

Effects of Polycyclic Aromatic Hydrocarbons in Urban Stormwater on Receiving Sediment

By

Dimitrios Athanasiou, B.S., M.S.

A Dissertation

In

Civil Engineering

Submitted to the Graduate Faculty
of Texas Tech University in
Partial Fulfillment of
the Requirements for
the Degree of

DOCTOR OF PHILOSOPHY

Danny Reible, Ph.D., P.E. BCEE, NAE
Chair of Committee

Andrew Jackson, Ph.D.

Todd Anderson, Ph.D.

Venkatesh Uddameri, Ph.D.

Mark Sheridan, Ph.D.
Dean of the Graduate School

August 2019

Copyright 2019, Dimitrios Athanasiou

Acknowledgments

I would like to express my deepest gratitude for my esteemed advisor, Dr. Danny Reible, for giving me the opportunity to be a part of his research team and his support throughout my Ph.D. His guidance helped me become a better researcher and a more mature conveyor of ideas. I would also like to thank my committee and faculty that contributed to my research and education, Professors Andrew Jackson, Todd Anderson, Venkatesh Uddameri, Juske Horita and Theo Udeigwe.

Furthermore, I would like to thank Dr. Magdalena Rakowska and Dr. Balaji Rao for showing me the ways around a lab and providing valuable insights and feedback on my research. Heartfelt thanks go to those who shared the graduate experience with me, Nomaan, Michelle, Tea, Songjing, Xiaolong, Tariq, Alex, Soraya, Adesewa, Uriel, Nahirobe, Aashik, Hsu and Paula.

I am grateful to Dr. Agamemnon Koutsospyros because he is the one that gave me the opportunity to come to the United States to further my education and laid the deep foundations for my consequent Ph.D. work

A very special thanks to my wife, Giovanna, for her continuous support, patience and encouragement during the harder days and for sharing the better ones.

Last but not least. I would not be here if it wasn't for my parents, brother and γαγιά Koula and I wouldn't be the same person if it wasn't for my friends Andreas, Nikos, Kostas, Vassilis and Alexandros.

TABLE OF CONTENTS

ACKNOWLEDGEMENTS	ii
ABSTRACT	vii
LIST OF TABLES	ix
LIST OF FIGURES	xi
1. Introduction	1
1.1 Overview	1
1.2 Research Objectives and Dissertation Organization	2
2. Literature Review	4
2.1 Polycyclic Aromatic Hydrocarbons	4
2.2 Pressurized Liquid Extraction	6
2.3 Sediment	8
2.4 Urban Stormwater Runoff	10
2.5 Bioaccumulation	11
2.6 Porewater	13
2.7 References	15
3. Pressurized Liquid Extraction of Polycyclic Aromatic Hydrocarbons from Weathered Sediment	20
3.1 Introduction	20
3.2 Materials and Methods	24
3.2.1 Chemicals	24
3.2.2 Reference material	24
3.2.3 Sample preparation	25
3.2.4 Instruments	28
3.2.5 Cell Cleaning after extraction	28
3.2.6 HPLC conditions	28
3.3 Results and Discussion	30
3.3.1 Method Blanks and Blank Spikes	30
3.3.2 Overall recovery comments	30

3.3.3 Effect of solvent mixture on PAHs based on number of rings	33
3.3.4 Effect of sorbents and their application	34
3.3.5 Effect of extraction time	36
3.3.6 Effect of extraction temperature	37
3.3.7 Effect of copper	39
3.4 Conclusions	40
3.5 References	42
4. Polycyclic Aromatic Hydrocarbons in Urban Runoff and Resulting Sediment Contamination	44
4.1 Introduction	44
4.2 Materials and Methods	47
4.2.1 Sampling Overview	47
4.2.2 Sample deployment and collection	51
4.2.2.1 Stormwater	51
4.2.2.2 Sediment cores	52
4.2.2.3 Settling traps	52
4.2.3 Sample preparation	53
4.2.3.1 Stormwater	53
4.2.3.2 Sediment	57
4.2.4 Chemicals, materials and instruments	59
4.2.5 Analysis	60
4.2.5.1 HPLC	60
4.2.5.2 GC-TQMS	61
4.2.6 Calculations and statistical analyses	61
4.2.6.1 Stormwater solids concentration for each particle size fraction	61
4.2.6.2 Stormwater PAH concentration in water for each particle size fraction	62
4.2.6.3 Stormwater PAH concentration on solids in water for each particle size fraction	62
4.2.7 PAH diagnostic ratios	63
4.3 Results and Discussion	64
4.3.1 Relative runoff contributions	64
4.3.2 Stormwater runoff	65

4.3.2.1	Runoff particle size and organic carbon content.....	66
4.3.2.2	Runoff PAHs.....	69
4.3.2.3	Time-series grab runoff.....	70
4.3.2.4	Stormwater runoff summary	73
4.3.3	Sediment	74
4.3.3.1	Settling material deposition profile, particle size and deposited PAH mass.....	75
4.3.3.2	Sediment PAH concentrations	79
4.3.3.3	Sediment TOC content.....	82
4.3.3.4	PAH ratios.....	83
4.3.3.5	Sediment summary.....	85
4.4	Conclusions	86
4.5	References	88
5.	Assessment of Polycyclic Aromatic Hydrocarbon Bioavailability in Sediments Impacted by Urban Runoff	92
5.1	Introduction	92
5.2	Materials and Methods	97
5.2.1	Sampling Overview	97
5.2.2	Sample deployment and collection.....	98
5.2.2.1	Sediment	98
5.2.2.2	Tissues.....	98
5.2.2.3	SPMEs.....	100
5.2.3	Chemicals, materials and instruments	101
5.2.4	Sample preparation.....	102
5.2.4.1	Sediment	102
5.2.4.2	Tissues.....	103
5.2.4.3	Passive Samplers.....	104
5.2.5	Analysis	104
5.2.5.1	HPLC	104
5.2.5.2	GC-TQMS.....	105
5.2.6	Statistical analysis.....	105
5.3	Results	107
5.3.1	Sediment.....	107

5.3.2 In-situ measurements	109
5.3.3 Ex-situ measurements.....	112
5.3.4 Relating bioaccumulation to freely dissolved and bulk sediment concentrations	116
5.3.5 Effects of storm runoff on receiving sediments	120
5.4 Conclusions	122
5.5 References	123
6. Conclusions and Future Works	125
APPENDIX	128

ABSTRACT

Urban stormwater runoff has long been identified as a major influence to the contamination of receiving water bodies and sediment. The episodic nature of storms combined with the imperviousness of urban surfaces, lead to stormwater discharges laden with high levels of solids-associated polycyclic aromatic hydrocarbons (PAHs). These compounds pose a concern due to their toxicity, mutagenicity and carcinogenicity, and many of them have been placed on USEPA Priority Pollutant List.

The core objective of this study was to determine the physical, chemical and biological characteristics of stormwater runoff from a mixed use urban watershed and determine the distribution and bioaccumulation potential of its effects on the receiving sediment. Historically, stormwater assessment has been focused on loads rather than impacts on sediments and different sampling approaches were needed to characterize those impacts. The experimental approach involved a 2-year sampling plan in Paleta creek at Naval Base San Diego (NBSD) involving a variety of sampling approaches including intensive sampling of individual storms, water and sediment collection before and after the winter rainy season and settling traps collecting depositing sediments throughout the storm season. Storm runoff samples from 2 storms in January 2016 were collected and size fractionated. Receiving sediments were monitored with water column, sediment and sediment trap measurements. Porewater passive samplers and both in-situ and ex-situ bioaccumulation studies using bent-nose clams (*Macoma Nasuta*) were conducted in cooperation with US Navy personnel to assess the response of the receiving benthos. Total Organic Carbon (TOC) and Black Carbon (BC) contents were measured to better understand the source of the depositing solids as well as to link PAHs in sediments to their bioaccumulation potential. Sediment and tissue was extracted by pressurized liquid extraction

(PLE), storm samples were liquid-liquid extracted (LLE) and final analysis was carried out by HPLC-FLD and GC-TQMS.

In preparation for the sediment sampling, a study of PLE was conducted in order to develop an in-house method that would allow us to process large amounts of sediment samples in an efficient and accurate way and, in particular, extract PAHs effectively from weathered and high BC sediment samples.

The combination of size fractionated stormwater loads with sediment traps was identified as the most effective monitoring tools to assess sediment recontamination. Analysis of stormwater samples showed most of the PAHs were associated with large particles in runoff and led to rapid near field deposition and sediment recontamination. SEM imaging confirmed the presence of large BC-rich particles in the near field traps. However, bioavailability was limited as indicated by bioaccumulation studies suggesting that sediment recontamination assessment should also be coupled with assessment of bioavailability. Porewater concentrations were also shown to correlate well with the observed bioaccumulation suggesting that either bioassays or porewater assessment could characterize bioavailability for PAHs. Parent and alkylated PAH ratios allowed stormwater from this watershed to be separated from sediments settling in areas away from the stormwater discharges.

LIST OF TABLES

3-1 Certified PAH concentrations of CRM and SRM.....25

3-2 List of tested methods with their respective parameters.....26

3-3 FLD excitation and emission wavelengths for the detection of different PAHs.....29

3-4 Average Σ PAH, Σ PAH-13, Σ (2-3 ring)PAH, Σ (4 ring)PAH and Σ (5-6 ring) PAH recoveries of each method on CRM and SRM.....31

3-5 List of methods (with their solvent and sorbent) that gave the best average recovery for each PAH.....33

A1 Extraction % recoveries of 15 PAHs from CRM for the 25 tested methods. In parenthesis the % relative standard deviation.....138

A2 Extraction % recoveries of 15 PAHs from SRM for the 5 tested methods. In parenthesis the % relative standard deviation.....139

A3 Storm 1 - Calculated aqueous runoff PAH concentrations in the corresponding size intervals.....140

A4 Storm 2 - Calculated aqueous runoff PAH concentrations in the corresponding size intervals.....141

A5 Storm 1 – TFS and calculated runoff solids concentrations of PAHs in the corresponding size intervals.....142

A6 Storm 2 – TFS and calculated runoff solids concentrations of PAHs in the corresponding size intervals.....143

A7 Average measured sediment core and settling trap Σ PAH concentrations at the receiving waters of Paleta creek.....144

A8 TOC content of solids deposited on filters/sieves of composite runoff collected during both storms.....145

A9 July 2015 - Average measured tissue, sediment and porewater concentrations for 7 PAHs at the receiving waters of Paleta creek.....146

A10 In-situ 2015-2016 - Average measured tissue, sediment and porewater concentrations for 7 PAHs at the receiving waters of Paleta creek.....147

A11 Ex-situ 2015-2016 - Average measured tissue, sediment and porewater concentrations for 7 PAHs at the receiving waters of Paleta creek.....	148
A12 Ex-situ 2016-2017 - Average measured tissue, sediment and porewater concentrations for 7 PAHs at the receiving waters of Paleta creek.....	149

LIST OF FIGURES

2-1 Structures and names of USEPA PAH-16 priority pollutants.....4

3-1 Annual number of publications on PLE for the period 1995-2018.
(Source: Web of Science).....20

3-2 Effect of in-cell and column clean-up processes on mean average
ΣPAH-13 recoveries for CRM.....35

3-3 Effect of extraction time on mean average ΣPAH-13 recoveries
for CRM.....36

3-4 Effect of extraction temperature on mean average ΣPAH-13
recoveries for CRM and SRM.....38

3-5 Effect of in-cell copper on mean average ΣPAH-13 recoveries for
CRM.....40

4-1 Sampling locations at Naval Base San Diego. Stormwater runoff
was sampled in yellow locations. Time series runoff grab samples
were collected in the black location. Sediment cores and settling traps
were sampled in red locations.....49

4-2 Precipitation and sampling events of the 2 year sampling period
between 2015 and 2017.....50

4-3 ISCO autosampler.....51

4-4 Stormwater sample collected in a 10 L carboy.....51

4-5 Van Veen grab.....52

4-6 Settling traps deployed (left) and retrieved (right).....52

4-7 Dekaport splitter.....53

4-8 Schematic of the stormwater particle size fractionation
methodology used in this study.....54

4-9 2-L separatory funnel setup.....56

4-10 Pressurized liquid extraction of sediment samples was
performed by the Dionex ASE 350 instrument.....57

4-11 Sample cleanup setup with 50 mL chromatographic columns loaded with alumina and sodium sulphate.....58

4-12 Total solids and PAH mass transported by runoff during storm 1. (Y-axis is log).....64

4-13 Total solids and total PAHs concentrations in different solid fractions of runoff during the two storms that were sampled in Paleta creek.....65

4-14 Total organic carbon content of solids deposited on filters/sieves of composite runoff collected at the mouth of Paleta creek during both storms.....66

4-15 SEM pictures and EDS spectra of runoff particles collected at the mouth of Paleta creek during storm 1.....68

4-16 Storm 1 - Mass of PHE, PYR and BaP in different fractions of composite runoff solids at Paleta creek. All values are from single measurements.....69

4-17 Storm 1 - Total solids and total PAH concentrations in different solid fractions of runoff grab samples at progressing time points at Paleta creek.....71

4-18 Total organic carbon content of ambient grab runoff solids deposited on filters/sieves at the mouth of Paleta creek during both storms.....72

4-19 One-dimensional model describing deposition of particles transported by storm runoff.....75

4-20 Mass of settling particles collected by the deployed traps in July 2015 and during season 2015-2016. The solid line represents the anticipated runoff contribution, the dashed line represents an imaginary second source and the double line represents the measured sum of the two sources.....76

4-21 Particle size distribution of the solids collected in the settling traps during deployments in July 2015 and season 2015-2016.....77

4-22 PAH mass deposited in the settling traps during deployments in July 2015 and season 2015-2016.....78

4-23 Sediment core and settling trap ΣPAH concentrations in all locations and for all sampling events at Paleta creek.....	80
4-24 PAH concentrations in settling traps and sediment cores during deployments in season 2015-2016.....	81
4-25 Receiving sediment (Pre and Post) and settling trap TOC content in all sampling locations during storm seasons 2015-2016 and 2016-2017.....	82
4-26 Three different PAH ratios of solids transported by storm 1 runoff upstream of NBSD (C2W) and at the discharge point (C1W) in red. Same ratios for the solids deposited in the 2015-2016 settling traps in all locations is in blue.....	83
5-1 (Left) Sampling locations. (Right-clockwise) SEA Rings (a) deployed in situ beside Henry rods (b) containing the SPME passive samplers (c). Retrieved sediment traps (d) and cores (e).....	97
5-2 ΣPAHHMW concentrations of settling trap material and pre/post-storm sediment cores collected during seasons 2015-2016 and 2016-2017.....	107
5-3 Season 2015/2016 in-situ porewater ΣPAHHMW concentrations per location for both SPME deployments.....	109
5-4 Season 2015/2016 in-situ lipid normalized ΣPAHHMW concentrations per location. Open, 80μm and 500μm refer to the existence or not of a pre-filter on the top of the bioassay chambers.....	110
5-5 Pre/post season 2015-2016 and 2016-2017 ex-situ porewater ΣPAHHMW concentrations per location.....	112
5-6 Pre/post season 2015-2016 and 2016-2017 ex-situ lipid normalized ΣPAHHMW concentrations per location.....	114
5-7 Log-log graph of measured normalized porewater concentrations versus lipid normalized ΣPAHHMW concentrations for all sampling events.....	116
5-8 Log-log graph of predicted porewater concentrations versus lipid normalized ΣPAHHMW concentrations for all sampling events.....	118
A1 Cumulative boxplots of triplicates of all methods for CRM and SRM PAH recoveries.....	128
A2 Comparison of CRM PAH recovery signatures of the 5 best extraction methods.....	129

A3 Comparison of CRM PAH recovery signatures of methods 8, 11 and 13.....	129
A4 Comparison of the average recoveries of 3 groups (2-3, 4 and 5-6 ring) of PAHs from CRM for methods 8, 11 and 13.....	130
A5 Chemical structures and selected properties of the 16 USEPA priority pollutant PAHs (source:www.enviro.wiki/index.php?title=Polycyclic_Aromatic_Hydrocarbons_(PAHs)).....	131
A6 Concentrations of PHE, PYR and BaP in different fractions of composite runoff solids for both storms at Paleta creek. All values are from single measurements.....	132
A7 Storm 2 - Total solids and total PAH concentrations in different solid fractions of runoff grab samples at progressing time points at Paleta creek.....	133
A8 ΣPAH of settling particles collected by the deployed traps in July 2015 and during season 2015-2016.....	134
A9 Receiving sediment (Pre and Post) and settling trap BC content in all sampling locations during storm seasons 2015-2016 and 2016-2017.....	135
A10 July 2015 in-situ and ex-situ porewater ΣPAH _{HMW} concentrations per location.....	136
A11 Histogram showing the distribution of the residuals following the regression of porewater and tissue measurements.....	137
A12 Annual precipitation in San Diego during the 2011-2018 period. (source: https://www.sdcwa.org/annual-rainfall-lindbergh-field).....	137

Chapter 1

Introduction

1.1 Overview

Polycyclic aromatic hydrocarbons (PAHs) are toxic and persistent organic pollutants strongly associated with urban sediments. Following the reduction and control of industrial point sources in the 1970's, stormwater runoff became a more important contributor of PAHs to receiving waters. Runoff discharges usually don't receive appropriate treatment and that can lead to water quality degradation and negative impacts on the benthic communities. Moreover, the effectiveness of sediment remediation may be limited or reversed by the presence of these continuing stormwater discharges of PAHs.

The complexity of the sedimentary matrix and the presence of varying levels of natural organic matter (NOM) and interferences, can make the analysis of PAHs difficult. Pressurized liquid extraction (PLE) is a recently developed method of extracting pollutants from different matrices and its two major advantages are low solvent use and rapid extraction times. However, sediment samples often need multiple cleanup steps in order to purify the final extracts before analysis. Several PLE procedures have been proposed although no single method is universally accepted as the standard. In order to effectively use PLE, optimization is needed to demonstrate the ability to measure PAHs in stormwater solids that often contain strongly sorbed PAHs.

Any discussion about the effects of urban storm runoff to the receiving sediment, must begin from an accurate characterization of both stormwater loads as well as the physical and chemical characteristics of that stormwater relative to their fate in receiving waters. The study of stormwater requires physical analysis of the particle loading and size distribution and PAH analysis on both the runoff water and solids. In order to evaluate the resulting impacts on

sediment, both sediment traps and sediment sampling can be used. Sediment traps are more closely linked to recent deposition events while the sediments represent an integrated record of past events. It is apparent that a thorough study of runoff and sediment impacts is very resource intensive and requires planning and coordination.

Traditionally, defining bulk sediment PAH concentrations has been the basis for assessing exposure and risk of contaminated sediments. However, there has been increasing evidence that in some matrices only part of those PAHs are available for biological effects including toxicity and bioaccumulation. The presence of condensed carbon phases, often referred to as black carbon, often leads to a large portion of PAHs inaccessible to organisms. Thus, bulk PAH sediment concentrations may be overestimating risks of bioaccumulation and leading to ill-advised decisions from policy-makers. Bioaccumulation studies in benthic organisms can be used to assess bioavailability and physical chemical measurements such as porewater measurements are increasingly used to indicate that availability. All of these measurements are needed to create a complete picture of not only stormwater loads but the extent and implications of the resulting sediment recontamination.

1.2 Research Objectives and Dissertation Organization

With sediment being a relatively recent addition to the list of environmental matrices that receive remedial attention, a lot of concern is associated with the potential ways that a remediated site could be recontaminated. In an urban setting, a major input of contaminants into sediments comes from storm runoff. Identifying the characteristics of urban runoff and linking them to physical, chemical and biological effects on the receiving sediment is a critical step in any attempt to remediate contaminated sediments or develop methods of controlling runoff. In

response to the above needs and to further the current knowledge on sediment, the following objectives were addressed in this dissertation with reference to the chapters in which these were addressed:

- 1) Chapter 3: Develop a rapid and robust PLE method that will extract PAHs from a wide range of urban weathered sediments. The method must be able to produce high quality extracts in a time efficient manner as it will be used on a great number of sediment samples from different locations.
- 2) Chapter 4:
 - a. Integrate multiple runoff and sediment sampling tools to achieve physical/chemical characterization of urban runoff and determine the magnitude and distribution of its effects on the receiving sediment.
 - b. Propose an effective methodology to measure runoff and its impacts on receiving sediment.
- 3) Chapter 5:
 - a. Quantify the bioaccumulation potential of urban runoff and assess the risk it presents to the receiving benthos.
 - b. Propose and test an effective physico-chemical measurement that can serve as a surrogate for measuring bioaccumulation.

The above objectives provide not only a holistic analysis of the effects of urban runoff on the receiving sediments but also present methodologies to be applied in future studies.

Chapter 2

Literature Review

2.1 Polycyclic Aromatic Hydrocarbons

Polycyclic aromatic hydrocarbons (PAHs) is an extensively studied class of organic contaminants that consist of two or more aromatic rings. Their importance stems from their ubiquity in the urban environment and their carcinogenic and mutagenic effects on different organisms (Achten and Andersson, 2015; Dickhut et al., 2000). PAHs started being regularly discovered in environmental and drinking water samples throughout the US from the early 1970's, effectively since the creation of the EPA in 1970. Just 6 years later, 16 PAHs (Figure

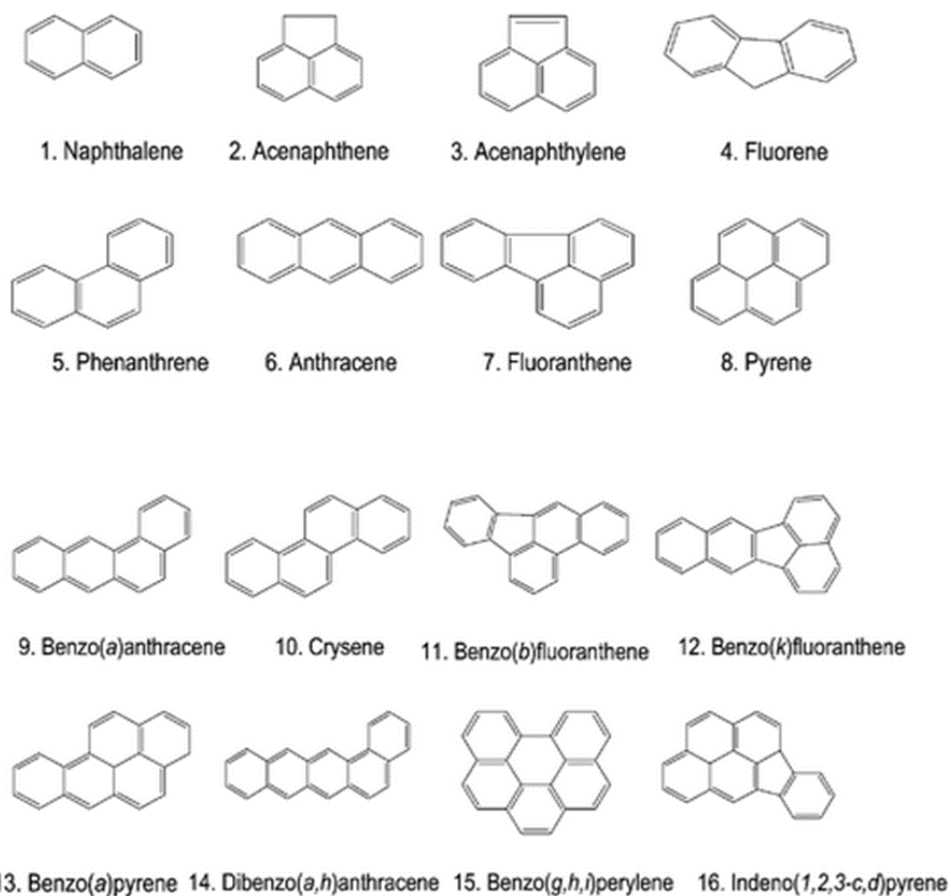


Figure 2.1: Structures and names of USEPA PAH-16 priority pollutants.

2.1) were included in a legal document known as “EPA’s 1976 Consent Decree” (Keith, 2015).

PAHs have a wide range of octanol-water ($3 < \log K_{ow} < 7$) and soil organic carbon ($3 < \log K_{oc} < 7$) partitioning coefficients as well as an 8-order-of-magnitude range of vapor pressures (10^{-2} - 10^{-10} mm Hg). Generally PAHs are relatively low in solubility and volatility and exhibit a strong affinity for particulate organic matter where they sorb and persist for considerable periods (Dickhut et al., 2000; Li et al., 2010).

Sources of PAHs can generally be divided into two categories, petrogenic and pyrogenic. Petrogenic sources include creosote and fossil fuels and their products (coal, tar, fuels, motor oil, asphalt etc.) (Li et al., 2014; Wolska et al., 2012). They are formed through incomplete combustion of organic matter or transformation of organic sediments over geologic time scales in subterranean anaerobic furnaces under elevated temperature and pressure and are typically abundant in 2-3 ring PAHs. Pyrogenic PAHs are formed during the aerobic high temperature combustion of petrogenic PAH sources (Kim et al., 2008; Stout et al., 2001) and exhibit an abundance of 4-6 ring PAHs.

In the urban environment, petrogenic PAHs sources can be asphalt (Abdel-Shafy and Mansour, 2016), pavement sealants (Mahler et al., 2012), vehicular tire and brake lining debris (Rogge et al., 1993), and leaked fuels (Hoffman et al., 1984; O’Reilly et al., 2014; Pengchai et al., 2004). The most prevalent urban pyrogenic source are vehicular exhaust particles (Abdel-Shafy and Mansour, 2016; Clark et al., 2015; Wang et al., n.d.; Zhang et al., 2012). Motor oil, despite being a petrogenic source when unused, picks up pyrogenic PAHs during its inevitable contact with the lower parts of combustion chambers.

2.2 Pressurized Liquid Extraction

Several methods have been developed to extract PAHs from soil and sediment. Traditional methods include ultrasonic agitation (Lau et al., 2010), mechanical agitation, maceration and percolation (Vazquez-Roig and Picó, 2015). Soxhlet extraction is probably the most trusted and most used method (Bjorklund et al., 2000; Lau et al., 2010; Nollet, 2006) as it is proven to give the highest extraction recoveries at the cost of high solvent use and very long processing times. Modern and more efficient extraction methods are microwave-assisted extraction (Qiao et al., 2018) and supercritical fluid extraction (Pakpahan, 2011).

Pressurized liquid extraction is another relatively recent method that offers much lower solvent use and rapid extraction times with comparable extraction potential to soxhlet (Heemken et al., 1997; Hawthorne et al., 2000). High operating pressure retains the solvent in the liquid phase while high temperature allows increased mass transfer of PAHs from the solid to the liquid phase (Richter et al., 1996). A number of different parameters are customizable with PLE; extraction temperature, adjustable ratio of up to 3 solvents, number and duration of extraction cycles and extraction cell volume are some of them.

One of the problems of PAH extraction from sediment is the extraction of interferences that lead to an impure sample. Usually, time consuming cleaning steps are required in order to have a clean extract (Kim et al., 2003). PLE has been shown to recover around 30% of the soil organic matter along with PAHs (Hawthorne et al., 2000). Sometimes, multiple cleanup steps are required in order to avoid introducing impurities in the analytical instrument and having high background. With ASE, one has the option of loading the extraction cell with one or more sorbents (alumina, silica gel, florisil) to remove analytes of non-interest such as lipids, pigments or cholesterol (Choi et al., 2014) during extraction. Activated copper can also be added in-cell

to remove elemental sulfur in the case of sediments because they often exhibit reducing conditions (Choi et al., 2014; Heemken et al., 1997; Pintado-Herrera et al., 2016). The addition of a sorbent and copper in-cell is a useful option as it minimizes sample processing time and solvent consumption (Choi et al., 2014; Kim et al., 2003; Pintado-Herrera et al., 2016).

Need for developing a PLE method for weathered solids

Different procedures have been proposed for the extraction of soils and sediments using PLE, but none is universally accepted. Development of methods appropriate for the extraction of PAHs from solids usually entails spiking an uncontaminated sample with the contaminant matrix of interest and acclimating for 2-48h (Choi et al., 2014; Fisher et al., 1997; Kim et al., 2003; Pintado-Herrera et al., 2016) instead of using weathered samples. The environmental relevance of desorption resistant (weathered) phases lies in their apparent lack of biological availability and their determination is crucial in assessing environmental risk. If total mass of contaminants on soils and sediments is required, however, extraction of this material would be desired and may be much more difficult by PLE than suggested by recoveries from recently inoculated matrices. Moreover, the extraction of this material may be uneven making it difficult to assess either an easily available form or total mass concentration from the amount extracted.

Another concern that has to be addressed is the productivity of relatively small laboratories with a high number of samples to process. The high mass of solids (5-30g) to be extracted by proposed PLE methods (Choi et al., 2014; Fisher et al., 1997; Saim et al., 1998; EPA Method 3545A) can lead to high amounts of NOM that will require multiple cleanup steps to purify before analysis. In chapter 3, we conduct a study and propose a method that can create a

high quality extract by extracting approximately 1 g of sediment and usually doesn't require further processing before analysis.

2.3 Sediment

Only recently did sediment emerge as an environmental domain that receives remedial attention. Following the implementation of the Clean Water Act in 1972, the introduction of the National Pollutant Discharge Elimination System (NPDES) led to a drastic reduction and control of industrial and municipal point sources in the 1970's. This reduction led to improvement of surface water quality but underlined the legacy of contaminated sediments as the terminal sink for HOCs (Reible, 2014). Natural attenuation was considered to be sufficient in recovering these sediments but we find persistent contamination even 50-100 years after contaminant deposition.

Sediments are often found in dynamic environments and are influenced by processes such as erosion and resuspension that can impair the overlying water. Under stable conditions, sediment contaminants are in equilibrium with the porewater, but groundwater upwelling, hyporheic exchange and bioturbation can lead to releases of these freely available contaminants to the overlying water column.

Organic pollutants in sediments are usually found in fine particulates which are rich in organic carbon. Worldwide, urban sediment is a compartment with elevated PAHs (Badin et al., 2008; Bian and Zhu, 2009; Cornelissen et al., 2008) and they are considered contaminants of primary concern due to their strong sorption on organic carbon (Accardi-Dey and Gschwend, 2002) and recalcitrance.

Sediment risk assessment is frequently focused on benthic organisms that lie at the bottom of the aquatic food chain. Infaunal and epibenthic species, are exposed to PAHs by

ingestion, inhalation and contact. Since ingestion of sediment is the most prominent route of uptake, bulk sediment concentrations were traditionally considered to be a good surrogate for sediment assessment. It is however important to understand that it is the biological response to a contaminated sediment that determines the risk of contamination, not the contaminant levels themselves. This became apparent when studies started revealing limited effects of relatively contaminated sediment or that contaminant concentrations in organisms were 1-2 orders of magnitude lower (Fernandez et al., 2009) than what would be expected if all contaminants were equally available. This led to more studies that revealed the presence of an organic carbon fraction, referred to as black carbon (BC) that is often present in soils and sediments and has high sorption capacity and renders organic contaminants largely unavailable to benthic organisms.

Black Carbon

It is well understood that organic contaminants in sediments mostly reside in the organic carbon fraction. With natural organic matter such as decaying leaf vegetation, the soil/sediment water sorption coefficient (K_d) can be separated into a measure of a compound's hydrophobicity, a compound's organic carbon sorption coefficient (K_{oc}), and the organic carbon content of the sediment (f_{oc}). In many soils and sediments, however, this approach is inaccurate and K_d is often much greater than $K_{oc} f_{oc}$. Studies that followed these observations revealed the existence of soots and biomass chars that are a condensed phase carbon and commonly referred to as BC (Gustafsson et al., 1997; Gustafsson and Gschwend, 1997). Lohmann et al. suggested that these materials despite contributing less than 10% of organic carbon, are responsible for the sorption of more than 90% of PAHs in Boston and New York harbor sediments (Lohmann et al., 2005).

The importance of measuring BC lies in helping to explain why increases in contaminant soil or sediment concentrations are not mirrored by body burden increases in bioaccumulation studies.

2.4 Urban Stormwater Runoff

Urban stormwater runoff has long been identified as a major influence to the contamination of receiving water bodies and sediment. The episodic nature of storms combined with the imperviousness of urban surfaces, lead to stormwater discharges laden with high levels of solids-associated organic contaminants. However, municipal storm drains were considered non-point sources and were not specifically addressed in the CWA of 1972. Following litigation, the D.C. Circuit Court of Appeals ruled in 1977 that stormwater discharges must be covered by the NPDES program. Further litigation ensued until 1987 when with the Water Quality Act, Congress addressed the stormwater problem by defining stormwater discharges as point sources and placing them under the NPDES umbrella.

Research conducted starting in the late 1970s and 1980s indicated that stormwater runoff was a significant cause of water quality impairment in many parts of the US. In the early 1980s, the EPA conducted the Nationwide Urban Runoff Program (NURP) to document the extent of the urban stormwater problem.

In an urban setting, the large proportion of impervious areas can rapidly lead to high volume runoff with enough kinetic energy to carry particles/contaminants to a receiving water body. Even low intensity precipitation that does not exceed the infiltration rate capacity of pervious surfaces, can lead to runoff in urban areas (Pitt et al., 1995). Physical characteristics (volume, total solids) of runoff can greatly vary according to drainage basin hydrology as well as

precipitation magnitude; chemical characteristics (contaminant loadings) will depend more on the level of urbanization and probably on the frequency of precipitation occurrence.

Characterization of urban runoff involves physical attributes, such as volume of runoff, total solids and organic matter content and contaminant load. These attributes can vary greatly according to drainage basin hydrology as well as precipitation magnitude. The chemical properties of stormwater depend mainly on the level of urbanization, potential contributing source areas and on the frequency of precipitation occurrence.

Historically, stormwater assessment has been focused on loads rather than impacts and this study aimed to more thoroughly characterize runoff and its effects on the receiving sediment.

2.5 Bioaccumulation

Bioaccumulation is the phenomenon where contaminant exposure and uptake by an aquatic organism leads to tissue concentration that exceeds that in the water (Gobas, 2001). Typically this is expressed as the bioaccumulation factor (BAF), a ratio of the contaminant concentrations in the organism tissue (C_{tissue}) and the surrounding media (C_m) (Eq. 1). If the route of contaminant uptake is from the freely dissolved phase (C_{pw}) via tissue sorption, the BAF is the ratio of the tissue concentration to the porewater concentration. In the case of hydrophobic organics (eg. PAHs) where lipids is the dominant phase of bioaccumulation in benthic organisms (Mackay, 1982) the bioaccumulation can be normalized to the lipid content as defined by the bioconcentration factor (BCF) (Eq. 2). If the bioaccumulating compound is hydrophobic, the porewater concentration would be proportional to the ratio of the sediment concentration to the fraction organic carbon and Eq.3 can be useful. Although these approaches have their basis in relating exposure to the porewater concentration and uptake from water, the major mode of

uptake for benthic organisms is ingestion of sediment. Despite this, porewater is increasingly being used as an indication of the available fraction of contaminants and the BCF may be useful even for deposit feeding routes of uptake.

$$BAF = \frac{C_{tissue}}{C_m} \quad (1) \quad BCF = \frac{\frac{C_{tissue}}{f_{lipids}}}{C_{pw}} \quad (2) \quad BSAF = \frac{\frac{C_{tissue}}{f_{lipids}}}{\frac{C_{sed}}{f_{oc}}} \quad (3)$$

Leo et al. studied the octanol-water model system and broadened its application to “partitioning-like” processes in more complex biological systems by showing that octanol is a satisfactory proxy model compound for lipid phases (Leo et al., 1971). In essence, this tells us that PAHs should partition approximately equally in lipids and octanol and the BCF should be approximately K_{ow} . We can thus define a biota-porewater accumulation factor that should be approximately unity (Eq. 4).

$$BPAF = \frac{\frac{C_{tissue}}{f_{lipids}}}{C_{pw} * K_{ow}} \cong 1 \quad (4)$$

According to the classic model, sediment porewater concentrations can be calculated by measuring organic carbon normalized sediment concentrations (C_{sed}/f_{oc}) and dividing by the organic carbon-water partition coefficient (K_{oc}) (Eq. 5). This paves the way for a predicted biota-porewater accumulation factor (Predicted BPAF) based on measured sediment concentrations (Eq. 6). We will examine this factor in Chapter 5 as well.

$$C_{pw} = \frac{C_{sed}}{f_{oc} * K_{oc}} \quad (5) \quad \longrightarrow \quad Predicted \ BPAF = \frac{\frac{C_{tissue}}{f_{lipids}}}{\frac{C_{sed}}{f_{oc} * K_{oc}} * K_{ow}} \quad (6)$$

2.6 Porewater

Freely dissolved concentration in sediment porewater is the aqueous concentration of compounds not associated with dissolved organic carbon, particulate matter or colloids (Schwarzenbach et al., 2003). The sorbing nature of sediments allows only a very small portion of PAHs to be found in the porewater and it's this fraction that rate-limits diffusive mass transfer processes (Rakowska et al., 2012). As noted above, this may also indicate the readily available contaminants that are readily taken up by deposit feeding organisms

As previously mentioned, the main route of PAH uptake for benthic organisms is sediment ingestion. However, the high amounts of BC found in urban sediments “tie up” a great portion of those PAHs and render them inaccessible. Studies have shown that porewater concentrations of hydrophobic organics correlate well with organism bioaccumulation (Gschwend et al., 2011; Lu et al., 2011; Sun and Ghosh, 2007; Vinturella et al., 2004) and can therefore be considered a better indicator of bioavailability. The use of passive sampling to measure freely dissolved concentrations and as a surrogate for bioaccumulation, could render standardized bioaccumulation studies unnecessary in the future.

Passive sampling

Recent advances in passive sampling have enabled direct measurement of freely dissolved concentrations of PAHs in porewater through the use of techniques such as solid phase microextraction (SPME) with polydimethylsiloxane (PDMS) fibers. PDMS fibers are inexpensive, can be rapidly deployed, minimally disturbing the sampling area and have been proven to accurately measure freely dissolved concentrations and to correlate well with organism

uptake (Lu et al., 2011). They consist of a glass cylindrical core coated with an annular layer of PDMS (a silicon-based organic polymer) that provides a high surface area to volume ratio.

Passive samplers can be deployed in-situ and ex-situ and they work by accumulating a minuscule amount of the target contaminant without affecting the equilibrium between free and sorbed phases (Van Der Wal et al., 2004). The amount of contaminant sorbed by the PDMS fiber at equilibrium is directly proportional (K_{pw}) to the freely dissolved concentration of that contaminant (Eq. 7).

$$C_{PDMS} = K_{PDMS-w} * C_{free} \quad (7)$$

Considering the different uptake kinetics that different PAHs exhibit, equilibration time can vary and it's not uncommon to have lower molecular weight PAHs at equilibrium while heavier ones not at equilibrium. It is therefore important to have a method of evaluating the equilibration stage that different compounds are at. This need led to the use of performance reference compounds (PRCs), substances that have similar characteristics to the pollutants of concern but are not naturally occurring at the sampling location (Fernandez et al., 2009; Karacik et al., 2013) and are analytically not interfering (Ghosh et al., 2014). In the case of PAHs, PRCs are usually deuterated (Vrana et al., 2014) or ^{13}C PAH (Karacik et al., 2013) isotopes. PRCs are pre-loaded onto the PDMS fibers prior to deployment and their release kinetics into the environment can be used to estimate the uptake kinetics of the parent compounds onto the fiber. Mass transfer models (Fernandez et al., 2009; Huckins et al., 1993; Lampert et al., 2015; Shen, 2017) have been created to link PRC release to more than the parent compound and that allowed for far fewer PRCs (but representing a broad range of hydrophobicities) needed to be pre-loaded in order to assess the uptake kinetics of all PAHs.

2.7 References

- Abdel-Shafy, H.I., Mansour, M.S.M., 2016. A review on polycyclic aromatic hydrocarbons: Source, environmental impact, effect on human health and remediation. *Egypt. J. Pet.* <https://doi.org/10.1016/j.ejpe.2015.03.011>
- Accardi-Dey, A.M., Gschwend, P.M., 2002. 23 Assessing the combined roles of natural organic matter and black carbon as sorbents in sediments. *Environ. Sci. Technol.* 36, 21–29. <https://doi.org/10.1021/es010953c>
- Achten, C., Andersson, J.T., 2015. Overview of Polycyclic Aromatic Compounds (PAC). *Polycycl. Aromat. Compd.* 35, 177–186. <https://doi.org/10.1080/10406638.2014.994071>
- Badin, A.-L., Faure, P., Bedell, J.-P., Delolme, C., 2008. Distribution of organic pollutants and natural organic matter in urban storm water sediments as a function of grain size. *Sci. Total Environ.* 403, 178–87. <https://doi.org/10.1016/j.scitotenv.2008.05.022>
- Bian, B., Zhu, W., 2009. Particle size distribution and pollutants in road-deposited sediments in different areas of Zhenjiang, China. *Environ. Geochem. Health* 31, 511–520. <https://doi.org/10.1007/s10653-008-9203-8>
- Bjorklund, E., Nilsson, T., Bowadt, S., 2000. Pressurised liquid extraction of persistent organic pollutants in environmental analysis. *Trends Anal. Chem.* 19, 434–445.
- Choi, M., Kim, Y.J., Lee, I.S., Choi, H.G., 2014. 4 Development of a one-step integrated pressurized liquid extraction and cleanup method for determining polycyclic aromatic hydrocarbons in marine sediments. *J. Chromatogr. A* 1340, 8–14. <https://doi.org/10.1016/j.chroma.2014.03.015>
- Clark, A.E., Yoon, S., Sheesley, R.J., Usenko, S., 2015. Pressurized liquid extraction technique for the analysis of pesticides, PCBs, PBDEs, OPEs, PAHs, alkanes, hopanes, and steranes in atmospheric particulate matter. *Chemosphere* 137, 33–44. <https://doi.org/10.1016/j.chemosphere.2015.04.051>
- Cornelissen, G., Pettersen, A., Nesse, E., Eek, E., Helland, A., Breedveld, G.D., 2008. The contribution of urban runoff to organic contaminant levels in harbour sediments near two Norwegian cities. *Mar. Pollut. Bull.* 56, 565–573. <https://doi.org/10.1016/j.marpolbul.2007.12.009>
- Dickhut, R.M., Canuel, E.A., Gustafson, K.E., Liu, K., Arzayus, K.M., Walker, S.E., Edgecombe, G., Gaylor, M.O., MacDonald, E.H., 2000. Automotive sources of carcinogenic polycyclic aromatic hydrocarbons associated with particulate matter in the Chesapeake Bay region. *Environ. Sci. Technol.* 34, 4635–4640. <https://doi.org/10.1021/es000971e>
- F.A.P.C. Gobas, Assessing Bioaccumulation Factors of Persistent Organic Pollutants in Aquatic Food-Chains. In: Harrad S. (eds) *Persistent Organic Pollutants* (2001) 145-165

- Fernandez, L.A., Macfarlane, J.K., Tcaciuc, A.P., Gschwend, P.M., 2009. Measurement of freely dissolved PAH concentrations in sediment beds using passive sampling with low-density polyethylene strips. *Environ. Sci. Technol.* 43, 1430–1436. <https://doi.org/10.1021/es802288w>
- Fisher, J.A., Scarlett, M.J., Stott, A.D., 1997. 2 Accelerated solvent extraction: An evaluation for screening of soils for selected U.S. EPA semivolatile organic priority pollutants. *Environ. Sci. Technol.* 31, 1120–1127. <https://doi.org/10.1021/es9606283>
- Ghosh, U., Kane Driscoll, S., Burgess, R.M., Jonker, M.T.O., Reible, D., Gobas, F., Choi, Y., Apitz, S.E., Maruya, K.A., Gala, W.R., Mortimer, M., Beegan, C., 2014. Passive sampling methods for contaminated sediments: practical guidance for selection, calibration, and implementation. *Integr. Environ. Assess. Manag.* 10, 210–223. <https://doi.org/10.1002/ieam.1507>
- Gschwend, P.M., Macfarlane, J.K., Reible, D.D., Lu, X., Hawthorne, S.B., Nakles, D. V., Thompson, T., 2011. Comparison of polymeric samplers for accurately assessing PCBs in pore waters. *Environ. Toxicol. Chem.* 30, 1288–1296. <https://doi.org/10.1002/etc.510>
- Gustafsson, O., Gschwend, P.M., 1997. Soot as a strong partitioning medium for polycyclic aromatic hydrocarbons in aquatic systems. *Mol. markers Environ. geochemistry ACS Sympos.* 365–381.
- Gustafsson, Ö., Haghseta, F., Chan, C., MacFarlane, J., Gschwend, P.M., 1997. Quantification of the Dilute Sedimentary Soot Phase: Implications for PAH Speciation and Bioavailability. *Environ. Sci. Technol.* 31, 203–209. <https://doi.org/10.1021/es960317s>
- Hawthorne, S.B., Grabanski, C.B., Martin, E., Miller, D.J., 2000. 9 Comparisons of Soxhlet extraction, pressurized liquid extraction, supercritical fluid extraction and subcritical water extraction for environmental solids: Recovery, selectivity and effects on sample matrix. *J. Chromatogr. A* 892, 421–433. [https://doi.org/10.1016/S0021-9673\(00\)00091-1](https://doi.org/10.1016/S0021-9673(00)00091-1)
- Heemken, O.P., Theobald, N., Wenclawiak, B.W., 1997. Comparison of ASE and SFE with Soxhlet, Sonication, and Methanolic Saponification Extractions for the Determination of Organic Micropollutants in Marine Particulate Matter. *Anal. Chem.* 69, 2171–80. <https://doi.org/10.1021/ac960695f>
- Hoffman, E.J., Mills, G.L., Latimer, J.S., Quinn, J.G., 1984. Urban Runoff as a Source of Polycyclic Aromatic Hydrocarbons to Coastal Waters. *Environ. Sci. Technol.* 18, 580–587. <https://doi.org/10.1021/es00126a003>
- Huckins, J.N., Manuweera, G.K., Petty, J.D., Mackay, D., Lebo, J.A., 1993. Lipid-Containing Semipermeable Membrane Devices for Monitoring Organic Contaminants in Water. *Environ. Sci. Technol.* 27, 2489–2496. <https://doi.org/10.1021/es00048a028>
- Karacik, B., Okay, O.S., Henkelmann, B., Pfister, G., Schramm, K.W., 2013. Water concentrations of PAH, PCB and OCP by using semipermeable membrane devices and sediments. *Mar. Pollut. Bull.* 70, 258–265. <https://doi.org/10.1016/j.marpolbul.2013.02.031>

- Keith, L.H., 2015. The Source of U.S. EPA's Sixteen PAH Priority Pollutants. *Polycycl. Aromat. Compd.* 35, 147–160. <https://doi.org/10.1080/10406638.2014.892886>
- Kim, J.H., Moon, J.K., Li, Q.X., Cho, J.Y., 2003. 7 One-step pressurized liquid extraction method for the analysis of polycyclic aromatic hydrocarbons. *Anal. Chim. Acta* 498, 55–60. <https://doi.org/10.1016/j.aca.2003.08.049>
- Kim, M., Kennicutt, M.C., Qian, Y., 2008. Source characterization using compound composition and stable carbon isotope ratio of PAHs in sediments from lakes, harbor, and shipping waterway. *Sci. Total Environ.* 389, 367–377. <https://doi.org/10.1016/j.scitotenv.2007.08.045>
- Lampert, D.J., Thomas, C., Reible, D.D., 2015. Internal and external transport significance for predicting contaminant uptake rates in passive samplers. *Chemosphere* 119, 910–916. <https://doi.org/10.1016/j.chemosphere.2014.08.063>
- Lau, E. V., Gan, S., Ng, H.K., 2010. Extraction techniques for polycyclic aromatic hydrocarbons in soils. *Int. J. Anal. Chem.* 2010, 398381. <https://doi.org/10.1155/2010/398381>
- Leo, A., Hansch, C., Elkins, D., 1971. Partition coefficients and their uses. *Chem. Rev.* 71, 525–616. <https://doi.org/10.1021/cr60274a001>
- Li, F., Zeng, X., Yang, J., Zhou, K., Zan, Q., Lei, A., Tam, N.F.Y., 2014. Contamination of polycyclic aromatic hydrocarbons (PAHs) in surface sediments and plants of mangrove swamps in Shenzhen, China. *Mar. Pollut. Bull.* 85, 590–596. <https://doi.org/10.1016/j.marpolbul.2014.02.025>
- Li, Z., Pittman, E.N., Trinidad, D.A., Romanoff, L.C., Mulholland, J., Sjödin, A., 2010. Determination of 43 polycyclic aromatic hydrocarbons in air particulate matter by use of direct elution and isotope dilution gas chromatography/mass spectrometry. *Anal. Bioanal. Chem.* 396, 1321–1330. <https://doi.org/10.1007/s00216-009-3297-4>
- Lohmann, R., Macfarlane, J.K., Gschwend, P.M., 2005. 25 Importance of black carbon to sorption of native PAHs, PCBs, and PCDDs in Boston and New York Harbor sediments. *Environ. Sci. Technol.* 39, 141–148. <https://doi.org/10.1021/es049424+>
- Lu, X., Skwarski, A., Drake, B., Reible, D.D., 2011. 1 Predicting bioavailability of PAHs and PCBs with porewater concentrations measured by solid-phase microextraction fibers. *Environ. Toxicol. Chem.* 30, 1109–1116. <https://doi.org/10.1002/etc.495>
- Mackay, D., 1982. Correlation of Bioconcentration Factors. *Environ. Sci. Technol.* 16, 274–278. <https://doi.org/10.1021/es00099a008>
- Mahler, B.J., Van Metre, P.C., Crane, J.L., Watts, A.W., Scoggins, M., Williams, E.S., 2012. Coal-tar-based pavement sealcoat and PAHs: Implications for the environment, human health, and stormwater management. *Environ. Sci. Technol.* 46, 3039–3045. <https://doi.org/10.1021/es203699x>
- Nollet, L.M.L., 2006. *Chromatographic Analysis of the Environment.*

<https://doi.org/9781420027983>

- O'Reilly, K.T., Pietari, J., Boehm, P.D., 2014. Parsing pyrogenic polycyclic aromatic hydrocarbons: forensic chemistry, receptor models, and source control policy. *Integr. Environ. Assess. Manag.* 10, 279–285. <https://doi.org/10.1002/ieam.1506>
- Pakpahan, E.N., 2011. Polycyclic Aromatic Hydrocarbons in Petroleum Sludge Cake : Extraction and Origin - a Case Study 1, 201–207.
- Pengchai, P., Furumai, H., Nakajima, F., 2004. Source Apportionment of Polycyclic Aromatic Hydrocarbons in Illinois River Sediment. *Polycycl. Aromat. Compd.* 24, 773–789. <https://doi.org/10.1080/10406630490487828>
- Pintado-Herrera, M.G., González-Mazo, E., Lara-Martín, P.A., 2016. 6 In-cell clean-up pressurized liquid extraction and gas chromatography-tandem mass spectrometry determination of hydrophobic persistent and emerging organic pollutants in coastal sediments. *J. Chromatogr. A* 1429, 107–118. <https://doi.org/10.1016/j.chroma.2015.12.040>
- Pitt, R., Field, R., Lalor, M., Brown, M., 1995. Urban Stormwater Toxic Pollutants: Assessment, Sources, and Treatability. *Water Environ. Res.* 67, 260–275. <https://doi.org/10.2175/106143095X131466>
- Qiao, X., Zheng, B., Guo, R., Cui, T., An, Y.-X., Liu, Y., Zhao, X., Wang, X., 2018. A clean-up method for determination of multi-classes of persistent organic pollutants in sediment and biota samples with an aliquot sample. *Anal. Chim. Acta* 1047, 71–80. <https://doi.org/10.1016/j.aca.2018.10.011>
- Rakowska, M.I., Kupryianchyk, D., Harmsen, J., Grotenhuis, T., Koelmans, A.A., 2012. In situ remediation of contaminated sediments using carbonaceous materials. *Environ. Toxicol. Chem.* <https://doi.org/10.1002/etc.1763>
- Reible, D.D., 2014. Processes, Assessment and Remediation of Contaminated Sediments, SERDP/ESTCP Environmental Remediation Technology. Springer New York, New York, NY. <https://doi.org/10.1007/978-1-4614-6726-7>
- Richter, B.E., Jones, B.A., Ezzell, J.L., Porter, N.L., Avdalovic, N., Pohl, C., 1996. 1 Accelerated Solvent Extraction: A Technique for Sample Preparation. *Anal. Chem.* 68, 1033–1039. <https://doi.org/10.1021/ac9508199>
- Rogge, W.F., Hildemann, L.M., Mazurek, M.A., Cass, G.R., Simoneit, B.R.T., 1993. Sources of Fine Organic Aerosol. 3. Road Dust, Tire Debris, and Organometallic Brake Lining Dust: Roads as Sources and Sinks. *Environ. Sci. Technol.* 27, 1892–1904. <https://doi.org/10.1021/es00046a019>
- Saim, N., Dean, J.R., Abdullah, P.M., Zakaria, Z., 1998. 3 An experimental design approach for the determination of polycyclic aromatic hydrocarbons from highly contaminated soil using accelerated solvent extraction. *Anal. Chem.* 70, 420–424. <https://doi.org/10.1021/ac970473x>

- Schwarzenbach, R.P., Gschwend, P.M., Imboden, D.M., 2003. Environmental organic chemistry, 2nd ed. Wiley, Hoboken, N.J.
- Shen, X. Developing models for the assessment and the design of the in situ remediation of contaminated sediments. (2017).
- Stout, S.A., Magar, V.S., Uhler, R.M., Ickes, J., Abbott, J., Brenner, R., 2001. Characterization of Naturally-occurring and Anthropogenic PAHs in Urban Sediments-Wycoff/Eagle Harbor Superfund Site. *Environ. Forensics* 2, 287–300. <https://doi.org/10.1080/713848281>
- Sun, X., Ghosh, U., 2007. PCB bioavailability control in *Lumbriculus variegatus* through different modes of activated carbon addition to sediments. *Environ. Sci. Technol.* 41, 4774–4780. <https://doi.org/10.1021/es062934e>
- Van Der Wal, L., Jager, T., Fleuren, R.H.L.J., Barendregt, A., Sinnige, T.L., Van Gestel, C.A.M., Hermens, J.L.M., 2004. Solid-phase microextraction to predict bioavailability and accumulation of organic micropollutants in terrestrial organisms after exposure to a field-contaminated soil. *Environ. Sci. Technol.* 38, 4842–4848. <https://doi.org/10.1021/es035318g>
- Vazquez-Roig, P., Picó, Y., 2015. Pressurized liquid extraction of organic contaminants in environmental and food samples. *TrAC - Trends Anal. Chem.* <https://doi.org/10.1016/j.trac.2015.04.014>
- Vinturella, A.E., Burgess, R.M., Coull, B.A., Thompson, K.M., Shine, J.P., 2004. Use of Passive Samplers to Mimic Uptake of Polycyclic Aromatic Hydrocarbons by Benthic Polychaetes. *Environ. Sci. Technol.* 38, 1154–1160. <https://doi.org/10.1021/es034706f>
- Vrana, B., Klučárová, V., Benická, E., Abou-Mrad, N., Amdany, R., Horáková, S., Draxler, A., Humer, F., Gans, O., 2014. Passive sampling: An effective method for monitoring seasonal and spatial variability of dissolved hydrophobic organic contaminants and metals in the Danube river. *Environ. Pollut.* 184, 101–112. <https://doi.org/10.1016/j.envpol.2013.08.018>
- Wang, X.S., Meng, •, Chen, Q., Zheng, X., n.d. Polycyclic aromatic hydrocarbons (PAHs) in Xuzhou urban street dust: concentration and sources. *Environ. Earth Sci.* 76. <https://doi.org/10.1007/s12665-017-6922-0>
- Wolska, L., Mechlińska, A., Rogowska, J., Namieśnik, J., 2012. Sources and fate of PAHs and PCBs in the marine environment. *Crit. Rev. Environ. Sci. Technol.* 42, 1172–1189. <https://doi.org/10.1080/10643389.2011.556546>
- Zhang, Y., Shi, G.-L., Guo, C.-S., Xu, J., Tian, Y.-Z., Feng, Y.-C., Wang, Y.-Q., 2012. Seasonal variations of concentrations, profiles and possible sources of polycyclic aromatic hydrocarbons in sediments from Taihu Lake, China. *J. Soils Sediments* 12, 933–941. <https://doi.org/10.1007/s11368-012-0526-9>

Chapter 3

Pressurized Liquid Extraction of Polycyclic Aromatic Hydrocarbons from Weathered Sediment

3.1 Introduction

Sediment has long been identified as a large sink of polycyclic aromatic hydrocarbons (PAHs). Either through stormwater runoff, atmospheric deposition or point sources, their hydrophobicity leads to accumulation in soils and sediments. The varying origin of these particles combined with different weathering processes that act upon them, contribute to the complexity of the sedimentary matrix. Due to their toxicity, carcinogenicity and bioaccumulation potential, their presence has been extensively monitored and documented.

Analysis of PAHs from soils and sediments requires extraction. Several extraction methods have been used in the past with the most prominent being Soxhlet (Bjorklund et al., 2000; Lau et al., 2010; Nollet, 2006). In recent years, pressurized liquid extraction (PLE) has

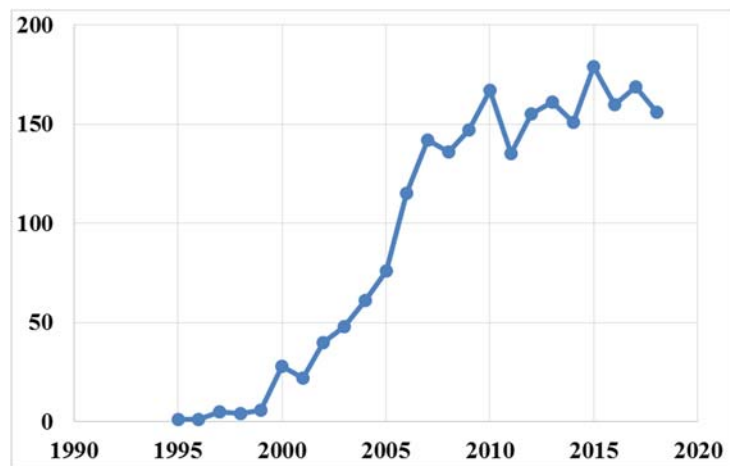


Figure 3-1: Annual number of publications on PLE for the period 1995-2018. (Source: Web of Science)

been gaining traction as a method of solid-liquid extraction as shown by the increasing number of publications since its introduction in 1995 (Figure 3-1). PLE has adequately fulfilled the promise of much lower solvent use, rapid extraction times and comparable performance to Soxhlet (Hawthorne et

al., 2000; Heemken et al., 1997; Lau et al., 2010). The high temperature possible with PLE, increases the mass transfer of PAHs by decreasing the viscosity of the solvent and weakening the

solute-matrix interactions (Fisher et al., 1997; Richter et al., 1996). At the same time, high pressure keeps the solvent in the liquid state and forces it into the matrix pores promoting high extraction recoveries (Kaufmann and Christen, 2002). Temperature, solvents, customizable ratio of up to three different solvents, number of cycles and duration of each cycle are some of the parameters that can be tailored with PLE. Appropriate selection of these parameters to maximize extraction from any soil or sediment, particularly from “aged” matrices, generally requires trial and error testing (Subedi et al., 2015). Pressure has only a minor effect on recoveries (Carabias-Martínez et al., 2005).

When extracting PAHs from sediment, attaining a clean extract ready for analysis can be very time consuming (Kim et al., 2003) as PLE has been shown to extract 25-33% of the soil organic matter along with PAHs (Hawthorne et al., 2000). Sometimes, multiple cleanup steps are required in order to avoid introducing impurities in the analytical instrument and having high background. With ASE, one has the option of loading the extraction cell with one or more sorbents (alumina, silica gel, florisil) to remove analytes of non-interest such as lipids, pigments or cholesterol (Choi et al., 2014) during extraction. Activated copper can also be added in-cell to remove elemental sulfur in the case of sediments because they often exhibit reducing conditions (Choi et al., 2014; Heemken et al., 1997; Pintado-Herrera et al., 2016). The addition of a sorbent and copper in-cell is a useful option as it minimizes sample processing time and solvent consumption (Choi et al., 2014; Kim et al., 2003; Pintado-Herrera et al., 2016).

PAHs represent a group of pollutants with a wide range of vapor pressures and water solubilities (as well as solubilities in extraction solvents) and thus show a broad range of extraction behavior (Hawthorne et al., 2000). Solvents typically used with PLE are dichloromethane (DCM), hexane (Hex) and acetone (Ace). DCM has been shown to

satisfactorily extract polar to non-polar compounds (Freitas et al., 2013; Saim et al., 1998) and has the added benefit of rapid concentration of the final extract due to its higher vapor pressure. Hexane has also been extensively used for PAH extraction because of its low polarity index and similar structure to (poly)aromatic compounds. As for Ace, its water solubility gives it the ability to penetrate particle pores that have trapped moisture and that way, provide access to another solvent to extract the analytes of interest from the solid phase. Past studies have shown that higher PAH recoveries are usually obtained using DCM-Hex (Pintado-Herrera et al., 2016) or Hex-Ace mixtures (Bjoërklund and Nilsson, 2000; Fisher et al., 1997; Saim et al., 1998).

Several PLE procedures have been proposed, although there is no single method universally accepted. The impact of different PLE variables on PAH recoveries has been previously explored (Richter et al., 1996), however most studies are conducted on spiked sediment, acclimated for 2-48h (Choi et al., 2014) and not weathered sediment. PAHs sorb on microporous materials very slowly and over long time periods, become “sequestered” (Jonker and Koelmans, 2002) and very resistant to desorption. The environmental relevance of these desorption resistant phases lies in their apparent biological availability and their determination is crucial in assessing environmental risk. If total mass of contaminants on soils and sediments is required, however, extraction of this material would be desired and may be much more difficult by PLE than suggested by recoveries from recently inoculated matrices. Moreover, the extraction of this material may be uneven making it difficult to assess either an easily available form or total mass concentration from the amount extracted.

EPA Method 3545A suggests PAH recoveries with PLE as a range of 27.8-107.3% of automated Soxhlet extraction with a mean recovery of 76.2%. The extraction mass proposed in the document (30g for a 34mL extraction cell) is large and combined with the lack of in-cell

sorbent and copper placement can lead to accumulation of NOM and sulfur in the final extract. Consequently, extracts derived from a highly humic or reduced samples will require multiple column cleanups to minimize interferences and carryover contamination in the analytical instrument of choice. The added processing time drastically limits applicability in real world samples, potentially leads to high losses, and may offset any initial sensitivity considerations (as implied by the very high extraction mass). Previous work in our laboratory has repeatedly shown that 0.5-1.5 g of dry sediment with cleanup in-cell, creates a high quality extract that will minimize further processing before analysis. There has also been criticism of EPA Method 3545A on the choice of Hex-Ace or DCM-Ace as the extraction solvents (Choi et al., 2014) and the use of 1 as opposed to 2 extraction cycles (Björklund et al., 1999; Popp et al., 1997).

In this work, conditions that optimize PAH extraction and sample cleanup from a weathered contaminated soil or sediment using a sample size of order 1 g is sought. The efforts were to identify conditions that would lead to good recoveries from reference weathered sediments with substantial fractions of PAHs expected to be in refractory, poorly extractable phases in order to be able to apply reasonable methods for weathered soils or sediments where actual concentration and therefore recovery was unknown. The reference materials selected for this purpose included CRM104 Certified Reference Sediment Material and Standard Reference Material 1941b (Organics in Marine Sediment). SRM has a total PAH-16 of 5.2 mg kg⁻¹, an organic carbon content of 3.1% of which 0.58% is black carbon (non-volatile for 24 hours at 375 C (Gustafsson et al., 1997). CRM has a total PAH-16 of 6.0 mg kg⁻¹, a total organic carbon content of 1.3% of which 0.11% is black carbon.

3.2. Materials and Methods

3.2.1 Chemicals

All solvents used (Hex, DCM, Ace and acetonitrile-ACN) were HPLC-grade from ThermoFisher Scientific (Phillipsburg, NJ, USA). Aluminum oxide (alumina) was purchased from Acros Organics (Phillipsburg, NJ, USA). Silica gel, florisil, sodium sulfate and copper powder were purchased from VWR (Radnor, PA, USA) and diatomaceous earth (DE) from ThermoFisher Scientific (Phillipsburg, NJ, USA). Research grade PAH-16 standards at a concentration of 100mg/L were purchased from Ultra Scientific (N. Kingstown, RI, USA). Ultrapure water was supplied by a GenPure Pro UV purification system (ThermoFisher Scientific, Phillipsburg, NJ, USA)

3.2.2 Reference material

Sigma-Aldrich (St. Louis, MO, USA) CRM104 Certified Reference Sediment Material from the southern branch of the Elizabeth River (Chesapeake Bay Area) and US National Institute for Standards and Technology (NIST in Gaithersburg, MD, USA) Standard Reference Material 1941b (Organics in Marine Sediment) from the mouth of the Baltimore (MD) harbor, were used to determine PAH recoveries. CRM was stored at 4 °C and SRM at 20 °C before and after each use. Reference concentrations of the 2 sediments can be seen in Table 3-1.

Table 3-1: Certified PAH concentrations of CRM and SRM.

Reference Concentrations						
	CRM concentration ($\mu\text{g}/\text{kg}$)			SRM concentration ($\mu\text{g}/\text{kg}$)		
	mean	deviation	RSD (%)	mean	deviation	RSD (%)
NAP	504	102	20.2	848	95	11.2
FL	270	37.6	13.9	85	15	17.6
ACE	575	92.5	16.1	38.4	5.2	13.5
PHE	202	27	13.4	406	44	10.8
AN	542	79	14.6	184	18	9.8
FLA	701	78.6	11.2	651	50	7.7
PYR	375	48.5	12.9	581	39	6.7
CHR	347	39.5	11.4	291	31	10.7
BaA	146	17.7	12.1	335	25	7.5
BbF	283	33.4	11.8	453	21	4.6
BkF	296	28.7	9.7	225	18	8.0
BaP	164	24.2	14.8	358	17	4.7
DBA	372	46	12.4	53	10	18.9
BghiP + InP	420+215	40+19.3	9.3	307+341	45+57	15.7

3.2.3 Sample preparation

Aliquots of 1.500 ± 0.001 g of reference material were weighed and mixed with DE. Stainless steel ASE cells (34 mL) were packed as follows; a cellulose filter was placed at the bottom followed by the sorbent, copper powder (when applicable), the sample/DE mix and any dead volume was filled with DE. Sorbents used in this study were 7.5 g of silica (activated according to EPA Method 3630c), 10 g of alumina (activated according to EPA Method 3610b), 8 g of florisil (activated according to EPA Method 3620c) or 5 g of alumina followed by 5 g of silica. Four of the methods involved no sorbent in the cell but cleanup by a 50 mL chromatographic column that had either 5 g of alumina or 4 g of silica with a small amount of pre-cleaned glass wool at the bottom. As for copper powder, either 4 or 8g were used (purified according to EPA Method 3660b).

The methods examined in this study were chosen as reduced permutations around the parameters that were selected to be explored, namely different solvent mixtures, temperature, extraction time per cycle, cleanup sorbent and desulphurization. All extraction methods (Table 3-2) had in common 2 static cycles with 6-8 mins of preheat time each, 100 s purge time and 10%

Table 3-2: List of tested methods with their respective parameters.

	Method	% Solvent used			Temperature (°C)	Extraction time/cycle (mins)	Sorbent in-cell
		DCM	Hex	Ace			
CRM	1	80	20		100	5	Al
	2	80	20		100	5	Al+4g Cu
	3	80	20		100	5	Al+8g Cu
	4	60	20	20	100	5	Al
	5	60	20	20	100	5	Al+4g Cu
	6	60	20	20	100	5	Al+8g Cu
	7		80	20	125	5	Al
	8		80	20	150	5	Al
	9		80	20	150	10	Al
	10	80	20		150	5	Al
	11	80	20		100	5	Si
	12	80	20		150	5	Si
	13	80	20		100	10	Si
	14	60	20	20	100	5	Si
	15		80	20	100	5	Si
	16		50	50	100	5	Si
	17	80	20		100	5	Al+Si
	18	60	20	20	100	5	Al+Si
	19	80	20		100	5	Column Al
	20	60	20	20	100	5	Column Al
	21	80	20		100	5	Column Si
	22	60	20	20	100	5	Column Si
	23		100		100	5	Si
	24	50	50		100	5	Si
	25	80	20		100	5	8g Florisil
SRM	1	80	20		100	5	Si
	2		80	20	100	5	Si
	3	80	20		150	5	Si
	4	80	20		100	5	Al
	5	80	20		100	5	Al+Si

rinse volume. Static pressure, as set by the instrument, was 1700 psi. The extracts were collected in 60mL amber vials and concentrated (with Rocket evaporator at 1700 rpm with 190 mbar vacuum for about 11mins) to approximately 1 mL. The samples were finally exchanged to acetonitrile, concentrated to 1mL and transferred into 2 mL vials for HPLC analysis. All analyses were performed in triplicates.

Calculation of the final volume was done by measuring the mass of the vial (plus a 300 μ L insert in the case of Method Blanks) before (m_i) and after (m_f) transferring the sample into it and using the density of ACN at 20 °C ($d_{ACN}=0.786 \text{ g cm}^{-3}$) in:

$$V_f = \frac{m_f - m_i}{d_{ACN}}$$

In general, the final volume was around 1mL for all samples.

Method Blanks

Background contamination of the solvents, sorbents and consumables as well as carryover contamination of the instrument, was assessed by a set of 3 ASE cells that were prepared in the same way as the rest (with silica in-cell) but had no reference material. The difference in volume was filled with DE and these cells were run at the start of every sequence. In total, 14 Method Blanks (MBs) were collected during this study with the final volume concentrated to 100-200 μ L to allow sufficient detection on the HPLC.

Blank Spikes / Spiked Method Blanks

Potential losses from this method were evaluated by a set of 3 cells that were prepared as the MBs but were spiked with 50 μ L of a 1 mg L⁻¹ mix of EPAs 16 priority PAHs in acetonitrile

on the top of the cell prior to extraction. In total, 13 Blank Spikes (BSs) were collected during this study.

The extraction of MBs and BSs was performed with Hex-Ace 1:1 v/v, 2 cycles of 5 mins, 100 °C and 10% rinse.

3.2.4 Instruments

Extractions were performed with a Dionex ASE™ (Accelerated Solvent Extraction) 350 PLE system and evaporations with a Rocket™ Evaporator, both from ThermoFisher Scientific (Phillipsburg, NJ, USA). Analysis of the extracts was done on an Agilent Technologies (Santa Clara, CA, USA) 1260 Infinity HPLC system.

3.2.5 Cell Cleaning after extraction

Although it has been reported that method blanks generated by ASE exhibit significant background (Fisher et al., 1997), there are no reports of a method that acceptably cleans ASE cells after use. In our lab, cells are emptied after extraction, disassembled, rinsed with DI water and placed in a plastic tub with soap. After sonicating the tub for 30 minutes, the disassembled cells are placed in an oven at 130 °C until dry. The frits are placed loosely in beakers filled with methanol and sonicated for 30 more minutes. After drying, cells are reassembled and ran on ASE with Hex-Ace (1:1 v/v) for 1 cycle of 10 minutes at 150 °C with 30% rinse.

3.2.6 HPLC conditions

Separation of analytes on the HPLC was carried out by a Phenomenex (Torrance, CA, USA) Luna 5µm C18 column (250 x 4.6 mm) set to 40 °C. Operation was under isocratic

conditions with 1 mL min⁻¹ flow rate of 70% acetonitrile and 30% water (v:v). For optimal sensitivity, the FLD detector was used with the Method Detection Limit (MDL) determined to be less than 0.5 µg/L for all parent PAHs. This method was able to analyze 15 PAHs (acenaphthylene does not fluoresce) with Benzo[g,h,i]perylene and Indeno[1,2,3-cd]pyrene taken as a single concentration because complete separation was not possible. PAH quantitation was achieved by nine-point calibration from 0.5 µg L⁻¹ to 200 µg L⁻¹ (0.5, 1, 2, 5, 10, 20, 50, 100, 200 µg L⁻¹) for the following compounds; Naphthalene (NAP), Fluorene (FL), Acenaphthene (ACE), Phenanthrene (PHE), Anthracene (AN), Fluoranthene (FLA), Pyrene (PYR), Chrysene (CHR), Benzo(a)anthracene (BaA), Benzo(b)fluoranthene (BbF), Benzo(k)fluoranthene (BkF), Benzo(a)pyrene (BaP), Dibenz(a,h)anthracene (DBA), Benzo(g,h,i)perylene (BghiP)+Indeno(1,2,3-cd)pyrene (InP).

Correlation coefficients were consistently greater than 0.9980. Calculation of PAH recoveries from the reference materials and the spiked method blanks was performed as:

$$PAH \text{ recovery } (\%) = \frac{\text{measured mass}}{\text{reference/spiked mass}} * 100$$

Table 3.3: FLD excitation and emission wavelengths for the detection of different PAHs

	NAP	FL, ACE PHE	AN	FLA	PYR,CHR, BaA, BbF, BkF, BaP	DBA, BghiP+InP
Excitation (nm)	280	260	260	260	260	305
Emission (nm)	340	352	420	440	420	430

3.3 Results and Discussion

3.3.1 Method Blanks and Blank Spikes

Carryover of individual PAHs as detected by the MBs (N=14) was in the range of 0-28ng. Most affected was NAP with a maximum carryover contribution in method 23 (lowest NAP recovery) of 7.6%. When average carryover was used, its mass contribution to the final extracted PAHs remained below 2%. The extraction of the BSs (N=13) had accuracy in the 92-124% range with an average of 96.4%.

3.3.2 Overall recovery comments

Average recoveries of AN and BaP from CRM were consistently lower than the rest of PAHs (Table A1) and incongruent to the recoveries of PAHs with similar structure (Figure A1). Mean recovery of AN was 19.1% (N=75) with 8.4% standard deviation and 3.5%-38.3% range. Mean recovery of BaP was 25.2% (N=75) with 6.2% standard deviation and 11.0%-39.6% range. The possibility of analytical error is very low due to the great number of extractions (N=75) and the fact that neither the SRM nor the spiked blanks exhibited the same trend. This observation could be attributed to an incorrect reference value. Following this observation, AN and BaP will be excluded from calculations of mean average PAH recovery from CRM which will henceforth be calculated based on the average of the 13 remaining PAHs and will be thus be referred to as “average Σ PAH-13 recovery”.

Average Σ PAH-13 extraction recoveries with different methods ranged between 48.9% (23.1%)¹ and 79.3% (1.3%) for CRM (Table 3-4) while between 62.6% (16.2%) and 79.1%

Table 3-4: Average Σ PAH, Σ PAH-13, Σ (2-3 ring)PAH, Σ (4 ring)PAH and Σ (5-6 ring)PAH recoveries of each method on CRM and SRM.

	Method	Average Σ PAH Recovery	Average RSD	Average Σ PAH-13 Recovery	Average RSD	Average Recovery		
						2-3 Ring PAHs	4 Ring PAHs	5-6 Ring PAHs
CRM	1	60.9	7.8	67.9	7.9	68.7	64.5	50.2
	2	64.2	5.3	71.8	4.7	74.0	70.8	49.1
	3	60.6	9.9	67.6	9.9	73.7	66.2	42.9
	4	59.5	2.9	66.0	2.7	62.6	65.9	51.2
	5	56.9	3.1	63.1	2.7	63.5	64.2	44.4
	6	54.1	6.3	60.0	6.6	61.7	63.9	38.7
	7	68.5	3.4	76.1	2.0	66.0	80.7	61.3
	8	70.1	6.8	77.6	2.4	67.2	80.9	64.4
	9	44.6	23.1	48.9	23.1	45.4	53.9	36.4
	10	62.2	2.8	68.4	2.7	62.9	72.6	53.1
	11	71.8	2.6	79.3	1.3	75.9	80.6	60.7
	12	66.0	7.1	72.2	7.3	69.8	74.9	55.0
	13	62.4	6.7	67.7	7.6	78.7	79.4	32.5
	14	66.7	3.5	73.3	3.3	67.5	75.3	59.0
	15	61.8	5.4	67.1	5.6	69.0	76.2	43.2
	16	58.2	9.5	63.6	7.9	70.3	70.5	36.3
	17	65.7	5.3	72.5	5.2	66.3	75.2	57.6
	18	68.1	8.3	74.9	8.0	68.7	77.2	60.1
	19	69.4	3.7	76.8	3.8	78.5	74.5	56.2
	20	66.3	2.5	73.0	2.7	69.0	73.9	57.6
	21	63.1	2.8	70.1	2.6	59.4	72.7	59.1
	22	61.0	3.8	67.4	3.2	54.0	70.7	60.2
	23	44.0	19.2	49.8	17.5	40.1	58.4	36.5
	24	57.6	8.4	65.6	8.6	54.9	69.0	51.2
	25	58.5	4.0	66.5	2.1	61.1	67.2	48.9
SRM	1	67.1	8.1	64.7	7.3	63.6	68.4	69.4
	2	65.1	11.4	64.4	11.7	62.0	68.4	65.6
	3	79.1	8.4	79.5	9.5	80.1	84.7	73.7
	4	69.3	18.6	68.0	19.4	75.8	68.2	63.6
	5	62.6	16.2	61.9	16.7	65.1	63.7	59.2

¹ Values in parentheses indicate relative standard deviation (RSD).

(8.3%) for Σ PAH² from SRM (Table A2). The robustness of 23 out of 25 methods was very good (1.3% < average RSD < 9.9%) for CRM and only methods 9 and 23 had incidentally the lowest recoveries (48.9 and 49.8% respectively) with the highest inaccuracy (23.1 and 17.5% respectively). SRM had higher uncertainty associated with its extraction as 3 out of the 5 tested methods had RSD greater than 10%.

Method 16, the most similar to the recommended EPA method with addition of silica in the cell, was 20th (out of 25) in terms of average Σ PAH-13 recovery (63.6%). There were 3 methods (8, 11, 19) that had higher average Σ PAH-13 recovery (>76.2%) than the recoveries reported in the EPA document. We see that when the method proposed by the EPA is applied on a small mass of weathered sediment and sorbent is added in the extraction cell, the recoveries are lower than reported and there are other methods that perform significantly better (method 11 led to almost 25% higher average Σ PAH-13 recovery) with an equal or better quality extract.

Method 11 (DCM-Hex 4:1, 5 min, 100 °C, in-cell silica) achieved the highest average Σ PAH-13 recovery overall at 79.3% (1.3%) on CRM. There were 4 methods (7, 8, 18 and 19) that were within 6% with very similar extraction signatures that can be seen in Figure A2 and 5 more methods (2, 12, 14, 17, and 20) within 10% of the average Σ PAH-13 recovery of method 11. Method 8 (Hex-Ace 4:1, 5 min, 150 °C, in-cell alumina) was best performing for 5 PAHs with method 13 (DCM-Hex 4:1, 10 min, 100 °C, in-cell silica) performing best for 4 PAHs (Table 3-5) and their extraction signatures can be compared in Figure A3 and Figure A4.

² Average Σ PAH recoveries for SRM represent all 15 PAHs.

3.3.3 Effect of solvent mixture on PAHs based on number of rings

Different size PAHs seem to be extracted better with different solvent mixtures. Lower molecular PAHs with 2-3 aromatic rings appear to have higher affinity for 80% DCM and 20% Hex (Table 3-5) as shown by the 5 methods (2, 3, 11, 13 and 19) that achieved highest extraction of them (Table 3-4) f. Higher molecular PAHs with 5-6 rings were best extracted almost exclusively with method 8 (Table 3-5) which entails 80% Hex and 20% Ace. Lastly, intermediate weight PAHs with 4 rings were extracted very well by both the above mixtures. The effect of used solvents on different PAHs, can be linked to solvent polarity as implied by the dielectric constant in parenthesis for Hex ($\epsilon=1.9$), DCM ($\epsilon=9.1$) and Ace ($\epsilon=20.7$). The above

Table 3-5: List of methods (with respective solvent and sorbent used) that gave the best average recovery from CRM for each PAH.

	Rings	Best Solvent	Best Sorbent	Best Method
Naphthalene	2	80% DCM – 20% Hex	Silica	13
Fluorene	3	80% DCM – 20% Hex	Column Alumina	19
Acenaphthene	3	80% DCM – 20% Hex	Silica	11
Phenanthrene	3	80% DCM – 20% Hex	Silica	13
Anthracene	3	80% DCM – 20% Hex	Silica	13
Fluoranthene	4	80%Hex–20%Ace	Alumina	7
Pyrene	4	80% DCM – 20% Hex	Silica	13
Chrysene	4	80% Hex – 20% Ace	Alumina	8
Benz[a]anthracene	4	80% Hex – 20% Ace	Alumina	18
Benzo[b]fluoranthene	5	80% Hex – 20% Ace	Alumina	8
Benzo[k]fluoranthene	5	80% Hex – 20% Ace	Alumina	8
Benzo[a]pyrene	5	80% Hex – 20% Ace	Alumina	8
Dibenz[a,h]anthracene	6	80% Hex – 20% Ace	Alumina	8
Benzo[g,h,i]perylene + Indeno[1,2,3-cd]pyrene	6	60%DCM–20%Hex-20%Ace	Column Silica	22

results are consistent with the idea that PAHs with higher hydrophobicities are extracted better with a less polar solvent mixture. Thus higher portions of Hex are favorable to the extraction of heavier PAHs. However, the use of 100% Hex (method 23) gave very low average recovery (49.8% - 2nd worst), as has been reported before (Choi et al., 2014), and can be attributed to its lowest polarity.

In SRM, 80% DCM and 20% Hex performed better than 80% Hex and 20% Ace for 2-3 and 5-6 ring PAHs and equally well for 4 ring PAHs. Having looked at the effectiveness of different solvent mixtures on 2 weathered sediments, 80% DCM and 20% Hex provided the most balanced recoveries across the entire PAH range. Given that the purpose of this study was to develop a robust method that would perform reasonably well across the PAH spectrum and on different matrices, we propose the use of 80% DCM and 20% Hex for PLE extractions of weathered sediment.

3.3.4 Effect of sorbents and their application

Sorbent selection and its method of application significantly influences average Σ PAH-13 recoveries from CRM (Figure 3-2). If temperature (100 °C), extraction time (5 min) and solvent ratio (DCM-Hex 4:1) remain constant, direct comparison of methods 1 and 19 shows that use of alumina as a sorbent in a column setup, leads to better (PStT: $p=0.086$) average Σ PAH-13 recoveries (76.8% vs 67.9%). Alumina use in column cleanup with DCM-Hex-Ace 3:1:1 solvent mixture (method 20) also leads to significantly improved (PStT: $p=0.013$) average Σ PAH-13 recoveries (73.0% vs 66.0%) when compared to in-cell (method 4). Silica on the other hand leads to better average Σ PAH-13 recoveries when used in-cell. This can be seen when comparing the recoveries of method 11 to method 21 (79.3% vs 70.1%, PStT: $p=0.007$) and method 14 to

method 22 (73.3% vs 67.4%, PStT: $p=0.029$). Visually and analytically, the quality of the extracts was not significantly different.

Based on these results, it is proposed that for the extraction of PAHs from weathered sediments, silica should be used in the cell as a first step to reduce interferences and compounds

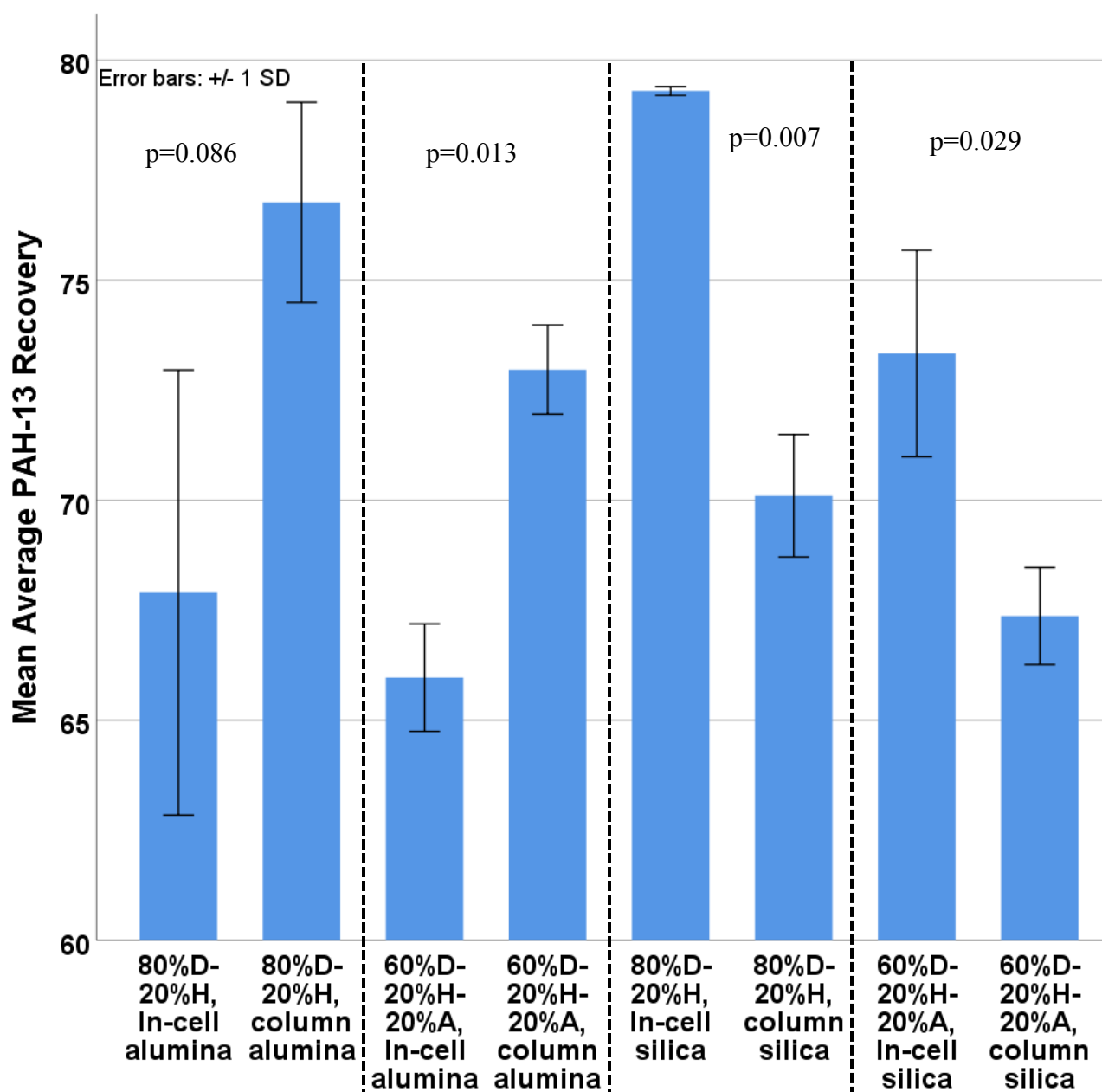


Figure 3-2: Effect of in-cell and column clean-up processes on mean average ΣPAH-13 recoveries for CRM.

of non interest. If further purification of the extracts is deemed necessary, column cleanup with alumina should be utilized.

3.3.5 Effect of extraction time

Increasing the extraction time led to lower average Σ PAH-13 recoveries (Figure 3-3). When 150 °C, alumina and Hex-Ace 4:1 are the extraction parameters, average Σ PAH-13 recovery drops significantly (PStT: $p=0.037$) from 77.6% with 5 mins extraction time (method 8) to 48.9% with 10 mins extraction time (method 9). In a similar fashion, with 100 °C, silica and DCM-Hex 4:1, average Σ PAH-13 recoveries are reduced (PStT: $p=0.061$) from 79.3% (method 11, 5 mins) to 72.2% (method 12, 10 mins). The quality of the extract was also affected by longer extraction times. Especially in the case of 150 °C, pigmentation was more prominent

and the HPLC chromatograms exhibited elevated background that contributed to the increased uncertainty during PAH quantification.

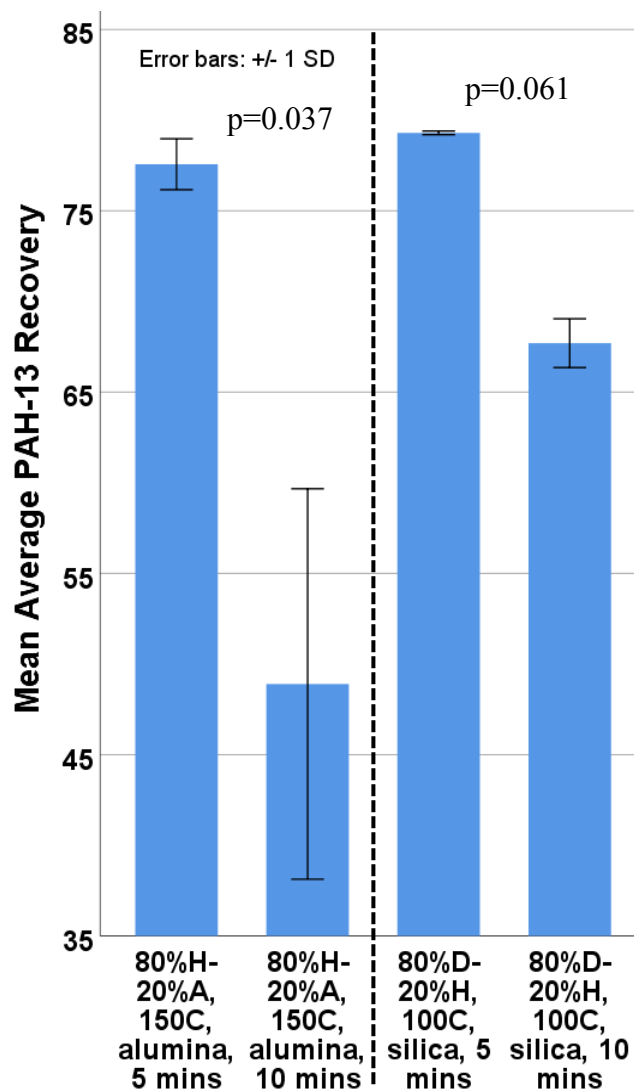


Figure 3-3: Effect of extraction time on mean average Σ PAH-13 recoveries for CRM.

Although we would tend to think that longer extraction time could improve recoveries, it has been reported in the past that extraction times longer than 5 mins do not improve recoveries

(Fisher et al., 1997). Reactions involving the soil organic matter and dissolved oxygen in the system (Fisher et al., 1997), especially at higher temperature, could potentially play a more pronounced role during prolonged extractions in transforming the PAHs in the cell, especially if a catalyst (eg. Nickel) is present. The much greater recovery decrease in the case of 150 °C compared to 100 °C aligns with the idea that at higher temperature, any transformation processes would have faster kinetics. It is harder to blame volatile losses as the extraction cell is a closed system and the air in the collection vial being displaced by the incoming solvent through the vent, should have a similar effect in both cases. The conclusion that can be drawn from these observations is that lengthening the extraction time, doesn't necessarily increase PAH recoveries, especially at elevated temperatures. Thus choosing 2 cycles of extraction of 5 mins each provides a good quality extract and improves productivity.

3.3.6 Effect of extraction temperature

Increased extraction temperature had various effects on average ΣPAH-13 extractions (Figure 3-4). When extracting CRM with DCM-Hex 4:1 and silica for 5 mins, method 12 (150 °C) had lower recoveries (PStT: $p=0.061$) than method 11 (100 °C). On the other hand, when extracting SRM with exactly the same parameters, method 3 (150 °C) led to higher recoveries (PStT: $p=0.102$) compared to method 1 (100 °C). The other two tested cases for CRM (method 7 vs 8 and method 1 vs 10), didn't produce significant differences (PStT: $p=0.286$ and $p=0.845$ respectively). One observation that was consistent across all these comparisons was a distinctly dark yellow color of the higher temperature extracts. This pigmentation is typical of high levels of NOM present in the sample and was confirmed by elevated HPLC UV absorbance. If NOM is not removed from the samples before HPLC analysis, it will lead to analytical downtime because

NOM will accumulate and subsequently act as another sorbing phase within the HPLC column leading to retention time shifts to the point of uncertainty in identifying the correct compounds in a chromatogram. Not long after that, repeated flushing of the column will be required in order to regenerate it. To avoid these analytical troubles, one or more column cleanups will be mandatory to reduce the NOM and that in itself will lead to evaporative and sorptive losses.

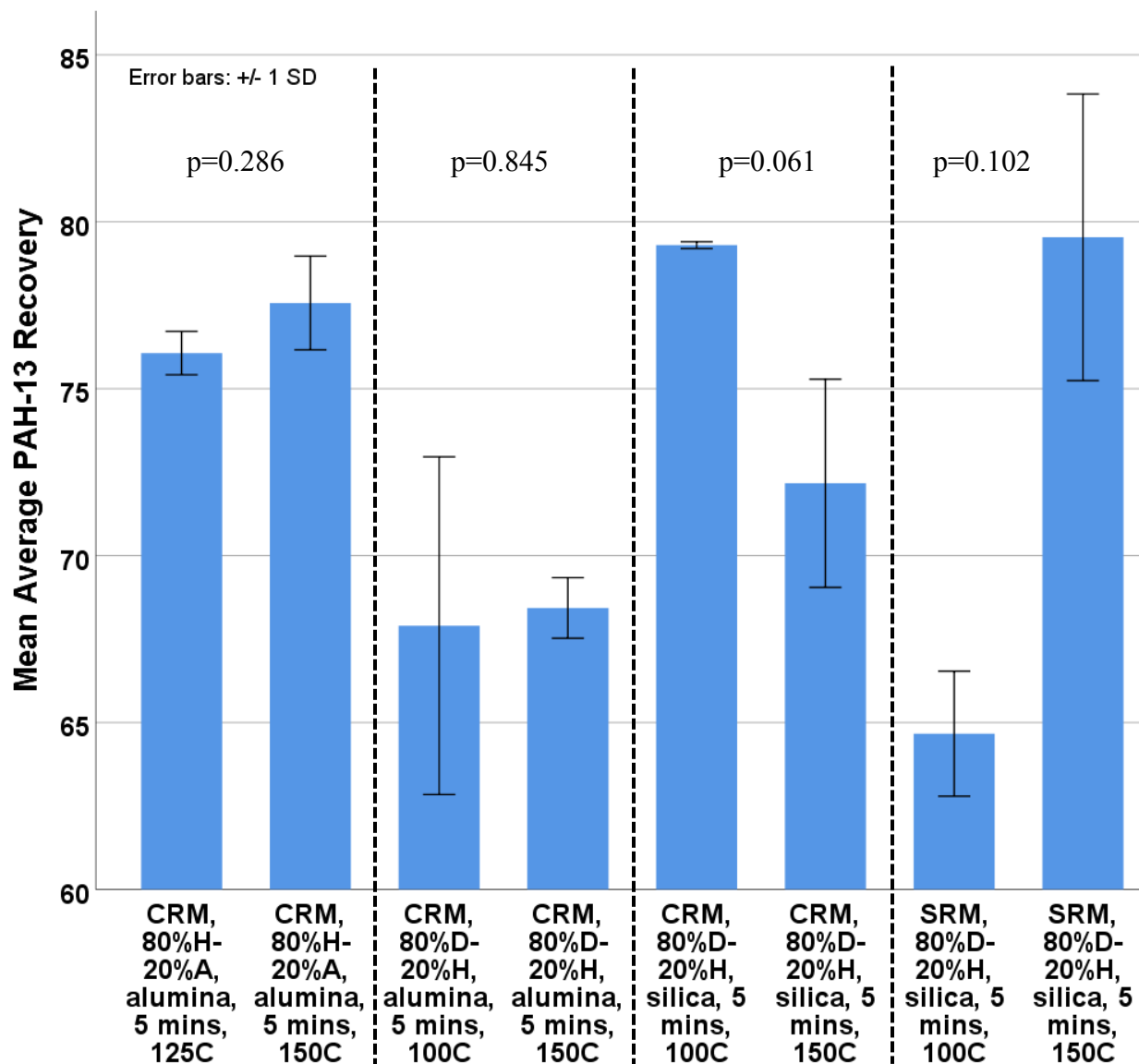


Figure 3-4: Effect of extraction temperature on mean average Σ PAH-13 recoveries for CRM and SRM.

These side effects of higher extraction temperatures combined with inconsistent effects on PAH recoveries, leads to the conclusion that PLE at 100 °C is the reasonable choice when productivity is taken into consideration. Studies have shown negligible (<5%) recovery gains with increased temperature (Pintado-Herrera et al., 2016) while others have reported evaporative and thermal degradation losses (Göbel et al., 2005) proposing 100 °C as a satisfactory extraction temperature (Choi et al., 2014).

3.3.7 Effect of copper

Addition of different masses of purified copper powder in-cell led to contrasting results (Figure 3-5). In the case of method 1 (DCM-Hex 4:1, 5 min, 100 °C, in-cell alumina without Cu), method 2 (method 1 plus 4 g of Cu) and method 3 (method 1 plus 8 g of Cu), there were no statistically significant differences in the means of average Σ PAH-13 recoveries. The recovery increase from method 1 to method 2 has 80% probability (PStT: $p=0.195$) being the result of the addition of 4 g of copper. However in the case of method 4 (DCM-Hex-Ace 3:1:1, 5 min, 100 °C, in-cell alumina without Cu), method 5 (method 4 plus 4 g of Cu) and method 6 (method 4 plus 8 g of Cu), there was a mild decrease of recoveries. The decrease in average Σ PAH-13 recovery from method 4 to method 5 as a result of the addition of 4g of copper can be considered statistically significant (PStT: $p=0.061$) but mild (2.9%). In past extractions, we have observed yellow sulfur crystals forming in the extracts of contaminated sediments. Copper in-cell addition at small doses (0.5 g) has been reported to not have an effect on recoveries (Pintado-Herrera et al., 2016). Since our study didn't show a significant difference arising from the use of much greater mass of copper, using approximately 4 g of purified copper inside the PLE cell during extraction can be a reasonable preemptive step to avoid sulfur removal later.

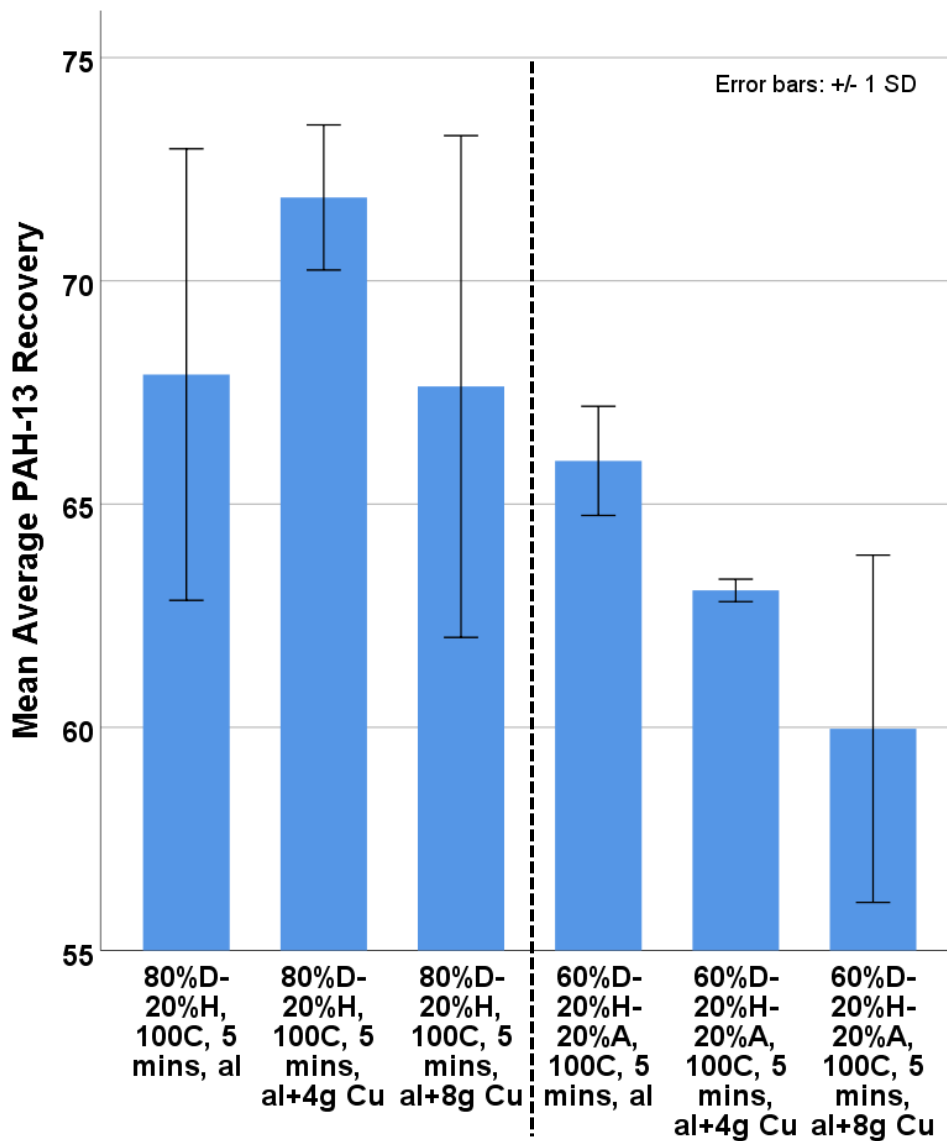


Figure 3-5: Effect of in-cell copper on mean average Σ PAH-13 recoveries for CRM.

3.4 Conclusions

Extracting PAHs from weathered sediment productively comes at a price. Compromises need to be made in the amount of PAHs that will be extracted from the sediment in order to be able to efficiently process large amount of samples with limited resources. Ideally, PLE methods

should be tailored to each sediment to achieve maximum extraction as sediment to sediment variations require different extraction parameters.

The results of this study propose that a lab performing extraction and analysis of weathered urban sediment with elevated organic content, should aim to use low sediment mass (0.5-1.5 g) and perform in-cell cleanup, preferably with silica and approx. 4 g of activated copper. If further purification is needed, alumina column cleanup should be employed. A solvent mixture of 80% DCM and 20% Hex at 100 °C with two 5-minute static cycles will result in very good extraction of PAHs from weathered sediment.

3.5 References

- Bjoerklund, E., Nilsson, T., 2000. Pressurised liquid extraction of persistent organic pollutants in environmental analysis. *Trends Anal. Chem.* 19, 434–445. [https://doi.org/10.1016/S0165-9936\(00\)00002-9](https://doi.org/10.1016/S0165-9936(00)00002-9)
- Bjoerklund, E., Bøwadt, S., Nilsson, T., Mathiasson, L., 1999. Pressurized fluid extraction of polychlorinated biphenyls in solid environmental samples. *J. Chromatogr. A* 836, 285–293. [https://doi.org/10.1016/S0021-9673\(99\)00077-1](https://doi.org/10.1016/S0021-9673(99)00077-1)
- Carabias-Martínez, R., Rodríguez-Gonzalo, E., Revilla-Ruiz, P., Hernández-Méndez, J., 2005. 10 Pressurized liquid extraction in the analysis of food and biological samples. *J. Chromatogr. A* 1089, 1–17. <https://doi.org/10.1016/j.chroma.2005.06.072>
- Choi, M., Kim, Y.J., Lee, I.S., Choi, H.G., 2014. 4 Development of a one-step integrated pressurized liquid extraction and cleanup method for determining polycyclic aromatic hydrocarbons in marine sediments. *J. Chromatogr. A* 1340, 8–14. <https://doi.org/10.1016/j.chroma.2014.03.015>
- Fisher, J.A., Scarlett, M.J., Stott, A.D., 1997. 2 Accelerated solvent extraction: An evaluation for screening of soils for selected U.S. EPA semivolatile organic priority pollutants. *Environ. Sci. Technol.* 31, 1120–1127. <https://doi.org/10.1021/es9606283>
- Freitas, L.D.S., Dariva, C., Jacques, R.A., Caramão, E.B., 2013. 5 Effect of experimental parameters in the pressurized liquid extraction of brazilian grape seed oil. *Sep. Purif. Technol.* 116, 313–318. <https://doi.org/10.1016/j.seppur.2013.06.002>
- Göbel, A., Thomsen, A., Mc Ardell, C.S., Alder, A.C., Giger, W., Theiß, N., Löffler, D., Ternes, T.A., 2005. Extraction and determination of sulfonamides, macrolides, and trimethoprim in sewage sludge. *J. Chromatogr. A* 1085, 179–189. <https://doi.org/10.1016/j.chroma.2005.05.051>
- Gustafsson, Ö., Haghseta, F., Chan, C., MacFarlane, J., Gschwend, P.M., 1997. Quantification of the Dilute Sedimentary Soot Phase: Implications for PAH Speciation and Bioavailability. *Environ. Sci. Technol.* 31, 203–209. <https://doi.org/10.1021/es960317s>
- Hawthorne, S.B., Grabanski, C.B., Martin, E., Miller, D.J., 2000. 9 Comparisons of Soxhlet extraction, pressurized liquid extraction, supercritical fluid extraction and subcritical water extraction for environmental solids: Recovery, selectivity and effects on sample matrix. *J. Chromatogr. A* 892, 421–433. [https://doi.org/10.1016/S0021-9673\(00\)00091-1](https://doi.org/10.1016/S0021-9673(00)00091-1)
- Heemken, O.P., Theobald, N., Wenclawiak, B.W., 1997. Comparison of ASE and SFE with Soxhlet, Sonication, and Methanolic Saponification Extractions for the Determination of Organic Micropollutants in Marine Particulate Matter. *Anal. Chem.* 69, 2171–80. <https://doi.org/10.1021/ac960695f>
- Jonker, M.T.O., Koelmans, A.A., 2002. 11 Sorption of polycyclic aromatic hydrocarbons and

- polychlorinated biphenyls to soot and soot-like materials in the aqueous environment: Mechanistic considerations. *Environ. Sci. Technol.* 36, 3725–3734. <https://doi.org/10.1021/es020019x>
- Kaufmann, B., Christen, P., 2002. 8 Recent extraction techniques for natural products: Microwave-assisted extraction and pressurised solvent extraction. *Phytochem. Anal.* 13, 105–113. <https://doi.org/10.1002/pca.631>
- Kim, J.H., Moon, J.K., Li, Q.X., Cho, J.Y., 2003. 7 One-step pressurized liquid extraction method for the analysis of polycyclic aromatic hydrocarbons. *Anal. Chim. Acta* 498, 55–60. <https://doi.org/10.1016/j.aca.2003.08.049>
- Lau, E. V, Gan, S., Ng, H.K., 2010. Extraction techniques for polycyclic aromatic hydrocarbons in soils. *Int. J. Anal. Chem.* 2010, 398381. <https://doi.org/10.1155/2010/398381>
- Nollet, L.M.L., 2006. *Chromatographic Analysis of the Environment*. <https://doi.org/9781420027983>
- Pintado-Herrera, M.G., González-Mazo, E., Lara-Martín, P.A., 2016. 6 In-cell clean-up pressurized liquid extraction and gas chromatography-tandem mass spectrometry determination of hydrophobic persistent and emerging organic pollutants in coastal sediments. *J. Chromatogr. A* 1429, 107–118. <https://doi.org/10.1016/j.chroma.2015.12.040>
- Popp, P., Keil, P., Möder, M., Paschke, A., Thuss, U., 1997. Application of accelerated solvent extraction followed by gas chromatography, high-performance liquid chromatography and gas chromatography-mass spectrometry for the determination of polycyclic aromatic hydrocarbons, chlorinated pesticides and polychlorin. *J. Chromatogr. A* 774, 203–211. [https://doi.org/10.1016/S0021-9673\(97\)00337-3](https://doi.org/10.1016/S0021-9673(97)00337-3)
- Richter, B.E., Jones, B.A., Ezzell, J.L., Porter, N.L., Avdalovic, N., Pohl, C., 1996. 1 Accelerated Solvent Extraction: A Technique for Sample Preparation. *Anal. Chem.* 68, 1033–1039. <https://doi.org/10.1021/ac9508199>
- Saim, N., Dean, J.R., Abdullah, P.M., Zakaria, Z., 1998. 3 An experimental design approach for the determination of polycyclic aromatic hydrocarbons from highly contaminated soil using accelerated solvent extraction. *Anal. Chem.* 70, 420–424. <https://doi.org/10.1021/ac970473x>
- Subedi, B., Aguilar, L., Robinson, E.M., Hageman, K.J., Björklund, E., Sheesley, R.J., Usenko, S., 2015. Selective pressurized liquid extraction as a sample-preparation technique for persistent organic pollutants and contaminants of emerging concern. *TrAC - Trends Anal. Chem.* <https://doi.org/10.1016/j.trac.2015.02.011>

Chapter 4

Polycyclic Aromatic Hydrocarbons in Urban Runoff and Resulting Sediment Contamination

4.1 Introduction

Water quality in coastal cities has been negatively affected by extensive urbanization that has been taking place since the last century. Dramatically increased human activity and landscape transformations have a detrimental effect on the condition of water bodies in close approximation to urban centers. The combination of altered watershed hydrology due to extensive impervious surfaces (Paul, M.; Meyer, 2005) and omnipresent priority organic pollutants (POPs) as a byproduct of a fossil-fuel-driven economy, has led to the emergence of stormwater runoff as the most significant mode of urban water quality degradation (according to the USEPA as mentioned in the National Water Quality Inventory 1996 Report to Congress).

Polycyclic aromatic hydrocarbons (PAHs) are common POPs associated with urban waters and sediments. Their presence poses a concern due to their toxicity, mutagenicity and carcinogenicity (Burgess et al., 2013; Cuypers et al., 2002; Hwang and Foster, 2006) and therefore many of them, have been placed on USEPA Priority Pollutant List (Figure A5). This class of contaminants consists of a variety of compounds characterized by two or more aromatic rings and a wide range of octanol-water partitioning coefficients ($3 < \log K_{ow} < 8$). Their generally low water solubility leads to their rapid sorption to organic carbon and their association with particulate matter has been well established (Dickhut et al., 2000; Li et al., 2010). Petroleum PAH sources (coal, tar, fuels, motor oil, asphalt etc.), also called petrogenic, are formed over geologic time scales in subterranean anaerobic furnaces under elevated temperature and pressure and are typically abundant in 2-3 ring PAHs. Pyrogenic PAHs are formed during the aerobic

high temperature combustion of petrogenic PAH sources and exhibit an abundance of 4-6 ring PAHs.

In modern urban environment, petrogenic PAHs can be found in asphalt (Abdel-Shafy and Mansour, 2016), pavement sealants (Barbara J Mahler et al., 2012), vehicular tire and brake lining debris (Rogge et al., 1993), and leaked fuels (Hoffman et al., 1984; O'Reilly et al., 2014; Pengchai et al., 2004). The most prevalent urban pyrogenic source are vehicular exhaust particles (Abdel-Shafy and Mansour, 2016; Clark et al., 2015; Zhang et al., 2012). Motor oil, despite being a petrogenic source when unused, soon picks up pyrogenic PAHs during its inevitable contact with the lower parts of combustion chambers.

Particles laden with PAHs such as the ones previously mentioned, can be suspended and transported by storm runoff (Corcoran et al., 2010). In an urban setting, the large proportion of impervious areas can rapidly lead to high volume runoff with enough kinetic energy to carry particles/contaminants to a receiving water body. Even low intensity precipitation that does not exceed the infiltration rate capacity of pervious surfaces, can lead to runoff in urban areas (Pitt et al., 1995). Physical characteristics (volume, total solids) of runoff can greatly vary according to drainage basin hydrology as well as precipitation magnitude; chemical characteristics (contaminant loadings) will depend more on the level of urbanization and probably on the frequency of precipitation occurrence.

Sediment is a relatively recent addition to the list of environmental matrices that receive attention and its importance stems from the fact that sorption strongly determines the fate of organic contaminants (Accardi-Dey and Gschwend, 2002). The complexity of this matrix can be attributed to its continuous shifting; deposition either directly from the atmosphere or by point/nonpoint discharges, resuspension by underwater currents/storm surges/propeller wash,

bioturbation and erosion are some of the mechanisms that can rapidly turn sediment from a sink to a source of pollutants. Worldwide, urban sediment is a compartment with elevated PAHs (Badin et al., 2008; Bian and Zhu, 2009; Cornelissen et al., 2008) that can degrade water quality, impair beneficial uses and stress the ecosystem. Benthic organisms that primarily lie at the bottom of the marine food chain, are exposed to PAHs by ingestion, inhalation and contact. That can have not only toxic and bioaccumulation effects on them but also poses a biomagnification risk.

Connecting stormwater with sediment contamination is a driving force behind this work. There are a number of studies on characterizing PAHs in urban runoff (Shinya et al., 2000; Zhang et al., 2008) and in urban road/highway runoff (Hoffman et al., 1984; Hwang and Foster, 2006), runoff from sealcoated pavements (Barbara J. Mahler et al., 2012; Watts et al., 2010) and PAH sources in urban runoff (Brown and Peake, 2006). There are also studies on characterizing PAHs in urban sediment (Stout et al., 2001) urban stream sediments (Bathi et al., 2012), particles collected in stormwater traps (Jartun et al., 2008) and PAH speciation in urban sediment particles (Ghosh et al., 2003). However, there have been very few studies that attempt linking the two (Cornelissen et al., 2008).

The goal of this study is to characterize the contribution and impact of urban runoff to sediment contamination in surface water bodies. Specific objectives of this work are to examine the solids distribution in stormwater discharge, with attention to the organic carbon content, in order to describe PAHs loading in size segregated runoff. The PAH signature in sediment and settling material collected from the receiving waters will be investigated, with the purpose of linking sediment contamination to stormwater discharges. The properties of solids collected from sediments, such as TOC and black carbon (BC), will indicate the mobile fraction of contaminant

adsorbed onto the sediment matrix. The behavior of different classes of PAHs will be studied by a cross-section of compounds, namely phenanthrene (PHE), pyrene (PYR) and benzo(a)pyrene (BaP), since different PAHs are associated with different levels of hydrophobicity which controls their environmental partitioning. The distribution of PAH sources is also used to differentiate impacts of stormwater versus other sources.

4.2 Materials and Methods

4.2.1 Sampling Overview

The Paleta creek watershed of Naval Base San Diego (NBSD) was chosen for the study area as a typical mixed used watershed with sources including industrial (Navy), residential (in the upper watershed) and roadway (interstate 5). The flow rate of the creek is highly associated with rain events and can have very low to no flow during the dry season or periods of drought. Precipitation events are almost entirely associated with winter periods with rain occurring rarely from April through October. The creek mouth discharges into the San Diego bay initially through a narrow channel that widens at about 1,200 ft. from the mouth. The California State Water Board has identified Paleta creek as a candidate toxic hot spot due to amphipod sediment toxicity.

Stormwater sampling was conducted via a variety of approaches including intensive stormwater sampling during two representative storm events, pre and post rainy season sediment sampling and bioassays, and settling chambers collecting sediment throughout the rainy season. The two sampled storm events took place on January 5-7, 2016 (storm 1 – 1.87in. of rain) and January 31 – February 1, 2016 (storm 2 – 0.16in. of rain). The stormwater samples were collected in two different ways. The major part of the sampling was performed by autosamplers

triggered by positive water flow and no salinity in order to insure the collection of runoff freshwater (storm 1: C1W, C2W, O1W, O2W, O3W and O4W, storm 2: C1W, C2W, O2W and O4W). The other part involved grab samples at different time points during storm 1 (A1W-01/05/2016, 13:27, A2W-01/05/2016, 19:47 and A3W-01/06/2016, 03:33) and storm 2 (A1W-01/30/2016, 09:00 and A2W-01/31/2016, 15:00) at the discharge point near C1W. These storm events are representative of 3/4 of the observed storms of the season that in general had 0.1-0.2 in. or 1-2 in. of total rainfall. This provided reassurance that the sampling was representative of the precipitation events taking place in San Diego.

The sediment and settling solids were sampled in 4 locations with increasing distance from the creek discharge point (P17, P11, P08 and P01). Intact sediment cores were collected by divers or by Van Veen grab samplers on 07/15/2015, 10/19/2015, 02/23/2016, 09/08/2016 and 03/08/2017 and stored at 4°C until processing or shipping to TTU. Sediment trap material was collected during the 2015 dry season (07/15/2015 – 08/12/2015) and over the course of the 2015-2016 wet season (10/19/2015 – 02/22/2016).

All sampling locations of this study can be seen in Figure 4-1 and all the sampling periods and events can be seen in Figure 4-2.



Figure 4-1: Sampling locations at Naval Base San Diego.. Stormwater runoff was sampled in yellow locations. Time series runoff grab samples were collected in the black location. Sediment cores and settling traps were sampled in red locations.

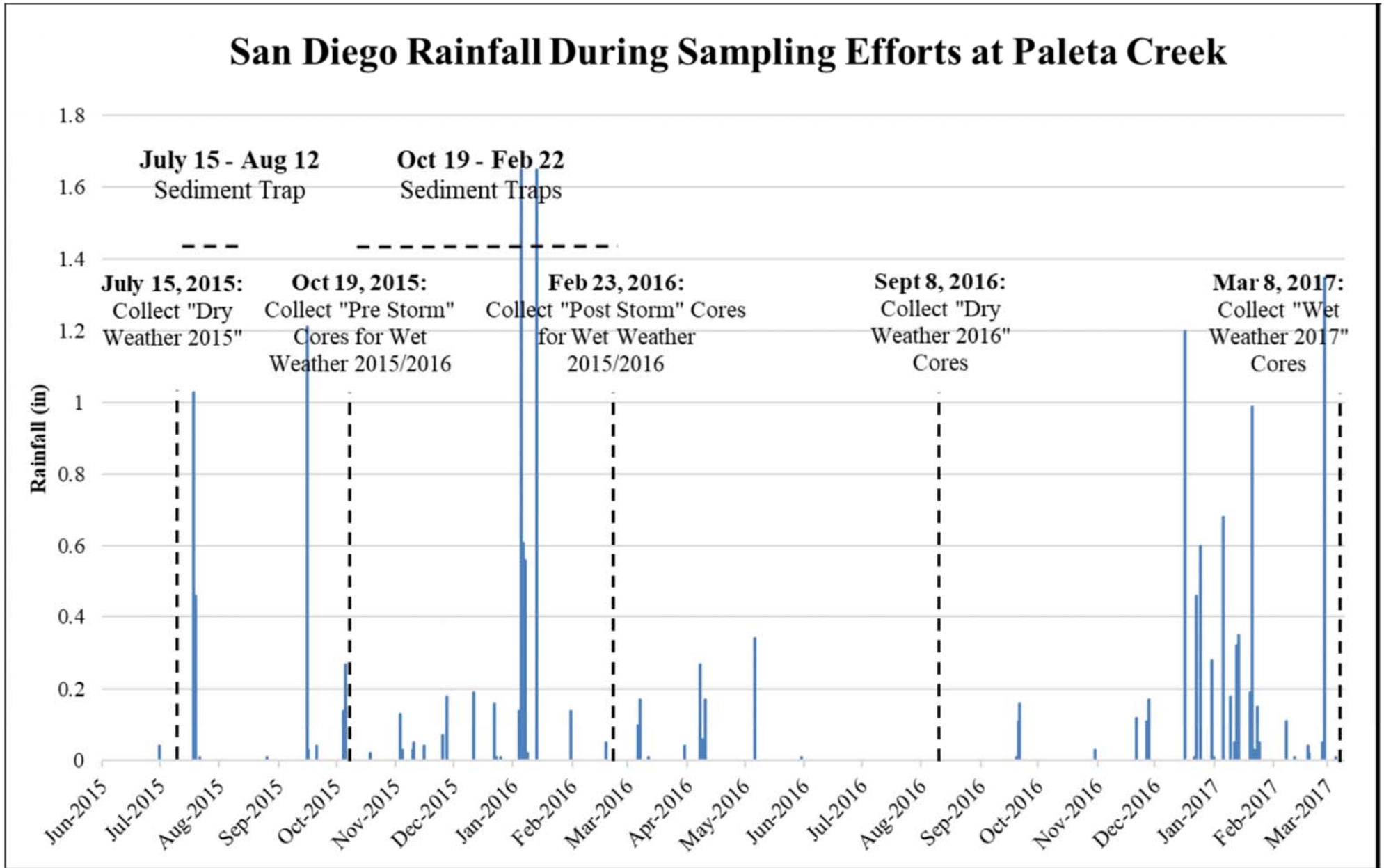


Figure 4-2: Precipitation and sampling events of the 2 year sampling period between 2015 and 2017.

4.2.2 Sample deployment and collection

4.2.2.1 Stormwater

The collection of stormwater consisted of time-spaced composite samples as well as time series of grab water samples. Stormwater sampling was conducted in 2016 during a storm on January 5-7 with 1.87 inches of rain and during another storm on January 31 to February 1 with 0.16 inches of rain. These two events captured 50% of the wet season total rainfall and represent small and large rains for the area as they were similar to approximately 75% of all storms during the 2015-2016 wet season.

A set of 10L glass carboys were cleaned by rinsing with organic solvents (hexane and acetonitrile), 10% v/v hydrochloric acid and MilliQ water. The carboys were shipped to the sampling site prior to stormwater sampling. Upon sampling, one carboy³ was placed inside each ISCO 6712 automatic water sampler (Figure 4-3) with sensors measuring salinity and flow velocity to ensure the collection of freshwater samples and minimize tidal effects. After retrieval, the carboys (Figure 4-4) were wrapped carefully by Geosyntec personnel for transportation to the SSC Bioassay Laboratory.



Figure 4-3: ISCO autosampler.



Figure 4-4: Stormwater sample collected in a 10 L carboy.

³ In storm 2, two carboys were used in each of the locations C1W, O2W, A1W and A2W to double detection limits.

4.2.2.2 Sediment cores

Sediment cores were hand-collected by SCUBA divers on 07/15/2015, 10/19/2015 and 02/23/2016. The divers pushed core liners 5 cm into the sediment in locations predetermined by GPS and then carefully capped the core on both sides. Once at the surface, cores were decanted of overlying water and the caps were secured with electrical tape. Sediment cores were collected with a Van Veen grab sampler on 09/08/2016 and 03/08/2017. After each grab, intact cores were sub-sampled by inserting core liners into the sampler (Figure 4-5). The sampler was thoroughly rinsed between stations to avoid cross-contamination, and sediment touching the sampler itself was avoided. After collection, all cores were stored at 4°C until processing or shipping to TTU.



Figure 4-5: Van Veen grab

4.2.2.3 Settling traps

Settling material was collected by single standard cylindrical sediment traps during the 2015 dry season (07/15/2015 – 08/12/2015) and by three standard cylindrical sediment traps per location (Figure 4-6) over the course of the 2015/2016 wet season (10/19/2015 – 02/23/2016). Dry season



Figure 4-6: Settling traps deployed (left) and retrieved (right).

sampling involved location P11 and P17 while wet season sampling took place in locations P01,

P08, P11 and P17. The traps were prefilled with hyper-saline brine, topped off with ambient seawater and capped. Divers lowered them into the water, secured them and removed the caps. Retrieval was performed by divers and a boat-mounted davit after capping them. Traps were transported back to the SSC laboratory, were allowed to settle and the overlying water was removed. All three traps at a given location were combined prior to analysis. All trap material was stored at 4°C until processing or shipping to TTU.

4.2.3 Sample preparation

4.2.3.1 Stormwater

The 10 L sample carboys containing the collected stormwater samples with suspended particulate matter, were equally split into 10⁴ 1-L bottles (7 glass amber for POP analysis and 3 plastic HDPE for metals analysis) using a Dekaport splitter (Figure 4-7). In storm 2, two carboys were used in each of the locations C1W, O2W, A1W and A2W. The Dekaport Sample Splitter is a 1-piece fluoropolymer device that was rinsed with MilliQ water at least 3 times before each use. The amber 1-L bottles were purchased certified clean by VWR

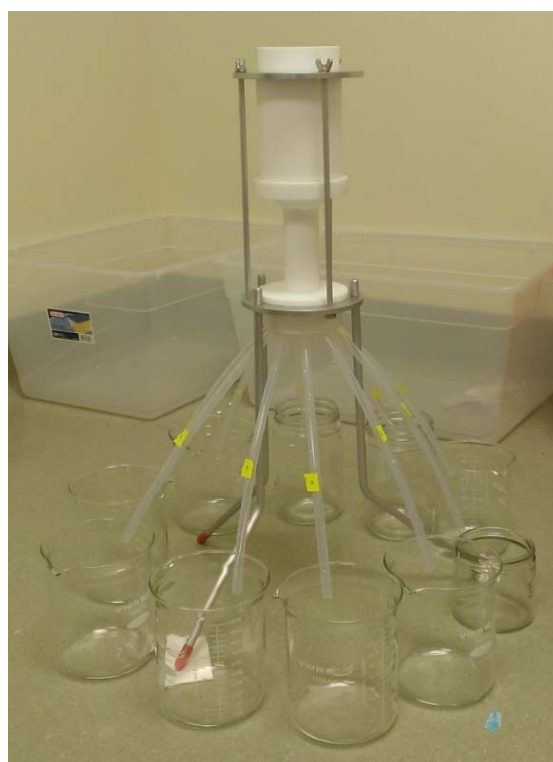


Figure 4-7: Dekaport splitter.

but were additionally cleaned in our lab by successively rinsing with hexane, acetonitrile and MilliQ water. After splitting, 3 of the 7 amber glass bottles were preserved at 4 °C as bulk

⁴ In the case of samples C1W, O2W, A1W and A2W of storm 2, 20 1-L bottles were generated.

subsamples and the other 4 were each filtered with 63 or 20 μm sieves and 2.7 or 0.7 μm glass fiber membrane filters (90 mm diameter) by a vacuum filtration system (Figure 4-8) and then stored at 4 $^{\circ}\text{C}$ until extraction. The particle size fractionation of stormwater runoff utilized in this study was a novelty that allowed us to link stormwater discharges with receiving water effects.

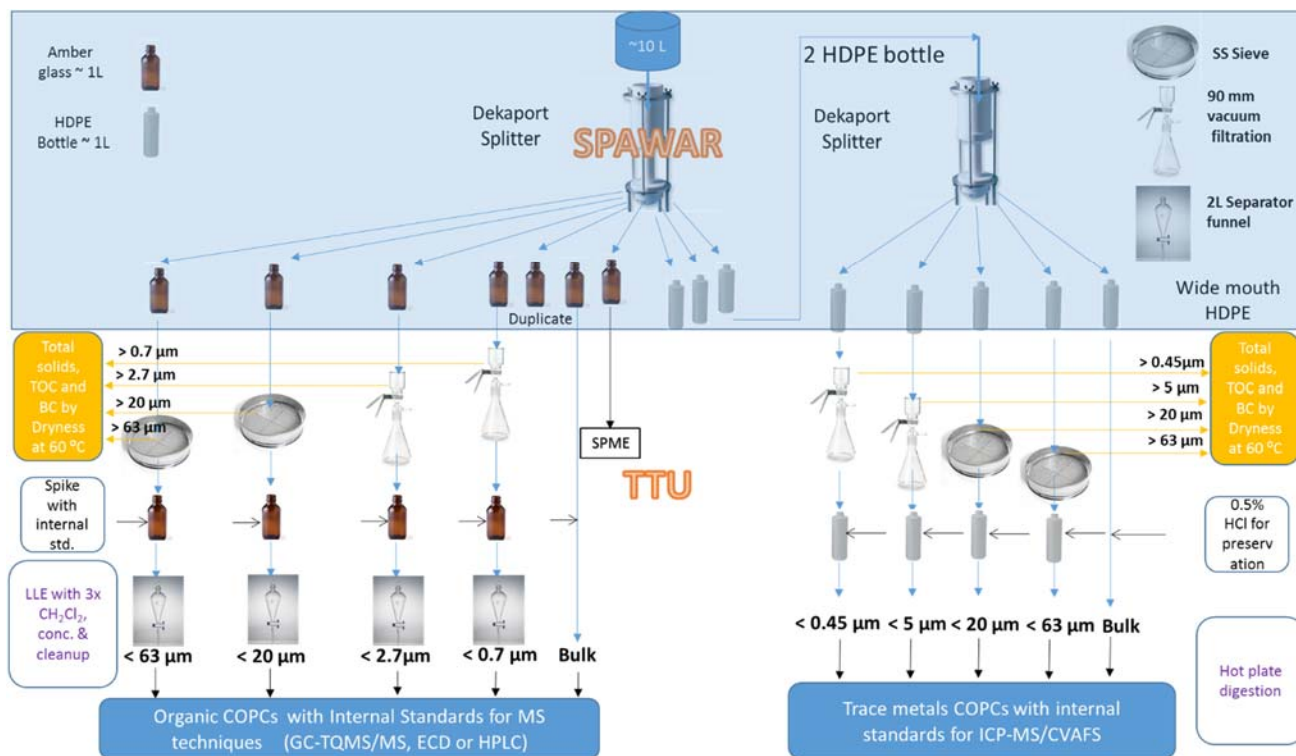


Figure 4-8: Schematic of the stormwater particle size fractionation methodology used in this study.

The mass of solids retained by the sieves and filters was measured in order to be able to calculate solids concentrations in each of the fractions. The filters used with the vacuum filtration system were pre-weighed to 1/100 of 1 mg before use. After filtering the samples, the filters were dried at 60 $^{\circ}\text{C}$ for 24 h and weighed again. Solids collected on the sieves were mobilized by spraying MilliQ water with a squirt-bottle and were transferred on pre-weighed 45 mm diameter glass fiber filters. Filters were dried at 60 $^{\circ}\text{C}$ for 24 h and weighed. Mass of collected solids in both cases was calculated as the difference between the two masses. The limited amount of solids collected on the sieves resulted in singular TOC measurements in storm

1 at 63 μm and duplicate measurements in storm 1 at 20 μm and storm 2 at 20 and 63 μm . Filter solids TOC measurements were in triplicates for storm 1 and 6 replicates for storm 2. Low flow runoff conditions during storm 2 led to high contribution of saline water in tidally influenced sampling locations, with high amounts of salts deposited on the fine particle filters when drying for solids weight estimation. This hindered the estimation of solids concentrations in those samples which were not used.

Dissolved organic carbon (DOC) analysis was performed in one of the bulk 1-L samples for each location. After filtering 30 mL of sample with a 0.7 μm glass fiber membrane, the filtrate was treated with 1 M hydrochloric acid (HCl) to remove inorganic carbon (carbonates) before analysis. The sample was then analyzed by the VarioCUBE TOC instrument with the combustion furnace set at 850 $^{\circ}\text{C}$. The instrument measures the carbon dioxide produced from the combustion of DOC and provides an aqueous DOC concentration.

The 4 filtrate fractions plus 1 of the bulk subsamples were liquid-liquid extracted in order to extract the PAHs. The process utilized 2-L separatory funnels (Figure 4-9) that were cleaned sequentially with soap, MilliQ water, acetone and dichloromethane before each use. The extraction method was based on EPA Method 3510c and entailed an initial spiking of the sample with 50 μL of a 1mg L^{-1} deuterated PAH solution in acetonitrile in order to monitor compound recoveries. The extraction itself was achieved adding 80 mL of dichloromethane in the funnel and vigorously shaking for 1 minute. After allowing the phases to separate for 10-60 minutes, dichloromethane was removed into a proprietary 500 mL flask and the above steps were repeated 2 more times. Due to initial sample volume limitations, each fraction led to a singular extract, there was no opportunity for triplicate extraction and analysis. The duplicate samples C1W,

O2W, A1W and A2W from storm 2 were extracted separately but the final extracts were combined to increase detection limits.

The solvent extracted fractions (approx. 240 mL) were then concentrated using Genevac Rocket™ rotary evaporator to 1 mL under 190 mbar pressure and 1700 rpm for 10-15 mins. The extracts were transferred to 2 mL amber HPLC autosampler vials using Pasteur pipettes and stored at -20 °C. Samples designated for HPLC analysis were exchanged to acetonitrile, whereas samples designated for GC-MS/MS analysis were exchanged to hexane.



Figure 4-9: 2-L separatory funnel setup.

Calculation of the final volume of the sample V_f transferred into the 2 mL vial was done by measuring the mass of the vial (plus a 300 μ L insert in the case of method blanks) before (m_i) and after (m_f) transferring the sample into it and using the density of ACN at 20 °C ($d_{ACN}=0.786$ g cm^{-3}) in the following equation:

$$V_f = \frac{m_f - m_i}{d_{ACN}} \quad (\text{Eq. 1})$$

4.2.3.2 Sediment

Total organic carbon (TOC) and black carbon (BC) analysis was performed on every sediment and settling trap sample in triplicates. Dried (at 60 °C overnight) sediment (10-40 mg) was weighed to the 1/100 of 1 mg and added in a small Ag boat. Samples designated for BC analysis received an extra step of treatment that involved oxidation at 375 °C for 24 h in a muffle furnace to remove volatile organic carbon (VOC) so that only BC remains (Gustafsson et al., 1997). The samples were then acidified with 100 µL of 1 M hydrochloric acid (HCl) for 1 h to remove inorganic carbon (mainly carbonates). The samples were finally burned at 950 °C inside the furnace of the VarioCUBE TOC instrument and the produced carbon dioxide (CO₂) was measured by an inline detector. The software of the instrument calculates a % TOC (m/m) value of the initial sample based on CO₂ produced and initial mass of the sample. Since we can only get % TOC and % BC values for the same sample, we can calculate % OC from the difference.

Extraction of PAHs from sediment core and settling trap material was realized by pressurized liquid extraction in triplicates using ASE 350 (Figure 4-10). Sediment was dried at 60 °C overnight and aliquots of 0.5-1.5 g were weighed and mixed with DE. Stainless steel ASE cells (34 mL) were packed as follows; a cellulose filter was placed at the bottom followed by 7.5 g silica gel (activated according to EPA Method 3630c), 5 g copper powder (purified

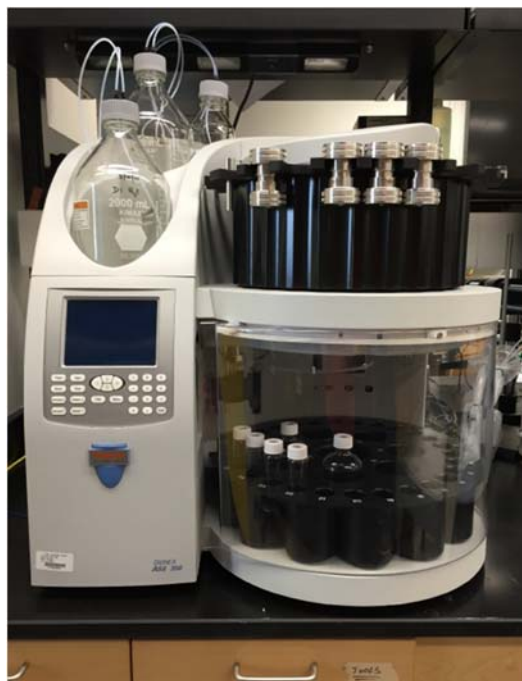


Figure 4-10: Pressurized liquid extraction of sediment samples was performed by the Dionex ASE 350 instrument.

according to EPA Method 3660b), the sample/DE mix and any dead volume was filled with DE. Extraction was performed with the following conditions; DCM-Hex (4:1 v/v), 2 static cycles of 5 minutes, 100 °C, 100 s purge time and 10% rinse volume. Static pressure, as set by the instrument, was 1700 psi. The extracts were collected in 60mL amber vials and concentrated (with Rocket evaporator at 1700 rpm with 190 mbar vacuum for about 11mins) to approximately 1 mL.

Samples that required purification were passed through a 50 mL chromatographic column (Figure 4-11) with a small amount of pre-cleaned glass wool at the bottom and loaded with 5 g of alumina (activated according to EPA Method 3610b) and 1 g of anhydrous sodium sulfate. All samples were finally exchanged to acetonitrile, concentrated to 1mL and transferred into 2 mL vials for HPLC

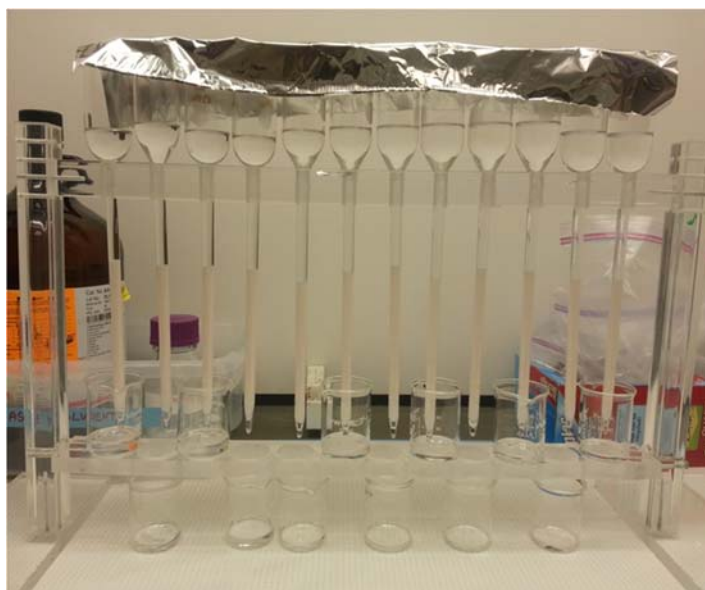


Figure 4-11: Sample cleanup setup with 50 mL chromatographic columns loaded with alumina and sodium sulphate.

analysis. All analyses were performed in triplicates. Calculation of the final volume of the sample in the 2 mL vials was done as in the case of Eq. 1.

Background contamination of the solvents, sorbents and consumables as well as carryover contamination of the instrument, was assessed by method blanks (MBs), a set of 3 ASE cells that were prepared in the same way as the rest of the samples. The difference in volume was filled with DE and these cells were run at the start of every sequence. Potential

losses from this method were evaluated by a set of 3 cells that were prepared as the MBs but were spiked with 50 μ L of a 1 mg L⁻¹ mix of EPAs 16 priority PAHs in acetonitrile on the top of the cell prior to extraction and run with every sequence. Quality control samples were extracted using the same method as the samples.

4.2.4 Chemicals, materials and instruments

The solvents used were hexane (Hex), dichloromethane (DCM), acetone (Ace) and acetonitrile (ACN) and were HPLC-grade from ThermoFisher Scientific (Phillipsburg, NJ, USA). Aluminum oxide (alumina) was purchased from Acros Organics (Phillipsburg, NJ, USA). Sodium sulfate and silica gel were purchased from VWR (Radnor, PA, USA) and diatomaceous earth (DE) from ThermoFisher Scientific (Phillipsburg, NJ, USA). Research grade PAH-16 (Naphthalene, Fluorene, Acenaphthylene, Acenaphthene, Phenanthrene, Anthracene, Fluoranthene (FLA), Pyrene (PYR), Chrysene (CHR), Benzo(a)anthracene (BaA), Benzo(b)fluoranthene (BbF), Benzo(k)fluoranthene (BkF), Benzo(a)pyrene (BaP), Dibenz(a,h)anthracene, Benzo(g,h,i)perylene, Indeno(1,2,3-cd)pyrene) standards at a concentration of 100 mg L⁻¹ and deuterated PAH (fluoranthene-d10, chrysene-d12, benzo[b]fluoranthene-d12, dibenzo[a,h]anthracene-d14) used as surrogate standards were purchased from Ultra Scientific (N. Kingstown, RI, USA). Research grade deuterated compounds (d-acenaphthene, d-phenanthrene and d-perylene) used as internal standards for gas chromatography triple quadrupole mass spectrometry (GC-TQMS) analysis were also purchased from Ultra Scientific. Ultrapure MilliQ water was supplied by a GenPure Pro UV purification system (ThermoFisher Scientific, Phillipsburg, NJ, USA)

Sediment extractions were performed with a Dionex ASE 350™ pressurized liquid extraction system and evaporations with a Rocket™ Evaporator, both from ThermoFisher Scientific (Phillipsburg, NJ, USA). Analysis of the extracts was done on an Agilent 1260 Infinity high performance liquid chromatography (HPLC) system and on an Agilent 7890B GC-TQMS, both from Agilent Technologies (Santa Clara, CA, USA).

4.2.5 Analysis

4.2.5.1 HPLC

Separation of analytes on the HPLC was carried out by a Phenomenex (Torrance, CA, USA) Luna 5µm C18 column (250 x 4.6 mm) set to 40 °C. Operation was under isocratic conditions with 1 mL min⁻¹ flow rate of 70% acetonitrile and 30% water (v:v). For optimal sensitivity, the FLD detector was used with the Method Detection Limit (MDL) determined to be less than 0.5µg/L for all parent PAHs. This method was able to analyze 15 PAHs (acenaphthylene does not fluoresce) with Benzo[g,h,i]perylene and Indeno[1,2,3-cd]pyrene taken as a single concentration because complete separation was not possible. PAH quantitation was achieved by nine-point calibration from 0.5 µg L⁻¹ to 200 µg L⁻¹ (0.5, 1, 2, 5, 10, 20, 50, 100, 200 µg L⁻¹) for the following compounds; Naphthalene (NAP), Fluorene (FL), Acenaphthene (ACE), Phenanthrene (PHE), Anthracene (ANT), Fluoranthene (FLA), Pyrene (PYR), Chrysene (CHR), Benzo(a)anthracene (BaA), Benzo(b)fluoranthene (BbF), Benzo(k)fluoranthene (BkF), Benzo(a)pyrene (BaP), Dibenz(a,h)anthracene (DBA), Benzo(g,h,i)perylene (BghiP)+Indeno(1,2,3-cd)pyrene (InP). Correlation coefficients were consistently greater than 0.9980.

4.2.5.2 GC-TQMS

The method used for the separation of PAHs on the GC/TQMS was based on EPA Method 8270 and has the following parameters: 60 m DB-5MS column (60 m × 0.25 mm × 0.25 μm; Agilent, USA), splitless mode, inlet temperature at 280 °C, injection volume 1 μL, flow of helium at 1.2 mL min⁻¹ and 54.5 min runtime. The mass spectrometer was set at SIM/SIM in electron ionization mode with at least two parent-product ion transitions monitored for quantitation/confirmation and the calibration ranged from 0.2 to 20 μg L⁻¹ with seven points.

4.2.6 Calculations and statistical analyses

The results are reported as contaminant (solids or PAHs) mass per runoff volume in a specific particle size fraction or contaminant (PAHs) mass per mass of solids in that specific particle size fraction.

4.2.6.1 Stormwater solids concentration for each particle size fraction

$$TFS_{0.7-2.7 \mu m} \left(\frac{mg}{L} \right) = TFS_{>0.7 \mu m} \left(\frac{mg}{L} \right) - C_{>2.7 \mu m} \left(\frac{mg}{L} \right)$$

$$TFS_{2.7-20 \mu m} \left(\frac{mg}{L} \right) = TFS_{>2.7 \mu m} \left(\frac{mg}{L} \right) - C_{>20 \mu m} \left(\frac{mg}{L} \right)$$

$$TFS_{20-63 \mu m} \left(\frac{mg}{L} \right) = TFS_{>20 \mu m} \left(\frac{mg}{L} \right) - C_{>63 \mu m} \left(\frac{mg}{L} \right)$$

“TFS” represents the total fraction solids (in mass per volume of processed water) as captured on the filter or sieve for the size fraction represented in the subscript.

4.2.6.2 Stormwater PAH concentration in water for each particle size fraction

$$C_{0.7-2.7 \mu\text{m}} \left(\frac{\text{ng}}{\text{L}} \right) = C_{<2.7 \mu\text{m}} \left(\frac{\text{ng}}{\text{L}} \right) - C_{<0.7 \mu\text{m}} \left(\frac{\text{ng}}{\text{L}} \right)$$

$$C_{2.7-20 \mu\text{m}} \left(\frac{\text{ng}}{\text{L}} \right) = C_{<20 \mu\text{m}} \left(\frac{\text{ng}}{\text{L}} \right) - C_{<2.7 \mu\text{m}} \left(\frac{\text{ng}}{\text{L}} \right)$$

$$C_{20-63 \mu\text{m}} \left(\frac{\text{ng}}{\text{L}} \right) = C_{<63 \mu\text{m}} \left(\frac{\text{ng}}{\text{L}} \right) - C_{<20 \mu\text{m}} \left(\frac{\text{ng}}{\text{L}} \right)$$

$$C_{>63 \mu\text{m}} \left(\frac{\text{ng}}{\text{L}} \right) = C_{\text{bulk}} \left(\frac{\text{ng}}{\text{L}} \right) - C_{<63 \mu\text{m}} \left(\frac{\text{ng}}{\text{L}} \right)$$

“C” represents the PAH concentration of the bulk, filtered or sieved water with the representative size fraction in the subscript.

4.2.6.3 Stormwater PAH concentration on solids in water for each particle size fraction

$$C_{0.7-2.7 \mu\text{m}} \left(\frac{\mu\text{g}}{\text{kg}} \right) = \frac{C_{<2.7 \mu\text{m}} \left(\frac{\text{ng}}{\text{L}} \right) - C_{<0.7 \mu\text{m}} \left(\frac{\text{ng}}{\text{L}} \right)}{TFS_{>0.7 \mu\text{m}} \left(\frac{\text{mg}}{\text{L}} \right) - TFS_{>2.7 \mu\text{m}} \left(\frac{\text{mg}}{\text{L}} \right)} \times 1000 \frac{\text{mg}}{\text{g}}$$

$$C_{2.7-20 \mu\text{m}} \left(\frac{\mu\text{g}}{\text{kg}} \right) = \frac{C_{<20 \mu\text{m}} \left(\frac{\text{ng}}{\text{L}} \right) - C_{<2.7 \mu\text{m}} \left(\frac{\text{ng}}{\text{L}} \right)}{TFS_{>2.7 \mu\text{m}} \left(\frac{\text{mg}}{\text{L}} \right) - TFS_{>20 \mu\text{m}} \left(\frac{\text{mg}}{\text{L}} \right)} \times 1000 \frac{\text{mg}}{\text{g}}$$

$$C_{20-63 \mu\text{m}} \left(\frac{\mu\text{g}}{\text{kg}} \right) = \frac{C_{<63 \mu\text{m}} \left(\frac{\text{ng}}{\text{L}} \right) - C_{<20 \mu\text{m}} \left(\frac{\text{ng}}{\text{L}} \right)}{TFS_{>20 \mu\text{m}} \left(\frac{\text{mg}}{\text{L}} \right) - TFS_{>63 \mu\text{m}} \left(\frac{\text{mg}}{\text{L}} \right)} \times 1000 \frac{\text{mg}}{\text{g}}$$

$$C_{>63 \mu\text{m}} \left(\frac{\mu\text{g}}{\text{kg}} \right) = \frac{C_{\text{Bulk}} \left(\frac{\text{ng}}{\text{L}} \right) - C_{<63 \mu\text{m}} \left(\frac{\text{ng}}{\text{L}} \right)}{TFS_{>63 \mu\text{m}} \left(\frac{\text{mg}}{\text{L}} \right)} \times 1000 \frac{\text{mg}}{\text{g}}$$

Statistical mean comparison of triplicate experimental data was conducted by paired sample T-test and cross-checked by Wilcoxon signed ranks test. All values reported in this study are from the paired sample T-test.

4.2.7 PAH diagnostic ratios

The temperature dependent (Budzinski et al., 1998; Katsoyiannis et al., 2007) ratio of ANT to the sum of ANT and PHE ($\text{ANT}/(\text{ANT}+\text{PHE})$) can be an indication of PAH sources (petrogenic: <0.1 , pyrogenic: >0.1). ANT and PHE are structural isomers with different thermodynamic properties (Soclo et al., 2000).

The photosensitive ratio (Tobiszewski and Namieśnik, 2012) of BaP to the sum of BaP and BeP ($\text{BaP}/(\text{BaP}+\text{BeP})$) can be an indication of particle age (~ 0.5 : “fresh” particles, <0.5 : aged particles). BaP is the isomer that photodegrades more rapidly and can thus a lower ratio can be an indication of prolonged exposure to sunlight.

Lastly, the ratio between the sum of 3-ring PAHs (ANT and PHE) and the sum of 6-ring PAHs (BghiP and InP) ($(\text{ANT}+\text{PHE})/(\text{BghiP}+\text{InP})$) is a novel ratio that can be an indication of direct atmospheric deposition of vehicle exhaust particles. It is inspired by the work of McVeety and Hites, 1988 on the atmospheric deposition of PAH-laden particles in a remote lake. They concluded that 80% of PHE and ANT on these pyrogenic exhaust particles is lost by volatilization while no loss was detected on heavier PAHs. This ratio is a more robust way to look at petrogenic and pyrogenic sources because it includes pyrogenic PAHs in both sides of the fraction. There are no specific ranges that signify the origin of the PAHs but the ratio can be used when comparing samples from different locations as we will see later.

4.3 Results and Discussion

4.3.1 Relative runoff contributions

Storm runoff makes its way to the San Diego bay by the Paleta creek (C1W) and outfalls O1W and O2W. The relative contributions of solids and PAHs from those 3 locations during storm 1, indicate that the creek itself is responsible for 97.3% of total solids mass and 98.3% of total PAH mass (Figure 4-12). Based on this observation, we will focus our runoff results on sampling location C1W as measured by composite (C1W) and ambient grab time series (A1W, A2W and A3W) water samples. It should be noted that a similar calculation could not be made

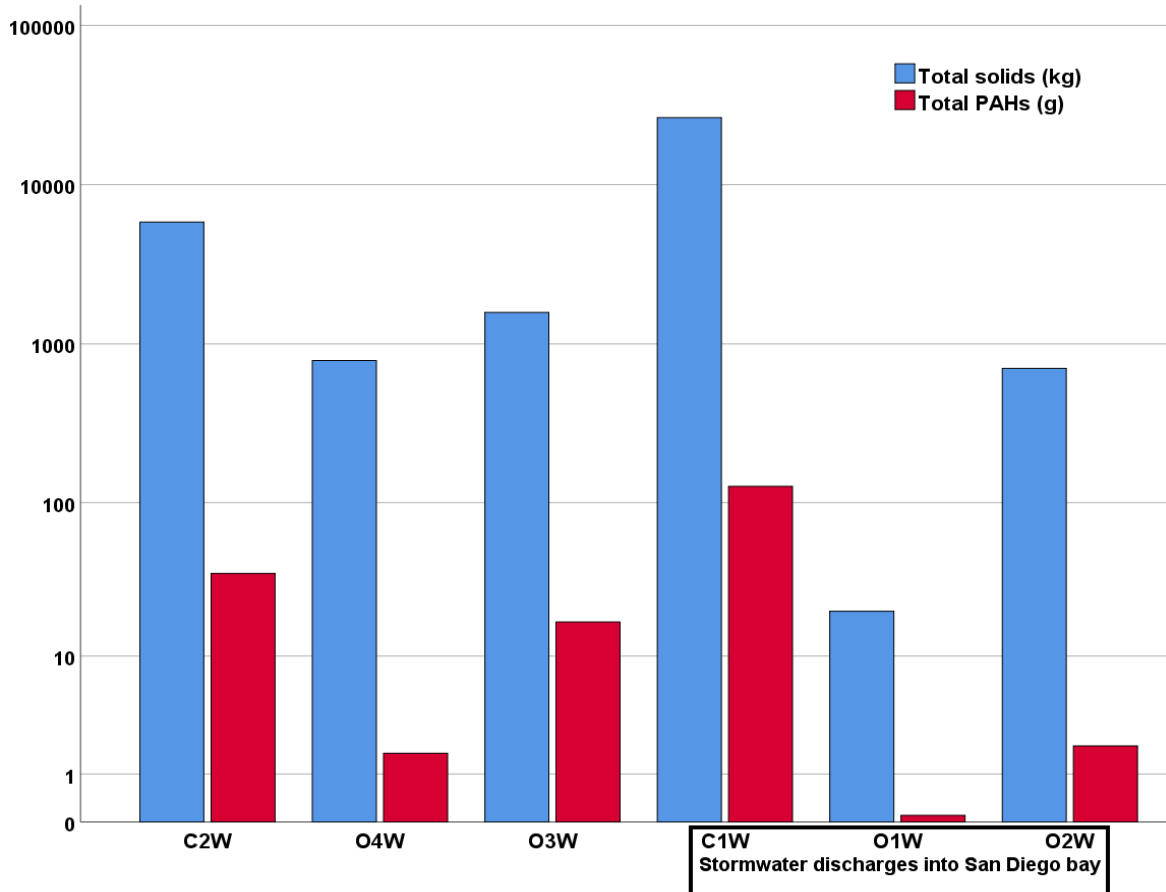


Figure 4-12: Total solids and PAH mass transported by runoff during storm 1. (Y-axis is log).

for storm 2 due to inaccurate flow measurements in C1W that led to significantly overestimating the total volume of discharging runoff (121,000 m³ in storm 2 vs 98,000 m³ in storm 1).

4.3.2 Stormwater runoff

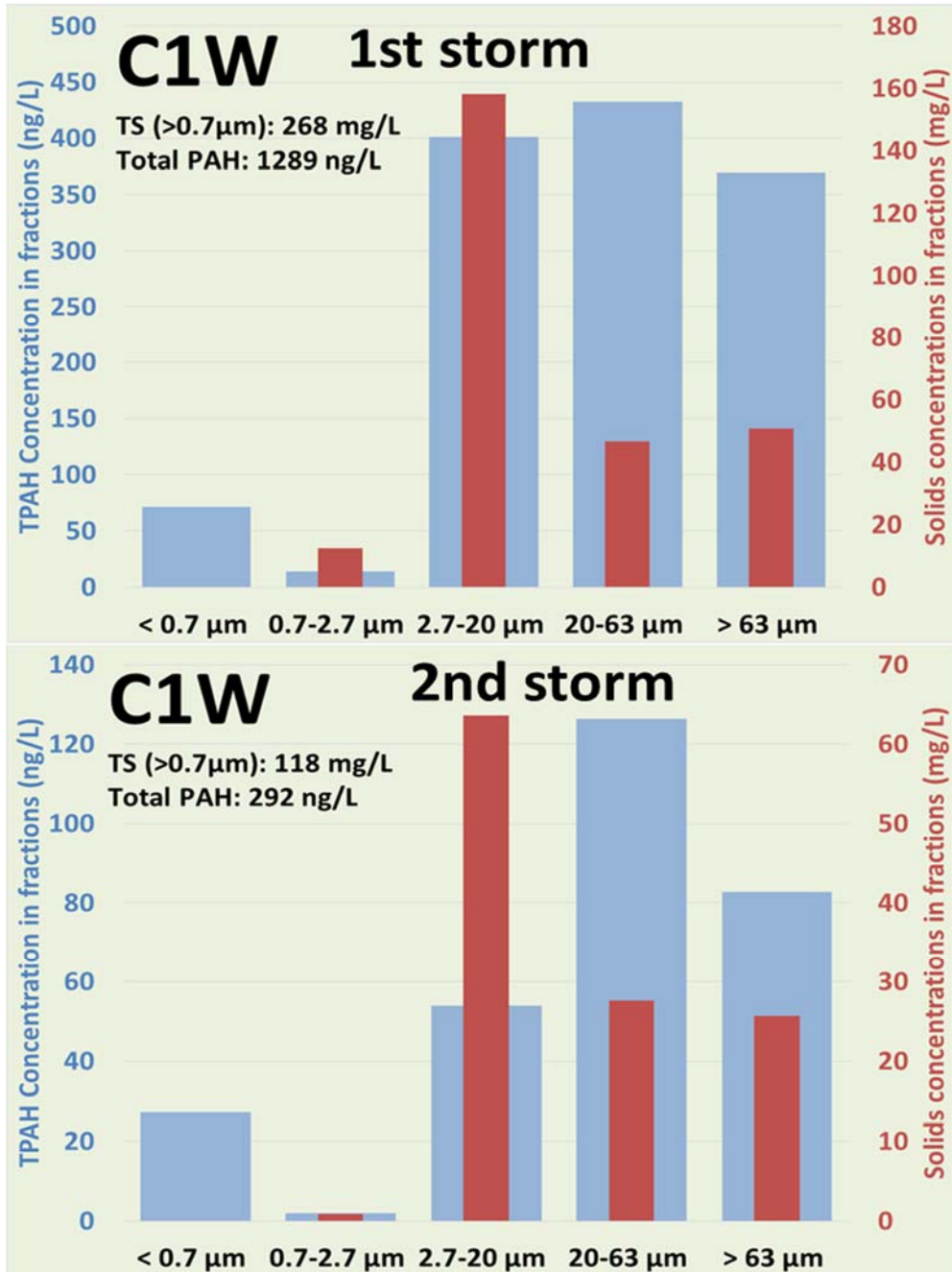


Figure 4-13: Total solids and total PAHs concentrations in different solid fractions of runoff during the two storms that were sampled in Paleta creek.

4.3.2.1 *Runoff particle size and organic carbon content*

The composite stormwater runoff of Paleta creek discharging into the San Diego bay (C1W) appears to have similar characteristics in both storms. The distribution of solids in both storm events (Figure 4-13, red bars) is dominated by fine/medium silt (2.7-20 μm), 59% (158 mg L⁻¹) in storm 1 and 54% (63.6 mg L⁻¹) in storm 2, with coarse silt (20-63 μm) and sand (>63 μm) having very similar concentrations; 46.6 mg L⁻¹ and 50.7 mg L⁻¹ in storm 1 and 27.6 mg L⁻¹ and 25.6 mg L⁻¹ in storm 2. There is a significant difference in the total amount of stormwater solids

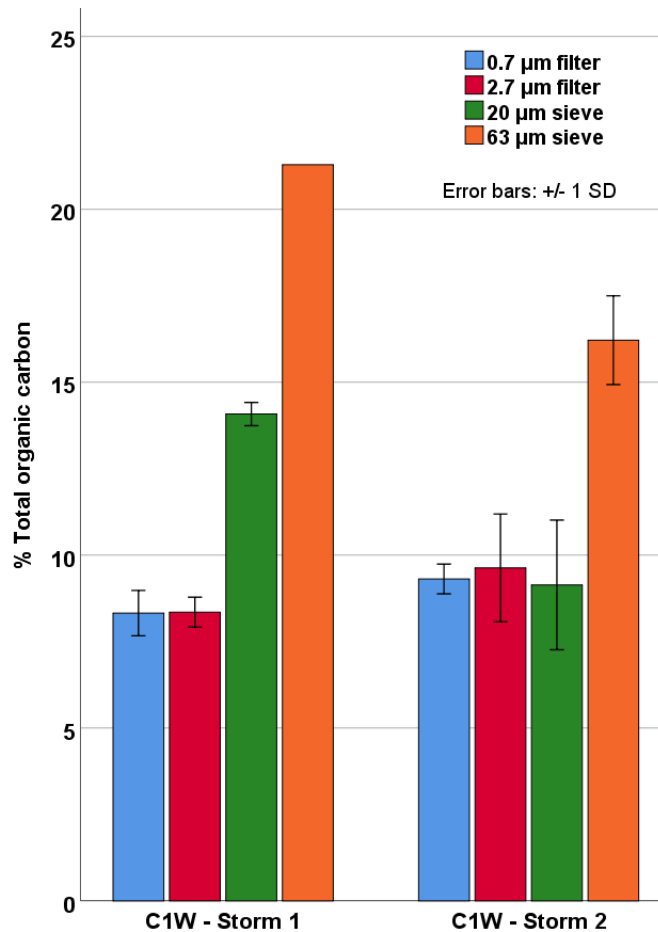


Figure 4-14: Total organic carbon content of solids deposited on filters/sieves of composite runoff collected at the mouth of Paleta creek during both storms.

(268 mg L⁻¹ in storm 1 vs 118 mg L⁻¹ in storm 2) and total rainfall (1.87in. in storm 1 vs 0.16in. in storm 2).

Total organic carbon (TOC) analysis of the above solids during both storms (Figure 4-14) reveals elevated content of organic carbon in coarser solids. Sand-size particles (>63µm) have the highest TOC content (storm 1 – 21%⁵, storm 2 – 16%⁶), coarse silt has elevated TOC only in storm 1 (14%⁴) while the remaining fractions have 8-10%⁷. We tend to think of organic carbon (and HOCs) as often being associated with fine solids but this was not the case in the stormwater solids. Analysis of the runoff solids, collected on the sieves and filters, by scanning electron microscopy (SEM) and energy-dispersive X-ray spectroscopy (EDS) shown in Figure 4-15, revealed the presence of large “carbon-rich” particles. Many of these particles appear to be originating from road debris (chipped gravel coated with asphalt) that has been eroded from the highway tarmac and was suspended and transported by the runoff. There were also particles resembling pieces of tire (rubber) that could also be originating from the highway or the paved portion of the upstream watershed.

⁵ Single measurement as there was not enough material for triplicate analysis.

⁶ Average of 2 measurements.

⁷ Values are averages of triplicate measurements except 20µm of storm 2 which is average of 2 measurements and 0.7 and 2.7 µm of storm 2 which are averages of 6 measurements.

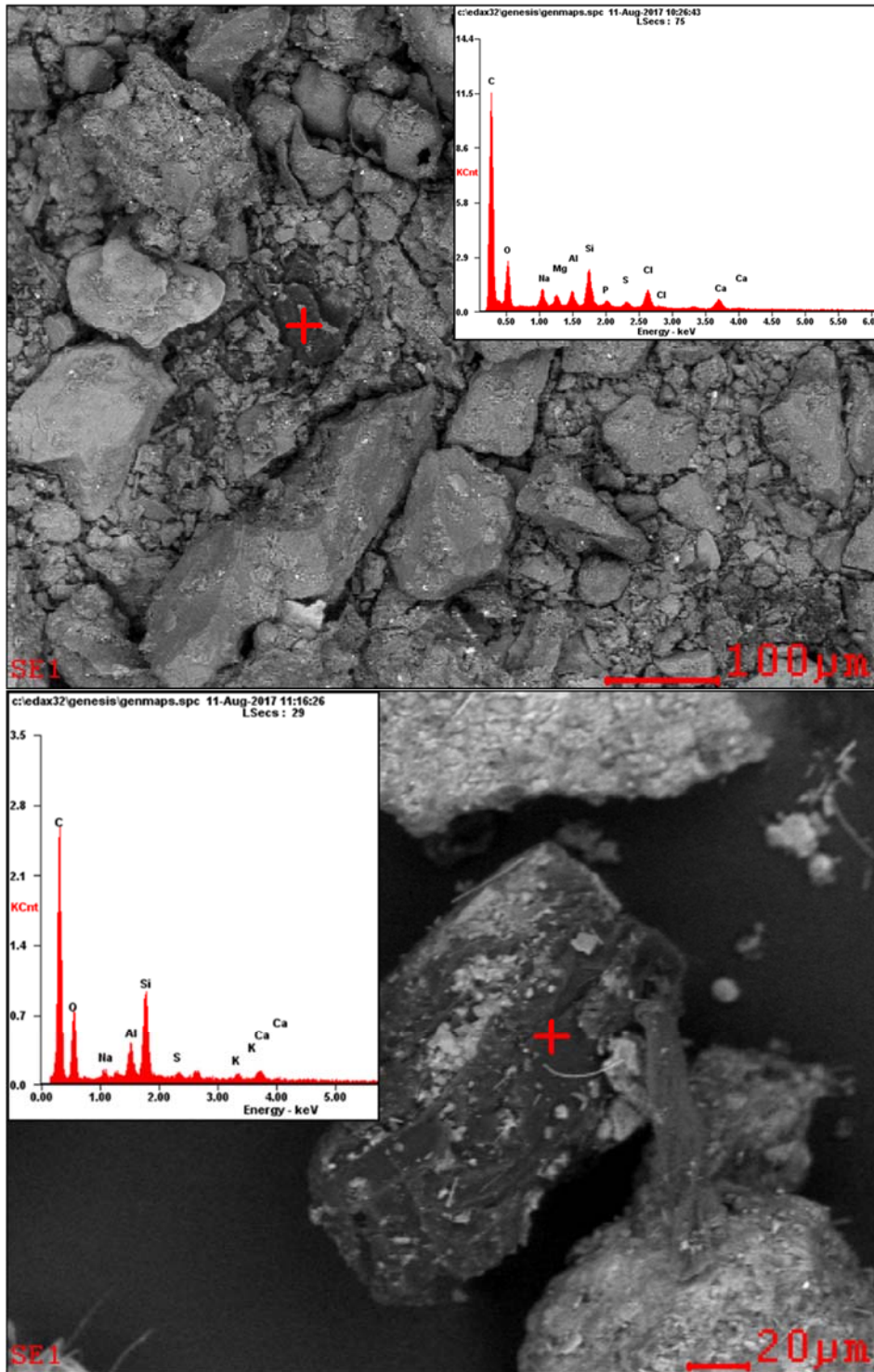


Figure 4-15: SEM pictures and EDS spectra of runoff particles collected at the mouth of Paleta creek during storm 1.

4.3.2.2 *Runoff PAHs*

There are also similarities between the two storms in the distribution of PAHs in the solids fractions (Figure 4-13, blue bars) as it appears that most of the Σ PAH mass burden is carried by larger particles. Around 66% and 75% of PAH mass during storm 1 and 2 respectively, are associated with coarse silt and sand particles ($>20\mu\text{m}$).

A look into 3 PAHs representing a wide range of hydrophobicities, reveals their different fractionation among the runoff solids (Figure 4-16). In storm 1, PHE and PYR are mainly associated with sand particles (72% and 47% respectively) with only 21% of BaP mass being carried by sand. Interestingly the mass ratio $m_{\text{sand}}/m_{\text{silt}}$ is decreasing from 2.6 in PHE to 0.92 in PYR to 0.27 in BaP. This trend indicates that as the size of PAHs increases, they associate more with finer particles that have no prior PAH load. It could also indicate that if sand-sized particles are sources of PAHs themselves, they have a more petrogenic origin as indicated by the higher abundance of lower molecular weight PAHs. Since we are examining mixed sources of particles, what we are witnessing is probably a combination of both.

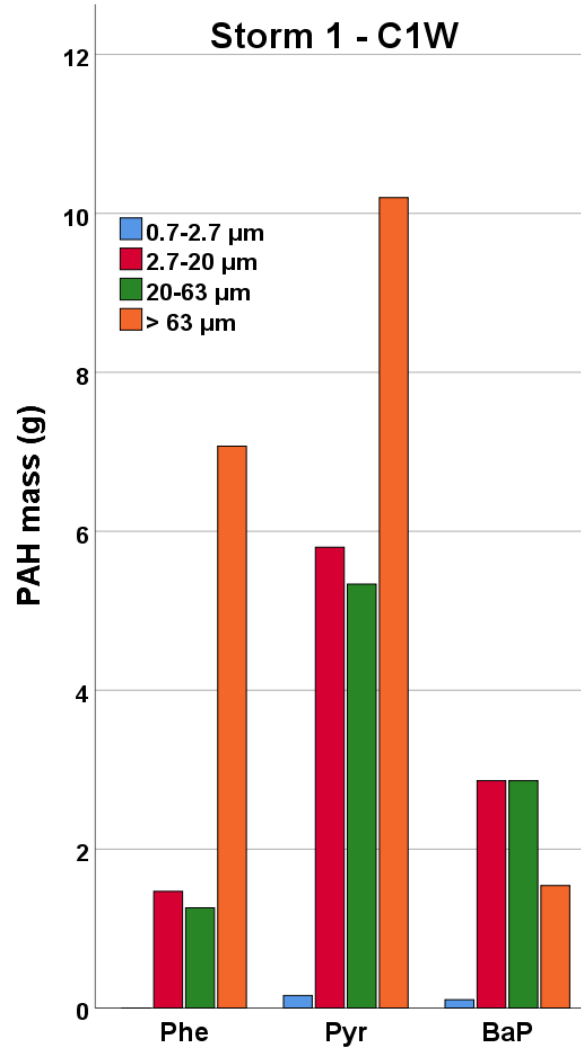


Figure 4-16: Storm 1 - Mass of PHE, PYR and BaP in different fractions of composite runoff solids at Paleta creek. All values are from single measurements.

The concentrations of the 3 PAHs on runoff solids in the different fractions range from 100 to 2000 $\mu\text{g kg}^{-1}$ (Figure A6). In general, storm 1 runoff appears to be carrying particles with significantly higher PAH concentrations compared to storm 2 runoff.

The PAH ratios of bulk solids in the composite runoff, were as follows. The ratio ANT/(ANT+PHE) of C1W discharge during storm 1 has a weak pyrogenic signature (0.13) while the upstream (C2W) sample during the same storm appears more petrogenic (0.07). Both upstream and discharge samples appear to be carrying more aged than fresh solids as their ratio of BaP/(BaP+BeP) was 0.45. Lastly, the ratio (ANT+PHE)/(BghiP+InP) was 1.19 in the case of storm 1 upstream runoff and 0.68 for the discharging runoff.

4.3.2.3 Time-series grab runoff

Ambient water grab samples (A1W-A3W) taken at different time points during the storms reveal that fine/medium silt (2.7-20 μm) is consistently the most represented fraction in storm 1 (Figure 4-17) and storm 2 (Figure A7). Coarser solids (>20 μm) are discharged almost entirely, early during storm 1 (A1W: 126 mg L^{-1} , A2W/A3W: 8 mg L^{-1}) and at much lower concentrations in storm 2 (A1W: 23 mg L^{-1} , A2W: 4 mg L^{-1}).

Total PAH concentrations have decreasing trend during storm 1 (A1W: 3598 ng L^{-1} , A2W: 337 ng L^{-1} and A3W: 184 ng L^{-1}) and storm 2 (A1W: 214 ng L^{-1} and A2W: 72.4 ng L^{-1}). The dominant fraction (where highest concentrations occur) shifts during storm 1 from sand (A1W) to fine/medium silt (A2W) to dissolved (A3W) and in storm 2 from sand (A1W) to dissolved (A2W). This shows that the larger particles are mobilized early in the storm, possibly with the initial runoff.

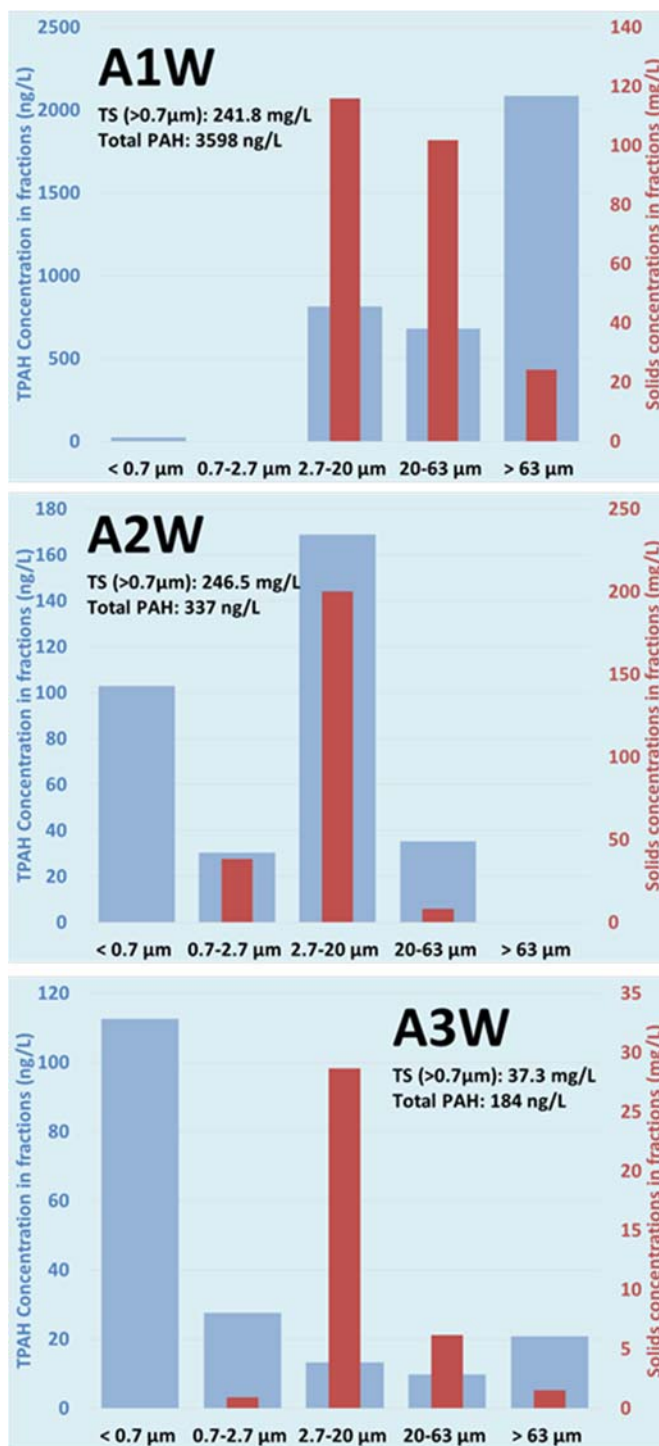


Figure 4-17: Storm 1 - Total solids and total PAH concentrations in different solid fractions of runoff grab samples at progressing time points at Paleta creek.

The earlier stages of the storm also carry particles with higher TOC content than later in the storm as shown by total organic carbon analysis of grab water solids (Figure 4-18). Initially

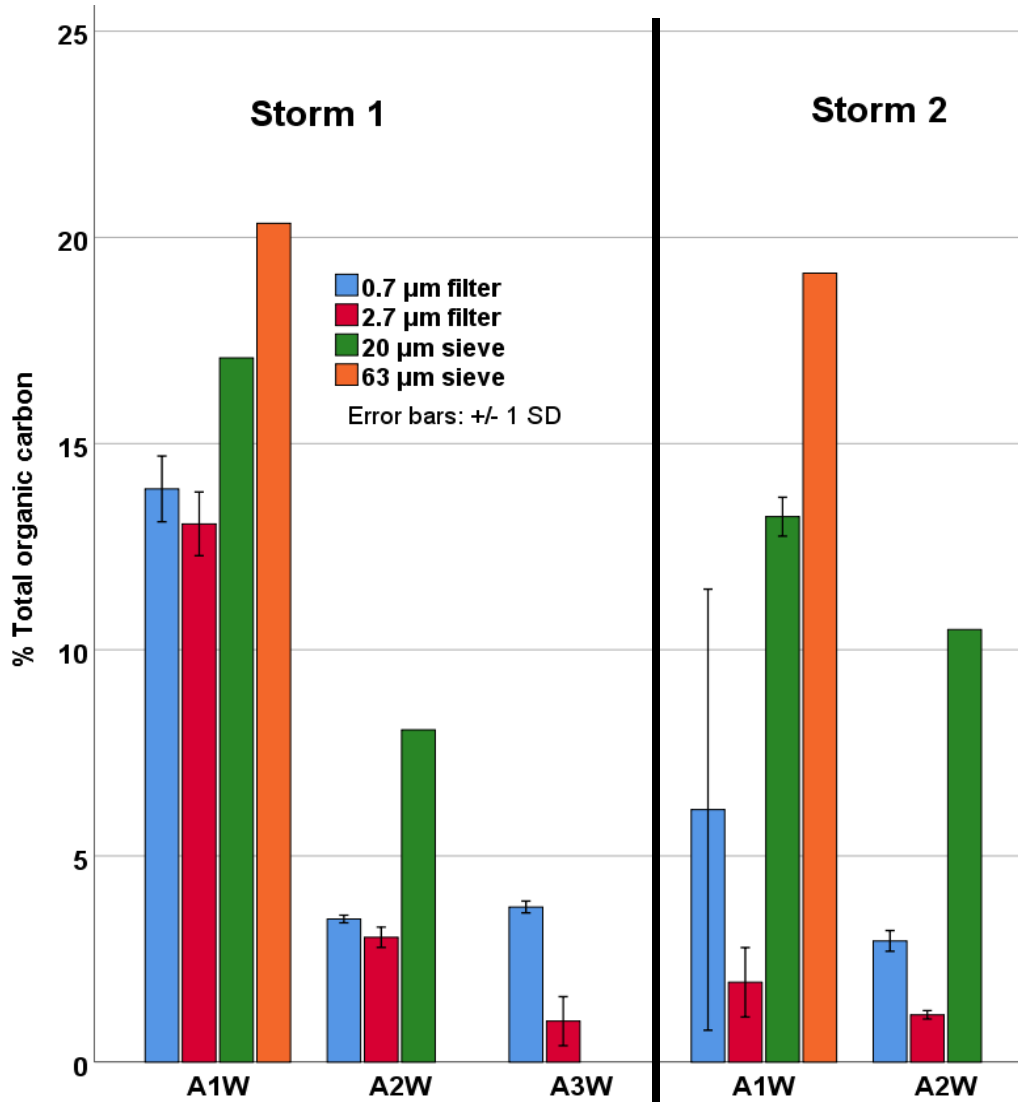


Figure 4-18: Total organic carbon content of ambient grab runoff solids deposited on filters/sieves at the mouth of Paleta creek during both storms.

in storm 1, the TOC content is on average around 15% (A1W) and later drops to less than 5% (A2W and A3W) while in storm 2 starts at around 10% (A1W) and drops to less than 5% (A2W). Coarser particles collected on the sieves (20 and 63 µm) have higher TOC content compared to solids collected on the filters (0.7 and 2.7 µm) with the sand particles always having the highest organic carbon mass in both storms. A rough average of solids TOC for A1W, A2W and A3W is on the same level (approx. 8%) as in the composite sample in the same location (C1W). The limited amount of solids collected on the filtration devices, resulted in no

measurement of TOC in storm 1 – A2W-63 μm , A3W-20/63 μm , storm 2 – A2W-63 μm ; singular TOC measurements in storm 1 – A1W-20/63 μm , A2 W-20 μm , storm 2 – A1W-63 μm , A2W-20 μm ; duplicate TOC measurements in storm 2 – A1W-20 μm . All 0.7/2.7 μm filter solids TOC measurements of storm 1 were in triplicates and of storm 2 in 6 replicates.

4.3.2.4 Stormwater runoff summary

It appears that the coarser particles ($>20 \mu\text{m}$) in the Paleta creek drainage basin carry the most ΣPAH mass, have higher TOC content than finer particles and are transported in the earlier phase of a storm. These results suggest that runoff's potential for contamination, should be spatially limited in the area close to the discharge point and should happen relatively soon after the runoff starts flowing. The great abundance of fine/medium silt particles in the watershed, is counterbalanced by low PAH concentrations and low settling velocity. When carried by runoff, that will probably lead to a widespread dilution of their PAH load and should not have strong contaminating impact in the receiving waters.

Most of the PAH mass in the coarse particles is made up of the lighter and less hydrophobic PAHs, as represented by PHE and PYR, that contribute to a less pyrogenic (more petrogenic) runoff signature in the near field. In contrast, heavier PAHs (represented by BaP) are relatively more abundant in the finer particles and should lead to a more pyrogenic signature further out in the bay.

Runoff solids originate from both pyrogenic and petrogenic sources and they appear to have been exposed to sunlight for prolonged periods of time. The major highway traversing the watershed could have a significant contribution of material to runoff. As our SEM images showed, eroded road debris, tire chips, leaked fuel and motor oil as well as exhaust particles, all

sunbathing on the surface of the tarmac, are washed away by the runoff and are being deposited in the San Diego bay.

More generally, solids and PAH distributions in the runoff, remain similar in both storms indicating that a watershed could have a distinct runoff profile indifferent to varying amounts of rainfall; a sort of signature that represents the type of activities taking place in the drainage basin.

4.3.3 Sediment

The primary mode of contamination caused by stormwater runoff is expected to be the settling of transported particles. A simple model that describes one-dimensional deposition of particles with distance from a point source at steady state, is shown in Figure 4-19. The system consists of a w -width channel on the y -axis, with advection on the x -axis, and settling on the z -axis. The mass balance for a differential element of this system is:

$$\begin{aligned}
 QC|x - QC|(x + \Delta x) - v_s Cw\Delta x &= 0 \Rightarrow \\
 \Rightarrow Q(C_x - C_{x+\Delta x}) &= v_s Cw\Delta x \Rightarrow \\
 \Rightarrow \frac{Q}{w} \frac{C_{x+\Delta x} - C_x}{\Delta x} &= -v_s C \xrightarrow{\text{limit } \Delta x \rightarrow 0} \\
 \xrightarrow{\text{limit } \Delta x \rightarrow 0} \frac{dC}{dx} &= -\frac{wv_s}{Q} C \Rightarrow \\
 \Rightarrow C = C_0 e^{-\frac{wv_s}{Q}x} & \quad \text{Eq. 2}
 \end{aligned}$$

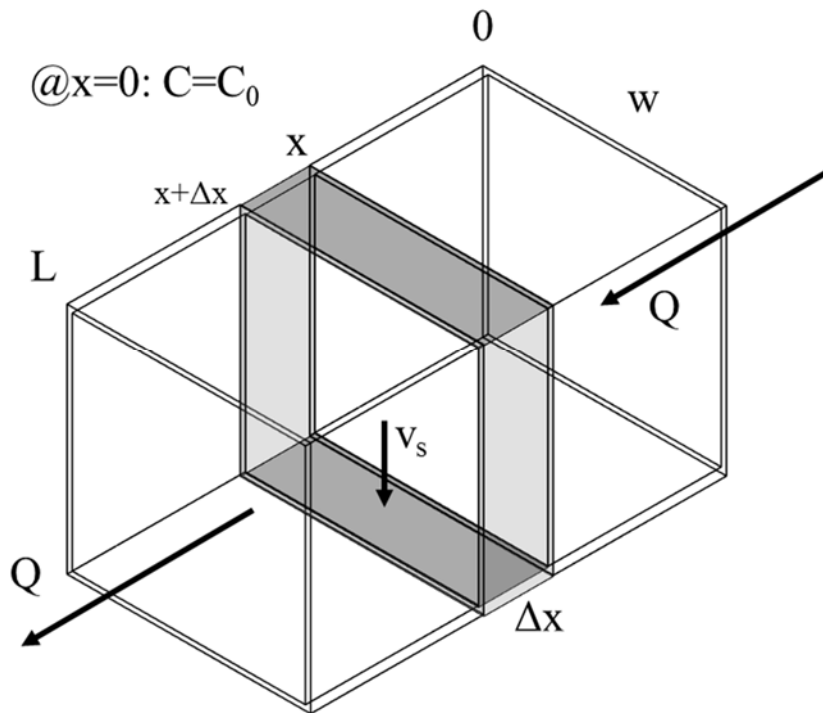


Figure 4-19: One-dimensional model describing deposition of particles transported by storm runoff

The model predicts highest reduction of solids concentration due to settling closest to the discharge point. In other words, most of the solids are expected to settle near the mouth of the creek. The above observation should be especially true in the case of larger particles that are characterized by higher settling velocities.

4.3.3.1 Settling material deposition profile, particle size and deposited PAH mass

The mass of the material collected by the settling traps during both deployments (Figure 4-20), has a “U” pattern (represented by the double line) in the case of season 2015-2016. This shape is counter intuitive as runoff contribution alone should have followed a continuous decreasing trend (solid line) with increasing distance from the discharge point, as predicted by the 1-dimensional deposition model described above. This leads to the conclusion that there is an

undefined amount of sources that are disproportionately contributing depositing material with increasing distance from the mouth of the creek (dashed line).

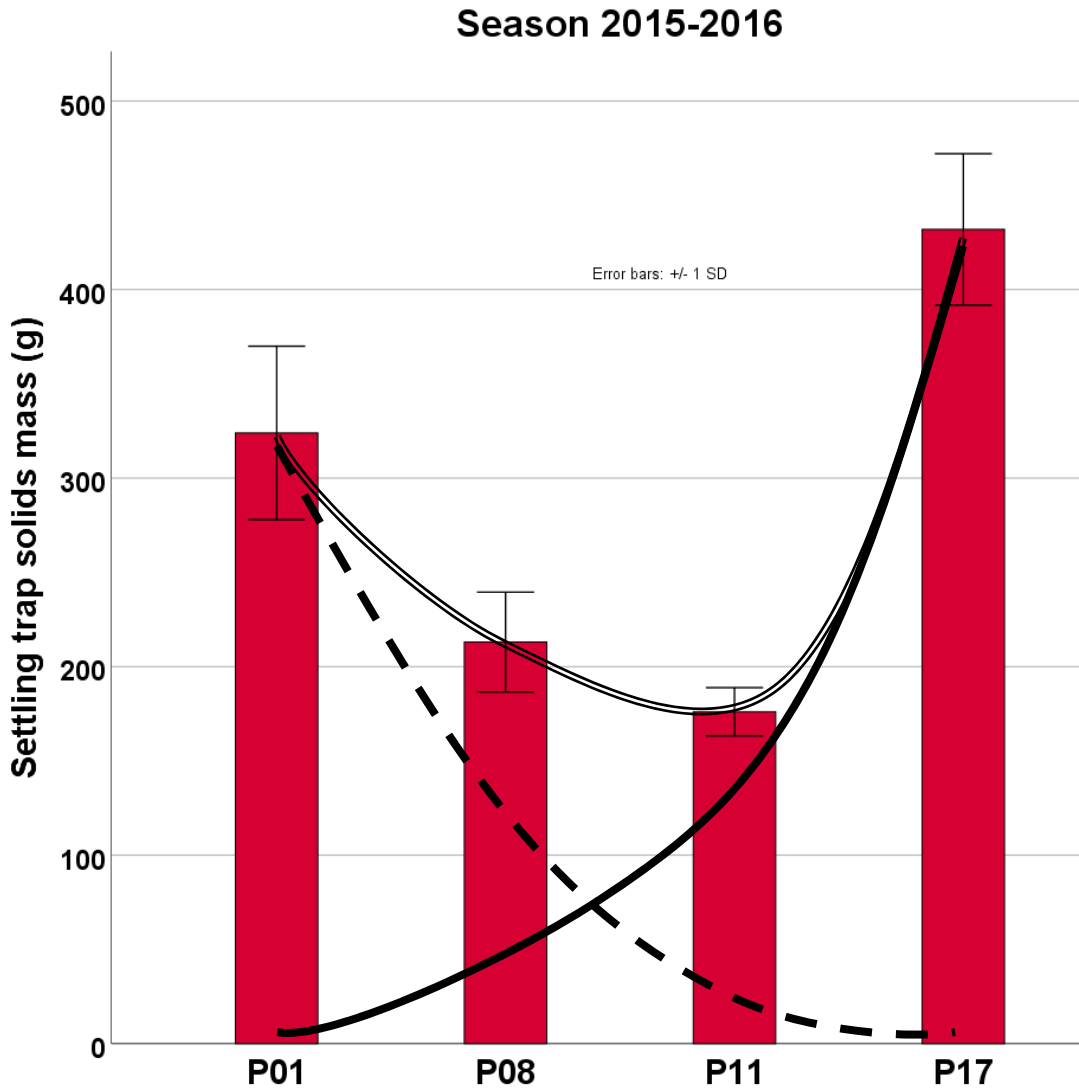


Figure 4-20: Mass of settling particles collected by the deployed traps during season 2015-2016. The solid line represents the anticipated runoff contribution, the dashed line represents an imaginary second source and the double line represents the measured sum of the two sources.

The size fractions of the solids collected in the traps (Figure 4-21), reveal that location P17 has greater abundance of sand particles than the other locations in both deployments. Coarse silt is also overrepresented in P17 in season 2015-2016. On the other hand, more fine/medium silt

was collected in location P01 in the 2015-2016 traps. During the short deployment (28 d) of the July 2015 traps, only 1 storm (approx. 1.5 in. of total rain) took place and we can assume that the collected solids were mainly deposited by that storm. This could also lead to the assumption that the “exaggerated” $>20 \mu\text{m}$ signature in P17 of the season 2015-2016 traps could be heavily attributed to the high magnitude of storm 1.

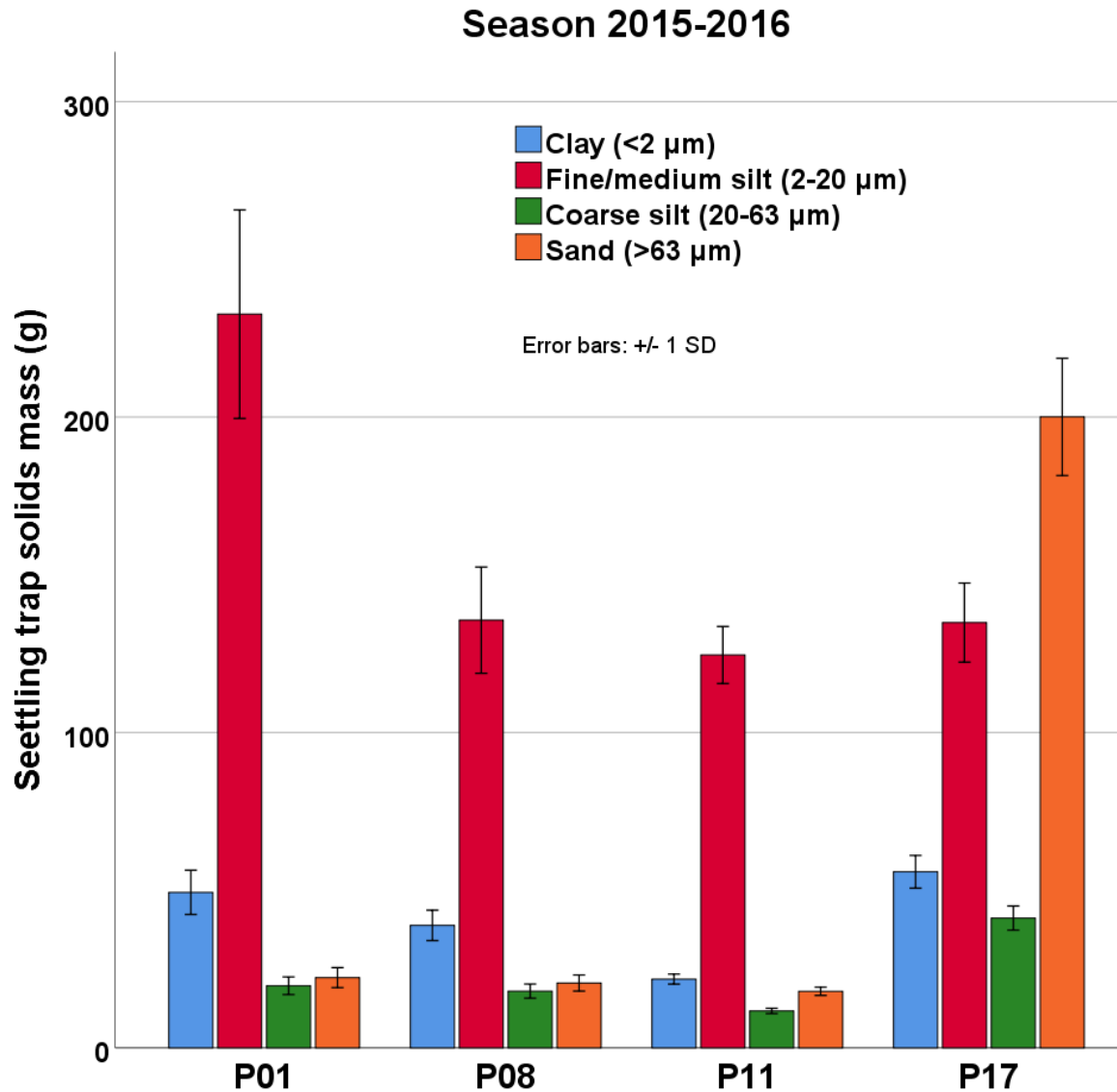


Figure 4-21: Particle size distribution of the solids collected in the settling traps during deployment in season 2015-2016.

The ΣPAH mass collected in the traps is 2-3 times higher in location P17 compared to the outer locations (Figure A8) and exhibits a U-shaped distribution but much less pronounced than the solids. Looking at the 3 individual PAHs (Figure 4-22), we see PHE and PYR mainly depositing at P17 while BaP has much less variation between all locations. Locations P01, P08 and P11 have very similar masses as well as distributions of the 3 PAHs.

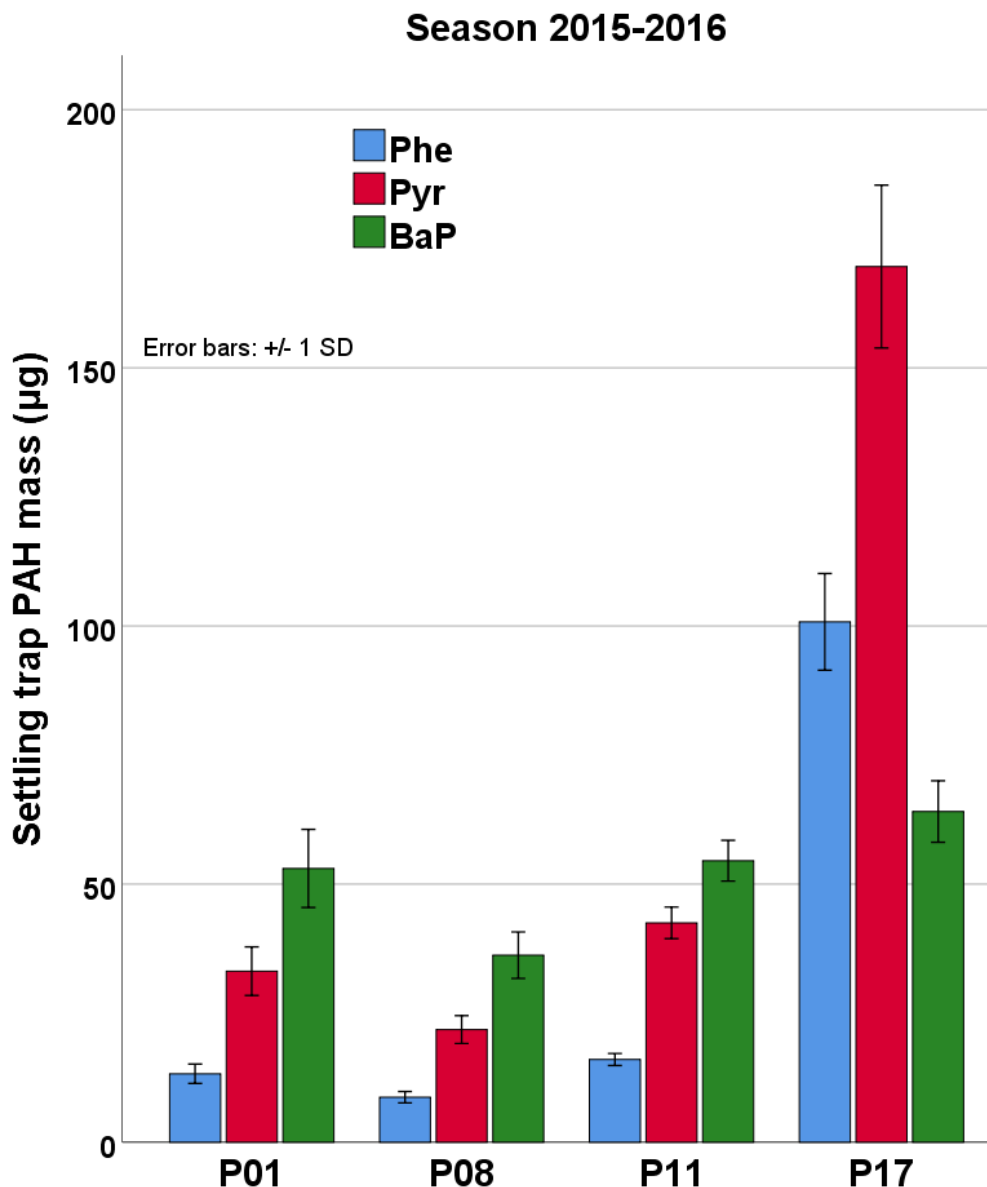


Figure 4-22: PAH mass deposited in the settling traps during deployments in season 2015-2016.

4.3.3.2 Sediment PAH concentrations

We observed seasonal fluctuations in the Σ PAH concentrations of the sediment as measured by sediment cores in the Paleta creek receiving waters (Figure 4-23). Looking at locations P11 and P17 for which we suspect the highest runoff contributions, Σ PAH concentrations start in the 1,000-4,000 $\mu\text{g kg}^{-1}$ range in October 2015 and increase to a maximum of 4,000-10,000 $\mu\text{g kg}^{-1}$ by February 2016 before dropping back to the 1,000-2,000 $\mu\text{g kg}^{-1}$ in September 2016 and finally rising to 2,000-3,000 $\mu\text{g kg}^{-1}$ in March 2017. Location P11 has higher Σ PAH concentrations than P17, albeit not statistically significant, in October 2015 ($p=0.112$) and February 2016 ($p=0.104$). In the 2016-2017 season this observation is inverted in September 2016 ($p=0.392$) and March 2017 ($p=0.027$). The most significant (2015-16: $p=0.013$, 2016-17: $p=0.016$) seasonal increases in Σ PAH concentrations were observed in location P11. The drastically high Σ PAH concentration with low uncertainty (relative standard deviation (RSD) is 4.8%) in the P11 February 2016 cores cannot be explained by particle deposition and could be the result of processes that result in sediment mixing such as bioturbation. It is also worth remembering that the sediment core samples are an integration of the top 5 cm of sediment.

Compared to post storm cores in season 2015-2016, settling trap average Σ PAH concentrations are significantly lower in P11 ($p=0.004$) and not significantly lower in P17 ($p=0.271$). The settling trap material is unaffected by sedimentary processes and this is a very good reason why it can be used to assess deposition of new material. Sediment cores (and sediment grab samples) are influenced by more processes than deposition alone and thus represent a synthesized picture of legacy and ongoing releases.

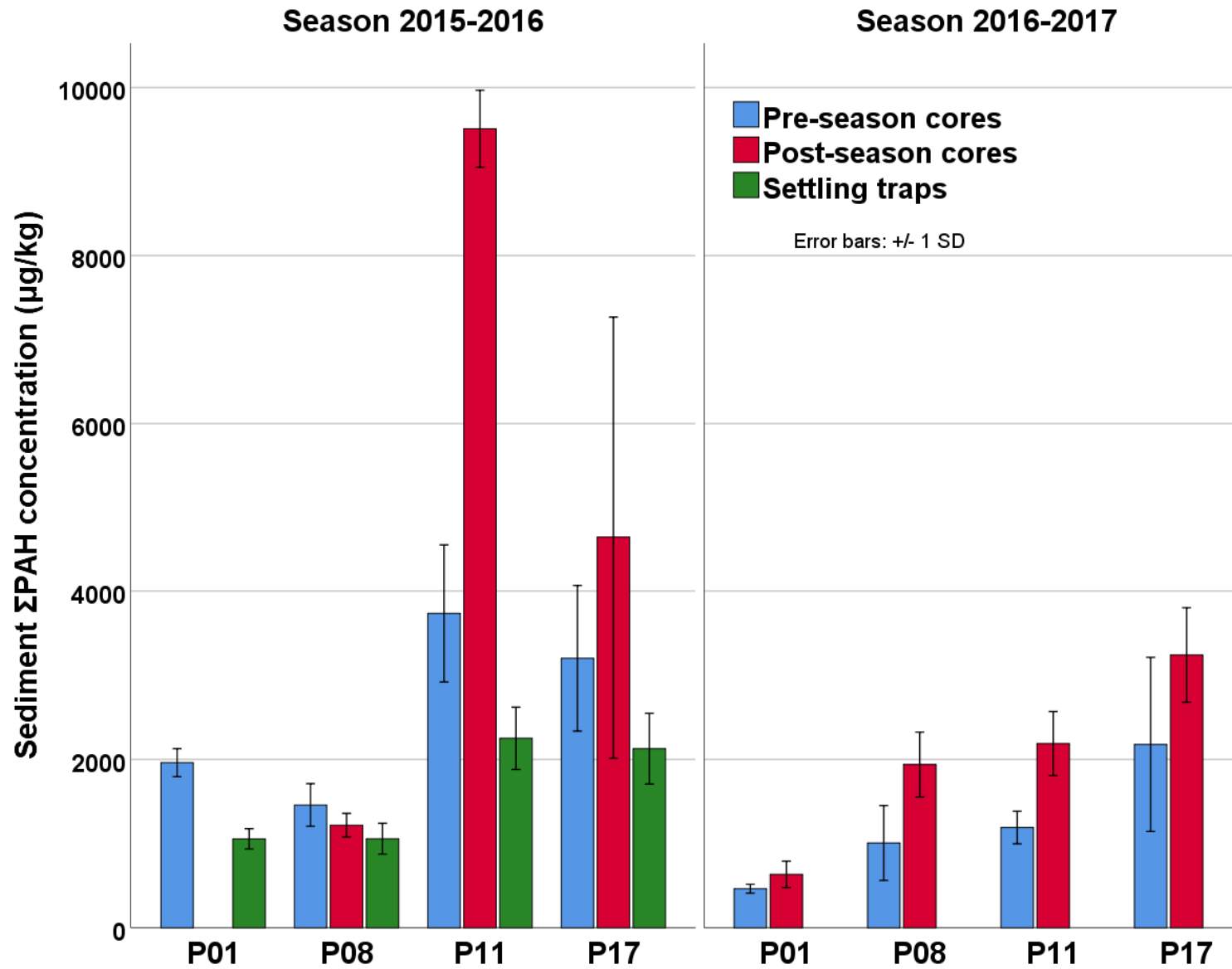


Figure 4-23: Sediment core and settling trap ΣPAH concentrations in all locations and for seasons 2015-2016 and 2016-2017 at Paleta creek.

Looking only into the 2015-2016 storm season for the 3 PAHs (Figure 4-24), we see that the higher molecular weight PAHs (PYR and BaP) have lower concentrations on the trap solids than in the cores. PHE concentrations are generally similar in the trap and core solids. As before, the elevated concentrations observed in locations P11 and P17 cannot be directly attributed to runoff and must be the result of other processes taking place in the sediment.

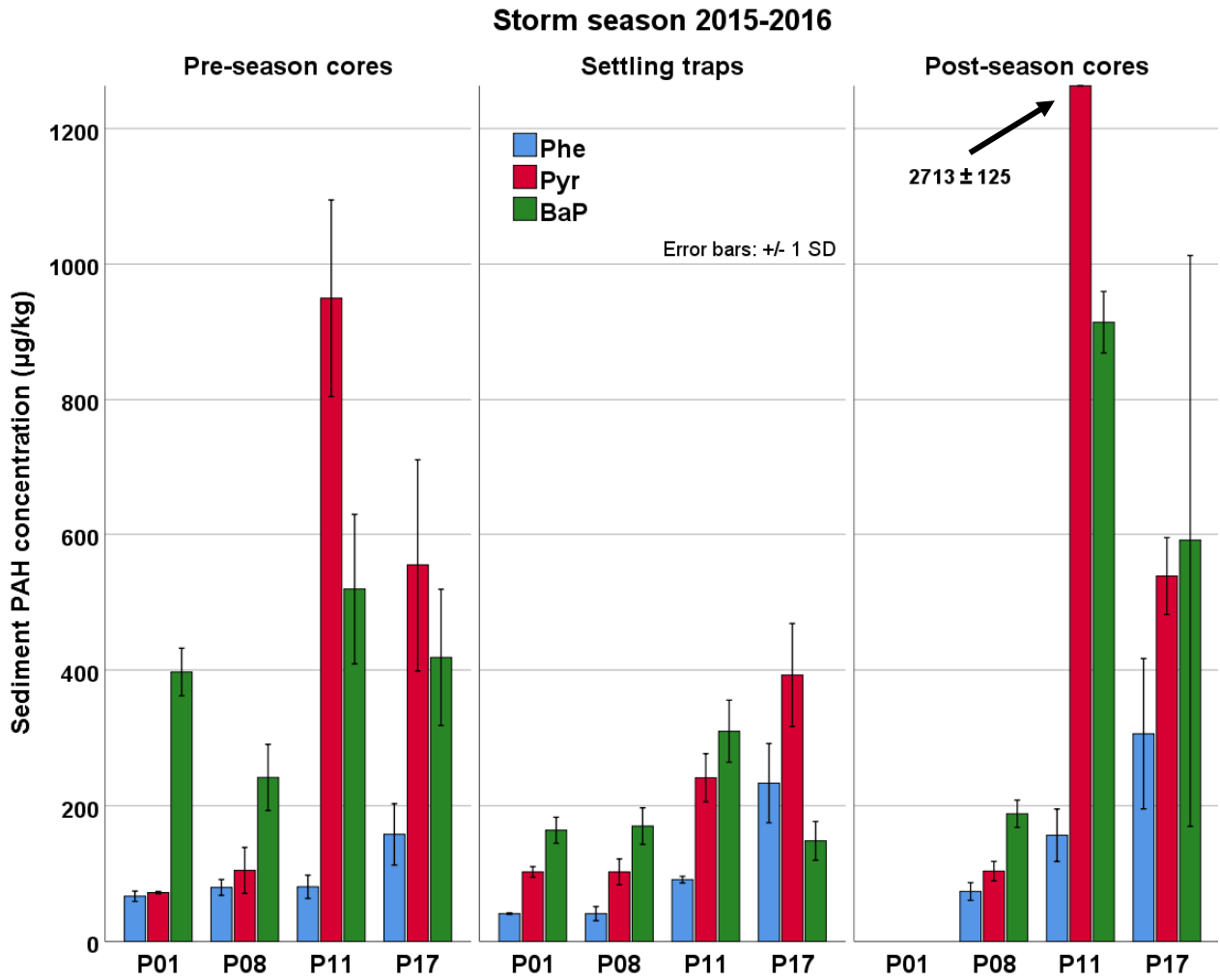


Figure 4-24: PAH concentrations in settling traps and sediment cores during deployments in season 2015-2016.

4.3.3.3 *Sediment TOC content*

The TOC content of the sediment core and settling trap solids in the near field (P17) is 2 times higher than further out in the bay (Figure 4-25). There is in fact a decreasing trend when moving away from the mouth of Paleta creek. The BC content (Figure A9) of the solids has a similar trend to TOC as it is highest in location P17 and drops in locations P11 to P01. In both cases there is a more significant increase at location P17 during the 2016-2017 storm season

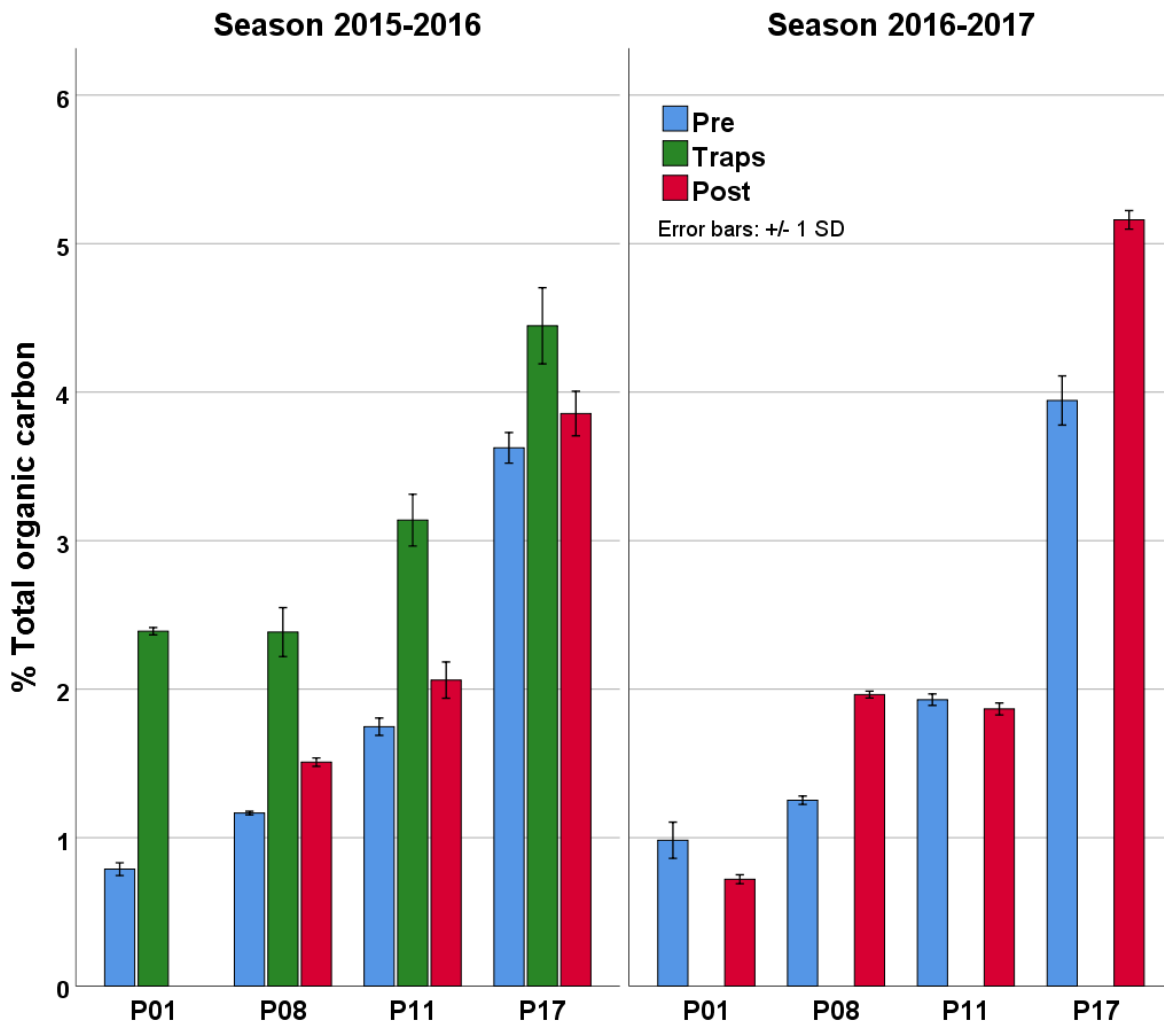


Figure 4-25: Receiving sediment (Pre and Post) and settling trap TOC content in all sampling locations during storm seasons 2015-2016 and 2016-2017.

compared to the 2015-2016 season. The material collected in the settling traps in 2015-2016 has significantly higher TOC content compared to the post sediment core solids in locations P08 ($p=0.008$), P11 ($p=0.002$) and P17 ($p=0.109$) and could explain the TOC increases from pre to post.

4.3.3.4 PAH ratios

The potential relation of particles transported by storm 1 runoff and particles collected by the settling traps in location P17 can be further substantiated using the 3 PAH ratios that were introduced earlier. The most clear observation from the 3 graphs in Figure 4-26 is the similarity of the PAH ratios of P17 trap solids with the runoff solids; in all 3 cases P17 signature is much more similar to the runoff than to the other locations. Another interesting result is the striking

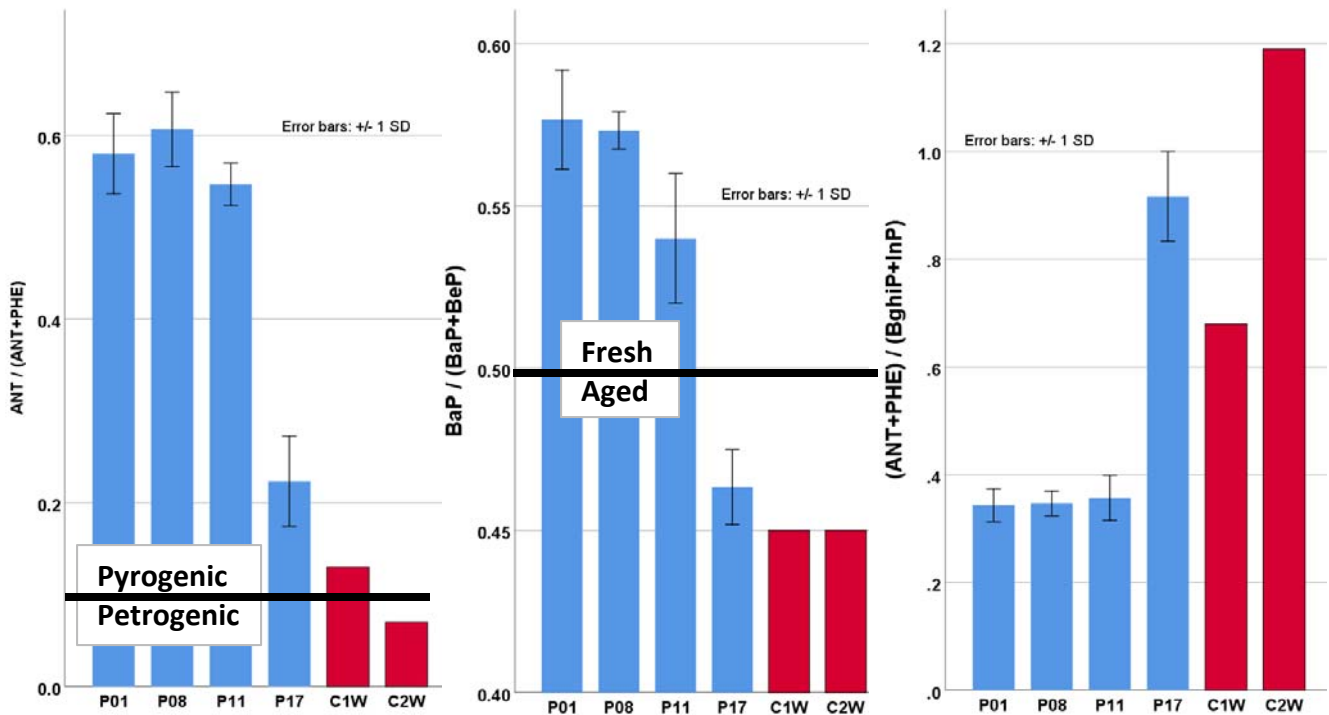


Figure 4-26: Three different PAH ratios of solids transported by storm 1 runoff upstream of NBSD (C2W) and at the discharge point (C1W) in red. Same ratios for the solids deposited in the 2015-2016 settling traps in all locations is in blue.

resemblance between the PAH ratios of locations P11, P08 and P01. It appears as if the solids in these 3 locations have a very similar origin. A final observation here is that this particle “source” is distinctly different from the runoff (which is also a source of particles), a distinction that is portrayed as two clusters of data in each graph (cluster 1: C1W, C2W and P17, cluster 2: P01, P08 and P11).

From the ratio values, we can see that locations P01, P08 and P11 have a much stronger pyrogenic ($[ANT/(ANT+PHE)] > 0.5$) signature, something that can be confirmed by the greater abundance of 6-ring PAHs (low $(ANT+PHE)/(BghiP+InP)$ ratio) compared to P17 and the runoff. The traps in the same locations also received material that is more “fresh” (less weathered) compared to the material collected in P17 and transported by the runoff ($[BaP/(BaP+BeP)] < 0.5$). These two observations are hinting towards runoff depositing PAHs mainly in P17 while the particles in P01, P08 and P11 have a different type of source. That source could be fresh vehicular exhaust particles that through atmospheric deposition are continuously precipitating in the San Diego bay where they escape significant photodegradation. One could make the case that the same particles are depositing in the watershed where they could be photodegraded before making their way in the bay by the runoff. A reason we’re not seeing a much less pyrogenic signature could be that the proportion of atmospherically deposited particles compared to the ones transported by runoff, is significantly higher. These directly deposited particles could also be resuspended by propeller wash of ships operating near the docks of NBSD and collected by the outer traps thus contributing to the increased amount of mass observed there.

4.3.3.5 *Sediment summary*

If stormwater runoff has any effect in the receiving sediment, it is mostly seen in the near field. Location P17 receives not only highest amount of total solids mass but almost all sand and most of the coarse silt particles. That was to be expected due to shallow depth (1-3 m), the rapid deposition of large particles and flocculation of finer particles due to the salt-saline water interface. P17 also receives the highest amount of Σ PAH mass, especially during the 2015-2016 wet season, most of which is comprising of low molecular weight (LMW) PAHs as represented by PHE and PYR. Total organic carbon is also much more abundant in P17 in practically every sediment measurement we made and decreases with increasing distance from the mouth of the creek.

Having said all the above, the increases in PAH concentrations during the wet season (as seen from Pre to Post core samples) are statistically “debatable” and when taking into account the settling solids concentrations as measured by the 2015-2016 traps, they would be difficult to be linked to runoff. Furthermore, the higher PAH concentrations on sediment solids in P11 for the 2015-2016 season (seen in both traps and cores) alone, would again challenge the idea that runoff has any effect in sediment contamination. These observations bring to the surface the inherent limitations that time-integrated sediment measurements, as sampled by sediment cores, possess. Sediment is affected by mixing processes which in the case of legacy contaminated sediments such as the ones in our study, make it more difficult to assess fresh deposition. This brings us to the conclusion that sediment traps are a great tool to use in assessing the contamination potential of runoff. Not only are they unaffected by mixing processes, but also provide the ability to measure the mass and contaminant burden of depositing material, thus illuminating spatial trends that cannot be observed by sediment cores.

The settling traps are also the ones who revealed the existence of one or more sources of particles and PAHs in the outer San Diego bay. The U-shaped solids and ΣPAH mass spatial distributions in the receiving waters prove that there is potentially a mix of processes that deposit increasing amount of material with increasing distance from the mouth of the Paleta creek. Some of these sources could be resuspension from propeller wash of ships and tug boats operating within the naval base or further out in the bay (SERDP ER-201031), resuspension from underwater currents, resuspension from runoff, bioturbation and atmospheric deposition. The PAH ratios we calculated are providing supporting evidence that atmospheric deposition may be a major contributor of pyrogenic PAHs in the area and its effects are obscured by runoff in P17. This could be further evidence that stormwater runoff has a very limited sphere of contaminating influence close to the discharge point.

4.4 Conclusions

Looking at our study more holistically, we can see some clear connections between our runoff and sediment measurements. Multiple lines of evidence, show that the large carbon rich particles with high PAH mass and weak pyrolytic signature that we saw in the stormwater, were primarily collected in the P17 traps. Considering the urban drainage basin with the existence of a major highway crossing it, these particles could be originating from eroded pieces of asphalt, chips of tarmac coated with pavement sealants, tire chips and even road debris glazed with spilled fuel and motor oils. These sources have a petrogenic signature that combined with their larger size (higher settling velocity) should contribute more heavily to near field contamination after discharge. However, the great abundance of silt particles with pyrogenic origin in the area counteract that petrogenic signature effectively leading to a more ambiguous one.

The above observations can also lead to the conclusion that most of the particles that are depositing in P17, have a high PAH content and can act as a source that releases PAHs in the overlying water column in the dry season as well as between storms. However, if we take into account the much higher TOC and BC content of those particles, a case can be made that they could in fact act as a sink, removing PAHs from the porewater and overlying water. This would effectively qualify them as a continuously self-replenishing capping material, already mildly depleted, but posing a barrier between the deeper legacy contaminated sediment and the overlying water. If any of this is true, we would expect the bioavailability of this layer to be severely restricted. This idea will be explored in the following chapter.

A significant lesson learnt from this study is the importance of using the right tools when attempting to link runoff to sediment effects. The choice of size segregating the stormwater and deploying settling traps in the receiving sediment, proved to be the combination that provided the opportunity to apply multiple physical and chemical tools that ultimately produced multiple lines of evidence.

4.5 References

- Abdel-Shafy, H.I., Mansour, M.S.M., 2016. A review on polycyclic aromatic hydrocarbons: Source, environmental impact, effect on human health and remediation. *Egypt. J. Pet.* <https://doi.org/10.1016/j.ejpe.2015.03.011>
- Accardi-Dey, A.M., Gschwend, P.M., 2002. 23 Assessing the combined roles of natural organic matter and black carbon as sorbents in sediments. *Environ. Sci. Technol.* 36, 21–29. <https://doi.org/10.1021/es010953c>
- Badin, A.-L., Faure, P., Bedell, J.-P., Delolme, C., 2008. Distribution of organic pollutants and natural organic matter in urban storm water sediments as a function of grain size. *Sci. Total Environ.* 403, 178–87. <https://doi.org/10.1016/j.scitotenv.2008.05.022>
- Bathi, J.R., Pitt, R.E., Clark, S.E., 2012. Polycyclic aromatic hydrocarbons in urban stream sediments. *Adv. Civ. Eng.* 2012, 1–9. <https://doi.org/10.1155/2012/372395>
- Bian, B., Zhu, W., 2009. Particle size distribution and pollutants in road-deposited sediments in different areas of Zhenjiang, China. *Environ. Geochem. Health* 31, 511–520. <https://doi.org/10.1007/s10653-008-9203-8>
- Brown, J.N., Peake, B.M., 2006. Sources of heavy metals and polycyclic aromatic hydrocarbons in urban stormwater runoff. *Sci. Total Environ.* 359, 145–155. <https://doi.org/10.1016/j.foreco.2006.01.031>
- Budzinski, H., Jones, I., Bellocq, J., Piérard, C., Garrigues, P., 1998. Evaluation of the sediment contamination by PAHs in the Gironde estuary. *Mar. Chem.* 58, 85–97.
- Burgess, R.M., Berry, W.J., Mount, D.R., Di Toro, D.M., 2013. Mechanistic sediment quality guidelines based on contaminant bioavailability: Equilibrium partitioning sediment benchmarks. *Environ. Toxicol. Chem.* 32, 102–114. <https://doi.org/10.1002/etc.2025>
- Clark, A.E., Yoon, S., Sheesley, R.J., Usenko, S., 2015. Pressurized liquid extraction technique for the analysis of pesticides, PCBs, PBDEs, OPEs, PAHs, alkanes, hopanes, and steranes in atmospheric particulate matter. *Chemosphere* 137, 33–44. <https://doi.org/10.1016/j.chemosphere.2015.04.051>
- Corcoran, A.A., Reifel, K.M., Jones, B.H., Shipe, R.F., 2010. Spatiotemporal development of physical, chemical, and biological characteristics of stormwater plumes in Santa Monica Bay, California (USA). *J. Sea Res.* 63, 129–142. <https://doi.org/10.1016/j.seares.2009.11.006>
- Cornelissen, G., Pettersen, A., Nesse, E., Eek, E., Helland, A., Breedveld, G.D., 2008. The contribution of urban runoff to organic contaminant levels in harbour sediments near two Norwegian cities. *Mar. Pollut. Bull.* 56, 565–573. <https://doi.org/10.1016/j.marpolbul.2007.12.009>

- Cuypers, C., Pancras, T., Grotenhuis, T., Rulkens, W., 2002. The estimation of PAH bioavailability in contaminated sediments using hydroxypropyl- β -cyclodextrin and Triton X-100 extraction techniques. *Chemosphere* 46, 1235–1245. [https://doi.org/10.1016/S0045-6535\(01\)00199-0](https://doi.org/10.1016/S0045-6535(01)00199-0)
- Dickhut, R.M., Canuel, E.A., Gustafson, K.E., Liu, K., Arzayus, K.M., Walker, S.E., Edgecombe, G., Gaylor, M.O., MacDonald, E.H., 2000. Automotive sources of carcinogenic polycyclic aromatic hydrocarbons associated with particulate matter in the Chesapeake Bay region. *Environ. Sci. Technol.* 34, 4635–4640. <https://doi.org/10.1021/es000971e>
- Ghosh, U., Zimmerman, J.R., Luthy, R.G., 2003. PCB and PAH speciation among particle types in contaminated harbor sediments and effects on PAH bioavailability. *Environ. Sci. Technol.* 37, 2209–2217. <https://doi.org/10.1021/es020833k>
- Gustafsson, Ö., Haghseta, F., Chan, C., MacFarlane, J., Gschwend, P.M., 1997. Quantification of the Dilute Sedimentary Soot Phase: Implications for PAH Speciation and Bioavailability. *Environ. Sci. Technol.* 31, 203–209. <https://doi.org/10.1021/es960317s>
- Hoffman, E.J., Mills, G.L., Latimer, J.S., Quinn, J.G., 1984. Urban Runoff as a Source of Polycyclic Aromatic Hydrocarbons to Coastal Waters. *Environ. Sci. Technol.* 18, 580–587. <https://doi.org/10.1021/es00126a003>
- Hwang, H.-M., Foster, G.D., 2006. Characterization of polycyclic aromatic hydrocarbons in urban stormwater runoff flowing into the tidal Anacostia River, Washington, DC, USA. *Environ. Pollut.* 140, 416–426. <https://doi.org/10.1016/j.envpol.2005.08.003>
- Jartun, M., Ottesen, R.T., Steinnes, E., Volden, T., 2008. Runoff of particle bound pollutants from urban impervious surfaces studied by analysis of sediments from stormwater traps. *Sci. Total Environ.* 396, 147–163. <https://doi.org/10.1016/j.scitotenv.2008.02.002>
- Katsoyiannis, A., Terzi, E., Cai, Q.Y., 2007. On the use of PAH molecular diagnostic ratios in sewage sludge for the understanding of the PAH sources. Is this use appropriate? *Chemosphere* 69, 1337–1339. <https://doi.org/10.1016/j.chemosphere.2007.05.084>
- Li, Z., Pittman, E.N., Trinidad, D.A., Romanoff, L.C., Mulholland, J., Sjödin, A., 2010. Determination of 43 polycyclic aromatic hydrocarbons in air particulate matter by use of direct elution and isotope dilution gas chromatography/mass spectrometry. *Anal. Bioanal. Chem.* 396, 1321–1330. <https://doi.org/10.1007/s00216-009-3297-4>
- Mahler, Barbara J, Van Metre, P.C., Crane, J.L., Watts, A.W., Scoggins, M., Williams, E.S., 2012. Coal-tar-based pavement sealcoat and PAHs: Implications for the environment, human health, and stormwater management. *Environ. Sci. Technol.* 46, 3039–3045. <https://doi.org/10.1021/es203699x>

- Mahler, Barbara J., Van Metre, P.C., Crane, J.L., Watts, A.W., Scoggins, M., Williams, E.S., 2012. Coal-tar-based pavement sealcoat and PAHs: Implications for the environment, human health, and stormwater management. *Environ. Sci. Technol.* 46, 3039–3045. <https://doi.org/10.1021/es203699x>
- McVeety, B.D., Hites, R.A., 1988. Atmospheric deposition of polycyclic aromatic hydrocarbons to water surfaces: A mass balance approach. *Atmos. Environ.* 22, 511–536. [https://doi.org/10.1016/0004-6981\(88\)90196-5](https://doi.org/10.1016/0004-6981(88)90196-5)
- O'Reilly, K.T., Pietari, J., Boehm, P.D., 2014. Parsing pyrogenic polycyclic aromatic hydrocarbons: forensic chemistry, receptor models, and source control policy. *Integr. Environ. Assess. Manag.* 10, 279–285. <https://doi.org/10.1002/ieam.1506>
- Paul, M.; Meyer, J., 2005. Streams in the Urban Landscape, in: *Urban Ecology. An International Perspective on the Interaction Between Humans and Nature*. pp. 207–231.
- Pengchai, P., Furumai, H., Nakajima, F., 2004. Source Apportionment of Polycyclic Aromatic Hydrocarbons in Illinois River Sediment. *Polycycl. Aromat. Compd.* 24, 773–789. <https://doi.org/10.1080/10406630490487828>
- Pitt, R., Field, R., Lalor, M., Brown, M., 1995. Urban Stormwater Toxic Pollutants: Assessment, Sources, and Treatability. *Water Environ. Res.* 67, 260–275. <https://doi.org/10.2175/106143095X131466>
- Rogge, W.F., Hildemann, L.M., Mazurek, M.A., Cass, G.R., Simoneit, B.R.T., 1993. Sources of Fine Organic Aerosol. 3. Road Dust, Tire Debris, and Organometallic Brake Lining Dust: Roads as Sources and Sinks. *Environ. Sci. Technol.* 27, 1892–1904. <https://doi.org/10.1021/es00046a019>
- Shinya, M., Tsuchinaga, T., Kitano, M., Yamada, Y., Ishikawa, M., 2000. Characterization of heavy metals and polycyclic aromatic hydrocarbons in urban highway runoff. *Water Sci. Technol.* 42, 201–208.
- Soclo, H.H., Garrigues, P.H., Ewald, M., 2000. Origin of polycyclic aromatic hydrocarbons (PAHs) in coastal marine. *Mar. Pollut. Bull.* 40, 387–396.
- Stout, S.A., Magar, V.S., Uhler, R.M., Ickes, J., Abbott, J., Brenner, R., 2001. Characterization of Naturally-occurring and Anthropogenic PAHs in Urban Sediments-Wycoff/Eagle Harbor Superfund Site. *Environ. Forensics* 2, 287–300. <https://doi.org/10.1080/713848281>
- Tobiszewski, M., Namieśnik, J., 2012. PAH diagnostic ratios for the identification of pollution emission sources. *Environ. Pollut.* 162, 110–119. <https://doi.org/10.1016/j.envpol.2011.10.025>
- Wang, X.S., Meng, •, Chen, Q., Zheng, X., n.d. Polycyclic aromatic hydrocarbons (PAHs) in Xuzhou urban street dust: concentration and sources. *Environ. Earth Sci.* 76. <https://doi.org/10.1007/s12665-017-6922-0>

Watts, A.W., Roseen, R.M., Ballesterio, T.P., Houle, J.J., Gilbert, H.L., 2010. Polycyclic Aromatic Hydrocarbons in Stormwater Runoff From Sealcoated 44, 8849–8854.

Zhang, W., Zhang, S., Yue, D., Wan, C., Ye, Y., Wang, X., 2008. Characterization and loading estimation of polycyclic aromatic hydrocarbons in road runoff from urban regions of Beijing, China. *Environ. Toxicol. Chem.* 27, 31–37. <https://doi.org/10.1897/07-030.1>

Zhang, Y., Shi, G.-L., Guo, C.-S., Xu, J., Tian, Y.-Z., Feng, Y.-C., Wang, Y.-Q., 2012. Seasonal variations of concentrations, profiles and possible sources of polycyclic aromatic hydrocarbons in sediments from Taihu Lake, China. *J. Soils Sediments* 12, 933–941. <https://doi.org/10.1007/s11368-012-0526-9>

Chapter 5

Assessment of Polycyclic Aromatic Hydrocarbon Bioavailability in Sediments Impacted by Urban Runoff

5.1 Introduction

One of the biggest contributors of contaminants in urban sediment is stormwater runoff. In contrast to urban wastewater, runoff often finds its way to a receiving water body untreated or with minimal treatment such as primary settling in detention basins. This can have a negative impact on water and sediment quality as well as the benthos. Epibenthic and infaunal species are exposed to elevated concentrations of urban contaminants like Polycyclic Aromatic Hydrocarbons (PAHs) with the potential of effects extending up the food chain.

Stormwater runoff from roads, parking areas and developed areas, may have a pronounced impact on sediments in coastal urban areas. The extensive impervious surfaces, gives runoff the kinetic energy to suspend and transport particles accumulated on the pavement into a receiving water body. Such particles can be pieces of tire, asphalt and soot, potentially coated with gasoline and motor oil, and may be laden with PAHs that contribute to sediment contamination as an episodic source. Assessing the significance of this source is particularly important in areas where sediment remediation is under consideration to manage a legacy of contamination in adjacent bodies of water. The presence of this ongoing source may slow, limit or even reverse recovery of the sediments affected by the stormwater.

In the previous chapter, we observed that PAHs in an urban watershed may be strongly associated with larger particles that settle quickly to the bottom of receiving waters contributing to bulk solid recontamination of the sediments. The significance of this bulk sediment recontamination, however, is largely a function of the bioavailability of the deposited

contaminants to the benthos that might inhabit those sediments. As noted previously, however, the stormwater sediments have a high black carbon (BC) content which could potentially render sorbed PAHs, significantly less bioavailable and effectively incurring reduced risk of adverse biological effects. In order to assess this question, the bioavailability of PAHs in stormwater loads and in depositing sediments was evaluated. The bioavailability of the PAHs was assessed by measuring interstitial or porewater concentrations of PAHs and comparing to expected toxicity in water and by assessing the bioaccumulation of PAHs to test organisms exposed to the depositing sediments.

In this study, our goal was to evaluate the biological impact that stormwater has on the receiving benthos and bioaccumulation can be a good indicator of that impact. Bioaccumulation is the phenomenon where contaminant exposure and uptake by an aquatic organism leads to tissue concentration that exceeds that in the water (Gobas, 2001). Now, a potential indicator of bioaccumulation is the bioaccumulation factor (BAF), a ratio of the contaminant concentrations in the organism tissue (C_{tissue}) and the surrounding media (C_m) (Eq. 1). For organic contaminants such as PAHs, the tissue concentration can often be normalized by the organic fraction of organisms (f_{lipids}) to better indicate the amount of bioaccumulation for a given level of contamination in the surrounding media. If the route of contaminant uptake is from the freely dissolved phase (C_{pw}) via tissue sorption, the BAF is the ratio of the tissue concentration to the porewater concentration. In the case of hydrophobic organics (eg. PAHs) where lipids is the dominant phase of bioaccumulation in benthic organisms (Mackay, 1982) the bioaccumulation can be normalized to the lipid content as defined by the bioconcentration factor (BCF) (Eq. 2). If the bioaccumulating compound is hydrophobic, the porewater concentration would be proportional to the ratio of the sediment concentration to the fraction organic carbon and Eq.3

$$BAF = \frac{C_{tissue}}{C_m} \quad (1) \quad BCF = \frac{\frac{C_{tissue}}{f_{lipids}}}{C_{pw}} \quad (2) \quad BSAF = \frac{\frac{C_{tissue}}{f_{lipids}}}{\frac{C_{sed}}{f_{oc}}} \quad (3)$$

can be useful. Although these approaches have their basis in relating exposure to the porewater concentration and uptake from water, the major mode of uptake for benthic organisms is ingestion of sediment. Despite this, porewater is increasingly being used as an indication of the available fraction of contaminants and the BCF may be useful even for deposit feeding routes of uptake.

Leo et al. studied the octanol-water model system and broadened its application to “partitioning-like” processes in more complex biological systems by showing that octanol is a satisfactory proxy model compound for lipid phases (Leo et al., 1971). In essence, this tells us that PAHs should partition approximately equally in lipids and octanol and the BCF should be approximately K_{ow} . We can thus define a biota-porewater accumulation factor that should approximate unity (Eq. 4).

$$BPAF = \frac{\frac{C_{tissue}}{f_{lipids}}}{C_{pw} * K_{ow}} \cong 1 \quad (4)$$

According to the classic model, sediment porewater concentrations can be calculated by measuring organic carbon normalized sediment concentrations (C_{sed}/f_{oc}) and dividing by the organic carbon-water partition coefficient (K_{oc}) (Eq. 5). This paves the way for a predicted biota-porewater accumulation factor (Predicted BPAF) based on measured sediment concentrations (Eq. 6).

$$C_{pw} = \frac{C_{sed}}{f_{oc} * K_{oc}} \quad (5) \quad \longrightarrow \quad Predicted \ BPAF = \frac{\frac{C_{tissue}}{f_{lipids}}}{\frac{C_{sed}}{f_{oc} * K_{oc}} * K_{ow}} \quad (6)$$

The organism chosen for the bioaccumulation studies was *Macoma Nasuta* (MN), the bent-nosed clam abundant in the North Pacific Ocean. Growing up to 5 cm in length, this infaunal species feeds with objects no larger than 500µm indiscriminately from surficial sediment as that material supports growth optimally. *Macoma Nasuta* typically feeds on the top millimeter of sediment (Hylleberg and Gallucci, 1975). Material extracted from the digestive tract of MN, showed many kinds of organisms, detritus as well as inorganic material, however the feces are in all cases richer in organic material than the surrounding sediment (Hylleberg and Gallucci, 1975). This selectivity towards organic matter (OM) leads to increased bioaccumulation risk as OM is a prime target for organic pollutants. The bioaccumulation assays that are part of this study were conducted at the US Navy Space and Naval Warfare Systems Command (SPAWAR) San Diego, (now called Naval Information Warfare Center, NIWC) while the extraction, analysis and evaluation of chemical body burdens were conducted in our lab.

One of the key drivers in characterizing risks of contaminated sediment is the evaluation of contaminant bioavailability. Traditionally, defining bulk sediment concentrations has been the basis for assessing biological and human health risk. In the Sediment Management Standards (Chapter 173-204 WAC) document submitted to the EPA in 2013 by the state of Washington, sediment quality standards that result in “no adverse effects on biological resources and no significant health risk to humans” in Puget Sound sediments, are defined by organic carbon normalized sediment PAH concentrations (WAC 173-204-320).

However, there has been increasing evidence that sediment porewater concentration can be a better indicator of bioavailability (Di Toro et al., 1991; Lu et al, 2014; Greenberg et al., 2014; Kraaij et al., 2003; You et al., 2006). These observations suggest that porewater contaminants might be controlling the steady-state bioaccumulation despite ingestion being the

route of uptake (Lu et al., 2011). Recent advances in passive sampling have enabled direct measurement of freely dissolved concentration of polycyclic aromatic hydrocarbons (PAHs) in porewater through the use of techniques such as solid phase microextraction (SPME) with polydimethylsiloxane (PDMS) fibers.

In our previous storm runoff analysis at Paleta creek in San Diego, we saw that a significant portion of runoff solids are coarse silt and sand. These particles are also carrying most of the Σ PAH and organic carbon mass, especially during the larger storm of the season. Analysis of the material collected by settling traps in the receiving waters throughout the wet season, revealed that solids collected close to the discharge point of the creek were mainly consisting of coarse silt and sand particles and had the highest Σ PAH and TOC mass. The close relationship of runoff and near field sediment was also confirmed by their PAH ratios which was very similar between them and distinctly different to the PAH ratios of the material collected further from the mouth of the creek. These results give us high confidence in determining that potential stormwater runoff effects will be disproportionately manifesting in the area close to the discharge point of the runoff.

In this work, our objective is to determine whether runoff has a contaminating effect on the receiving sediment. Following our conclusions from the previous work, we expect any impacts to be accentuated in the near field and also be represented by differences between pre-storm and post-storm season samples. To achieve the above, we measure porewater and bulk sediment PAH concentrations in bioassays of sediment impacted by stormwater discharges in which tissue samples are also collected. This provided an opportunity to study the partitioning of PAHs in these 3 compartments and assess the bioavailability of the contaminants residing in the sediment but also correlate physicochemical to biological measurements.

5.2 Materials and Methods

5.2.1 Sampling Overview

The sediment samples used in bioassays are from the receiving waters of stormwater discharges from Paleta Creek at Naval Base San Diego (NSBD) in California. Paleta Creek is a channelized urban stormwater conveyance system discharging into San Diego Bay. This location is designated as a toxic hotspot by the California State Water Board due to contamination of sediments and impacts on the benthic community. Sampling took place at 4 locations, with increasing distance from the mouth of Paleta creek (Figure 5-1 - left) prior to the winter storm season in 2015 and 2016 and after these same storm seasons. Sediment sampling and bioassays were conducted in July 2015, October 2015, February 2016, September 2016 and March 2017. October 2015 to September 2016 will be referred to as 2015-2016 storm season while September 2016 to March 2017 as 2016-2017 season.

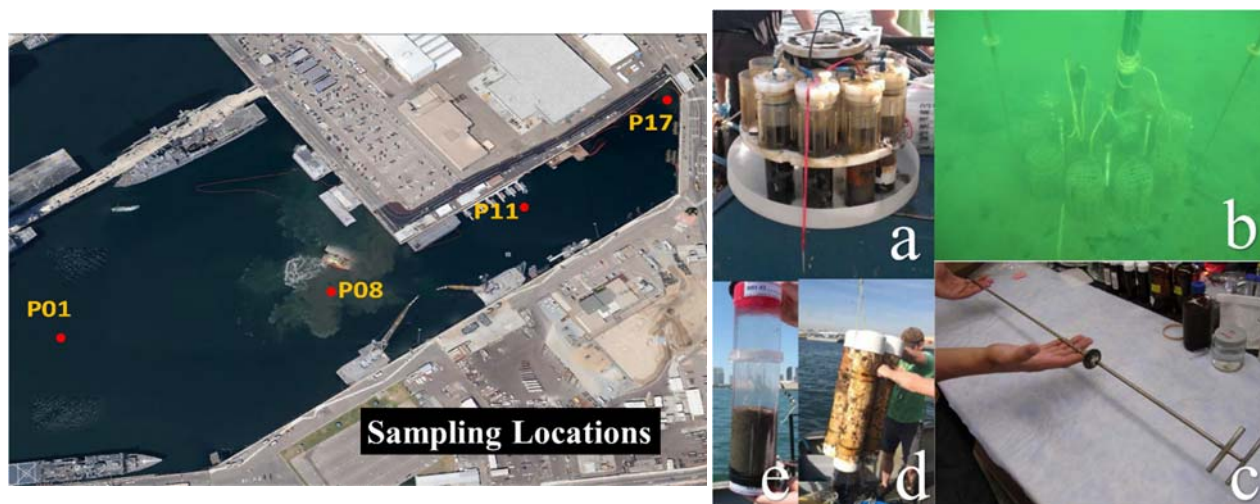


Figure 5-1: (Left) Sampling locations. (Right-clockwise) SEA Rings (a) deployed in situ beside Henry rods (b) containing the SPME passive samplers (c). Retrieved sediment traps (d) and cores (e).

In-situ bioaccumulation was measured by Sediment Ecosystem Assessment (SEA) Rings (ESTCP ER-201130) (Figure 5-1a) loaded with bent-nosed clams (*Macoma Nasuta*). In-situ sediment porewater was sampled by SPME passive samplers (Figure 5-1b and 5-1c). Sediment cores (Figure 5-1e) were collected and settling traps were deployed (Figure 5-1d) and retrieved after the storm seasons. Ex-situ passive sampling and bioassays (exposures were conducted at the SSC Pacific Bioassay Laboratory) were also performed on dry weather (pre storm season) and wet weather (post storm season) sediments. Additional bioassays were conducted with sediment collected during dry weather and spiked with settling trap material.

5.2.2 Sample deployment and collection

5.2.2.1 Sediment

Intact cores were collected by divers or by Van Veen grab samplers on 07/15/2015, 10/19/2015, 02/23/2016, 09/08/2016 and 03/08/2017 and stored at 4°C until processing or shipping to TTU. Sediment trap material was collected during the 2015 dry season (07/15/2015 – 08/12/2015) and over the course of the 2015/2016 wet season (10/19/2015 – 02/22/2016).

5.2.2.2 Tissues

In-situ bioaccumulation exposures utilized the Version 3.0 Sediment Ecotoxicity Assessment Rings (SEA Rings - SERDP #ER-1550, ESTCP #ER-201130). The SEA Ring is an integrative sediment and water quality assessment tool, which was developed by the University of Michigan and Space and Naval Warfare Systems Command (SPAWAR) under the Strategic Environmental Research and Development Program (SERDP). It is a device that consists of cylindrical chambers where organisms are deposited before in-situ deployment and constitutes a

controlled way of exposing an organism to the field in order to assess the bioaccumulation potential of native sediments. In our study, SEA Rings were used to assess not only sediment bioaccumulation but also biological effects of urban runoff.

SEA Rings consist of 10 exposure chambers with coarse stainless-steel mesh fastened to the top and bottom. Water pumps on the assembly were programmed to achieve 138 turnovers of overlying water per day for each chamber. Four of the chambers were fitted with an 80 μ m pre-filter on top and four were fitted with a 500 μ m pre-filter on top. During deployment, commercially available or field collected bent-nosed clams (*Macoma Nasuta*), acclimated to site conditions, were directly loaded into the chambers (5 clams per chamber). The SEA Rings were lowered, gently pushed approximately 5 inches into the sediment and an open cage with 15 clams was deployed next to them. After a 28 day exposure (01/26/2016 – 02/23/2016), SEA Rings were recovered and the clams were removed, counted for mortality and depurated overnight in clean seawater. Finally, the soft-body tissue was frozen and shipped for analysis.

Ex-situ exposures were conducted at the SSC Pacific Bioassay Laboratory with sediment cores (from now on called bioassay cores) and settling trap material during 07/17/2015 – 08/14/2015, 03/01/2016 – 03/29/2016, 09/13/2016 – 10/11/2016 and 03/10/2017 – 04/07/2017. Trap material was proportionally (to the volume of the material recovered from each station) added on top of the corresponding bioassay core collected at the beginning of the wet season. Approximately 100 g of each sediment type was placed into 1L glass mason jars with 500-750 mL of overlying uncontaminated 0.45 μ m filtered seawater (FSW) that was continuously aerated with filtered laboratory air delivered through Pasteur pipettes at a rate of approximately 100 bubbles per minute. A 24-h equilibration period with the overlying water was allowed prior to the introduction of test organisms or passive sample devices. *Macoma Nasuta* were received 4-6

days prior to exposure to allow for acclimation and to observe for mortalities. Organisms were introduced randomly to test chambers and renewals of the overlying water were made three times per week over the course of the 28 day exposure. Upon termination of the exposure period, surviving organisms were recovered, enumerated and then transferred to clean FSW overnight to purge digested sediment. Lastly, the soft body portions of the clams were dissected from each replicate, rinsed with Milli-Q water, weighed and frozen in sample collection jars until shipping for analysis.

5.2.2.3 SPMEs

Predetermined (5 and 30 cm) lengths of PDMS fiber were cleaned consecutively with dichloromethane, hexane, methanol and ultrapure water. The cleaned fibers were then placed in a water-methanol (4:1 v/v) solution with 2500 ng mL⁻¹ concentration of performance reference compounds (PRCs) where they remained no less than 8 days and until preparation for deployment. PRCs are non-interfering deuterated PAHs (more information in section 2.3) that are preloaded on the fibers to help define the extent of equilibration of the fibers during deployment. The stainless steel rods with a slit that would support the fibers during sediment deployment, were also cleaned sequentially with detergent and hot water, dichloromethane, hexane, methanol and ultrapure water.

For in-situ (field) deployment, the 30 cm fibers were laid into a groove cut into stainless steel holders, attached with waterproof caulk (hydrocarbon-free silicon) and inserted into the outer sheath. Three PDMS samplers were deployed very close to the SEA Rings (Figure 1b) by divers 15cm into the sediment during 10/19/2015 - 01/26/2016 and 01/26/2016 – 02/23/2016 at each location where SEA Rings were deployed. During retrieval, the depth of each sampler in

the sediment was noted. The fibers were immediately removed from the holder cleaned with a lint-free tissue wetted with Milli-Q water and segmented with ceramic column cutters every 5 cm to create a depth profile.

For ex-situ (laboratory) deployment, three 5 cm fibers were inserted into separate septas/envelopes and placed vertically directly in 20 ml vials containing the respective bioassay core and including the ones with added trap material on top of pre storm season bioassay core sediment. After exposure, the fibers were removed from the 20 mL vial, cleaned with a lint-free tissue wetted with Milli-Q water and segmented with ceramic column cutters.

All fiber segments from their corresponding locations and/or depths were transferred to 2 mL amber vials until further analysis.

Quality of the PRC loading was assured by randomly extracting and analyzing loaded fibers prior to field deployment. Deployment blanks, which are fibers shipped to the field, never deployed but otherwise processed in the same manner as the deployed fibers and solvent blanks, which confirm the purity of the extraction solvent, were utilized during all deployments.

5.2.3 Chemicals, materials and instruments

Research grade PAH-16 (Naphthalene, Fluorene, Acenaphthylene, Acenaphthene, Phenanthrene, Anthracene, Fluoranthene (FLA), Pyrene (PYR), Chrysene (CHR), Benzo(a)anthracene (BaA), Benzo(b)fluoranthene (BbF), Benzo(k)fluoranthene (BkF), Benzo(a)pyrene (BaP), Dibenz(a,h)anthracene, Benzo(g,h,i)perylene, Indeno(1,2,3-cd)pyrene) standards at a concentration of 100 mg L⁻¹ and deuterated PAH (fluoranthene-d10, chrysene-d12, benzo[b]fluoranthene-d12, dibenzo[a,h]anthracene-d14) used as surrogate standards and performance reference compounds (PRCs) at a concentration of 100 mg L⁻¹, were purchased

from Ultra Scientific (N. Kingstown, RI, USA). Research grade deuterated compounds (d-acenaphthene, d-phenanthrene and d-perylene) were used as internal standards for gas chromatography – triple quadrupole mass spectrometry (GC-TQMS) analysis and were purchased from Ultra Scientific. Ultrapure water was supplied by a GenPure Pro UV purification system (ThermoFisher Scientific, Phillipsburg, NJ, USA)

Solid phase micro-extraction polydimethylsiloxane fibers were purchased from Polymicro Technologies™ (Molex, Phoenix, AZ, USA) and Fiberguide (NJ, USA). Henry samplers were manufactured by M.H.E. Products (East Tawas, MI, USA).

Sediment extractions were performed with a Dionex ASE 350™ pressurized liquid extraction system and evaporations with a Rocket™ Evaporator, both from ThermoFisher Scientific (Phillipsburg, NJ, USA). The solvents hexane (Hex), dichloromethane (DCM), Acetone (Ace), Methanol (MeOH) used for sediment extraction and acetonitrile (ACN) for PDMS extraction were HPLC-grade from ThermoFisher Scientific (Phillipsburg, NJ, USA). Sample cleanup included aluminum oxide (alumina) from Acros Organics (Phillipsburg, NJ, USA), sodium sulfate from VWR (Radnor, PA, USA) and diatomaceous earth from ThermoFisher Scientific (Phillipsburg, NJ, USA). Analysis of the ACN extracts was done on an Agilent 1260 Infinity high performance liquid chromatography (HPLC) system and other solvent extracts were analyzed on an Agilent 7890B GC-TQMS, both from Agilent Technologies (Santa Clara, CA, USA).

5.2.4 Sample preparation

5.2.4.1 Sediment

Sediment sample extraction and analysis is described in detail in the previous chapter.

5.2.4.2 Tissues

Upon receipt, tissues were stored in a freezer until further processing. Sample preparation commenced by allowing them to thaw to room temperature, homogenizing each sample with the Omni homogenizer (OMNI International, Kennesaw, GA, USA), adding DE to remove the moisture and homogenizing further. Stainless steel ASE cells (34 mL) were packed as follows; a cellulose filter placed at the bottom followed by the sample/DE mix and any dead volume filled with DE. The cell was then spiked with 25 μL of a 4 mg L^{-1} mix of deuterated PAHs and placed on ASE carousel for extraction. Samples were extracted by a 4:1 (v/v) mixture of Hex-Ace, 100 $^{\circ}\text{C}$, 2 static cycles of 5 minutes, 50% rinse, 100 sec purge with ultrapure nitrogen gas and collected in 60 mL amber vials. Static pressure, as set by the instrument, was 1700 psi. The extract is concentrated (with Rocket evaporator at 1700 rpm with 190 mbar vacuum for about 11 mins) to 1 mL and then purified through a 50 mL chromatographic column with a small amount of pre-cleaned glass wool at the bottom and loaded with 5 g of alumina (activated according to EPA Method 3610b) and anhydrous sodium sulfate. The samples were finally exchanged to acetonitrile, concentrated to 1mL and transferred into 2 mL vials for HPLC analysis. All analyses were performed in triplicates.

Following extraction, evaporation and solvent exchange, calculation of the final sample volume was done by measuring the mass of the vial (plus a 300 μL insert in the case of method blanks) before (m_i) and after (m_f) transferring the final sample into it and using the density of ACN at 20 $^{\circ}\text{C}$ ($d_{\text{ACN}}=0.786 \text{ g cm}^{-3}$) in:

$$V_f = \frac{m_f - m_i}{d_{\text{ACN}}}$$

Background contamination of the solvents, sorbents and consumables as well as carryover contamination of the instrument, was assessed by method blanks (MBs), a set of 3

ASE cells that were prepared in the same way as the rest of the samples. The difference in volume was filled with DE and these cells were run at the start of every sequence. Potential losses from this method were evaluated by a set of 3 cells that were prepared as the MBs but were spiked with 50 μ L of a 1 mg L⁻¹ mix of EPA's 16 priority PAHs in acetonitrile on the top of the cell prior to extraction and run with every sequence. Quality control samples were extracted using the same method as the samples

5.2.4.3 Passive Samplers

The SPME fibers in the 2 mL amber vials, are extracted with an appropriate solvent (acetonitrile for HPLC analysis or hexane for GC-TQMS analysis) overnight. The fibers were removed from the extract and the vials were stored at 4 °C until analysis. Appropriate laboratory, field and PRC blanks were processed in a similar fashion for quality control and method performance.

5.2.5 Analysis

5.2.5.1 HPLC

Separation of analytes on the HPLC was carried out by a Phenomenex (Torrance, CA, USA) Luna 5 μ m C18 reverse phase column (250 x 4.6 mm) set to 40 °C. Operation was under isocratic conditions with 1 mL min⁻¹ flow rate of 70% acetonitrile and 30% water (v:v). For optimal sensitivity, the FLD detector was used with the Method Detection Limit (MDL) determined to be less than 0.5 μ g/L for all parent and deuterated PAHs. This method was able to analyze 15 PAHs (acenaphthylene does not fluoresce) with Benzo[g,h,i]perylene and Indeno[1,2,3-cd]pyrene taken as a single concentration because complete separation was not

possible. PAH quantification was achieved by nine-point calibration from $0.5 \mu\text{g L}^{-1}$ to $200 \mu\text{g L}^{-1}$ ($0.5, 1, 2, 5, 10, 20, 50, 100, 200 \mu\text{g L}^{-1}$) with correlation coefficients were consistently greater than 0.9980 for all parent and deuterated PAHs.

Data points refer to the following PAHs: Fluoranthene, Pyrene, Chrysene, Benz(a)anthracene, Benzo[b]fluoranthene, Benzo[k]fluoranthene and Benzo(a)pyrene. Since these compounds have 4-5 aromatic rings and are considered high molecular weight (HMW) PAHs, henceforth the sum of their concentrations in a samples will be referred to as $\Sigma\text{PAH}_{\text{HMW}}$.

5.2.5.2 GC-TQMS

The method used for the separation of PAHs on the GC/TQMS was based on EPA Method 8270 and has the following parameters: 60 m DB-5MS column, splitless mode, inlet temperature at $280 \text{ }^{\circ}\text{C}$, injection volume $1 \mu\text{L}$, flow at 1.2 mL min^{-1} and 54.5 min runtime. The mass spectrometer was set at SIM/SIM mode and the calibration ranged from 0.2 to $20 \mu\text{g L}^{-1}$ with seven points.

5.2.6 Statistical analysis

As our datasets consist of triplicate measurements, comparing the means by parametric statistical analysis is not reliable. There is uncertainty in fulfilling the normality assumption as it is not possible to declare with certainty that the population from which the 3 measurements originate is normally distributed. There are statisticians that believe that the t-Test is robust and can be indicative even in cases where normal distribution of the measurements cannot be established.

In order to cross check the results provided by the conducted t-Tests, we also conducted the non-parametric Wilcoxon signed ranks test. This test is agnostic to the normality assumption but as a test, it is very conservative when comparing means of triplicates. As an example, the comparison between the mean of a group with values: 1, 1, 2 and a group with values 1001, 1001, 1002, returns a p-value of 0.102.

The p-values calculated in this work are indicative and the graphs with the respective means and standard deviations should always be the main source of confidence regarding the differences between two sets of measurements.

5.3 Results

5.3.1 Sediment

Sediment $\Sigma\text{PAH}_{\text{HMW}}$ concentrations for the 2015-2016 and 2016-2017 storm seasons appear to increase in general during the storm season as indicated by collected pre and post-season sediment cores (Figure 5-2). The increases observed in location P17, were not statistically

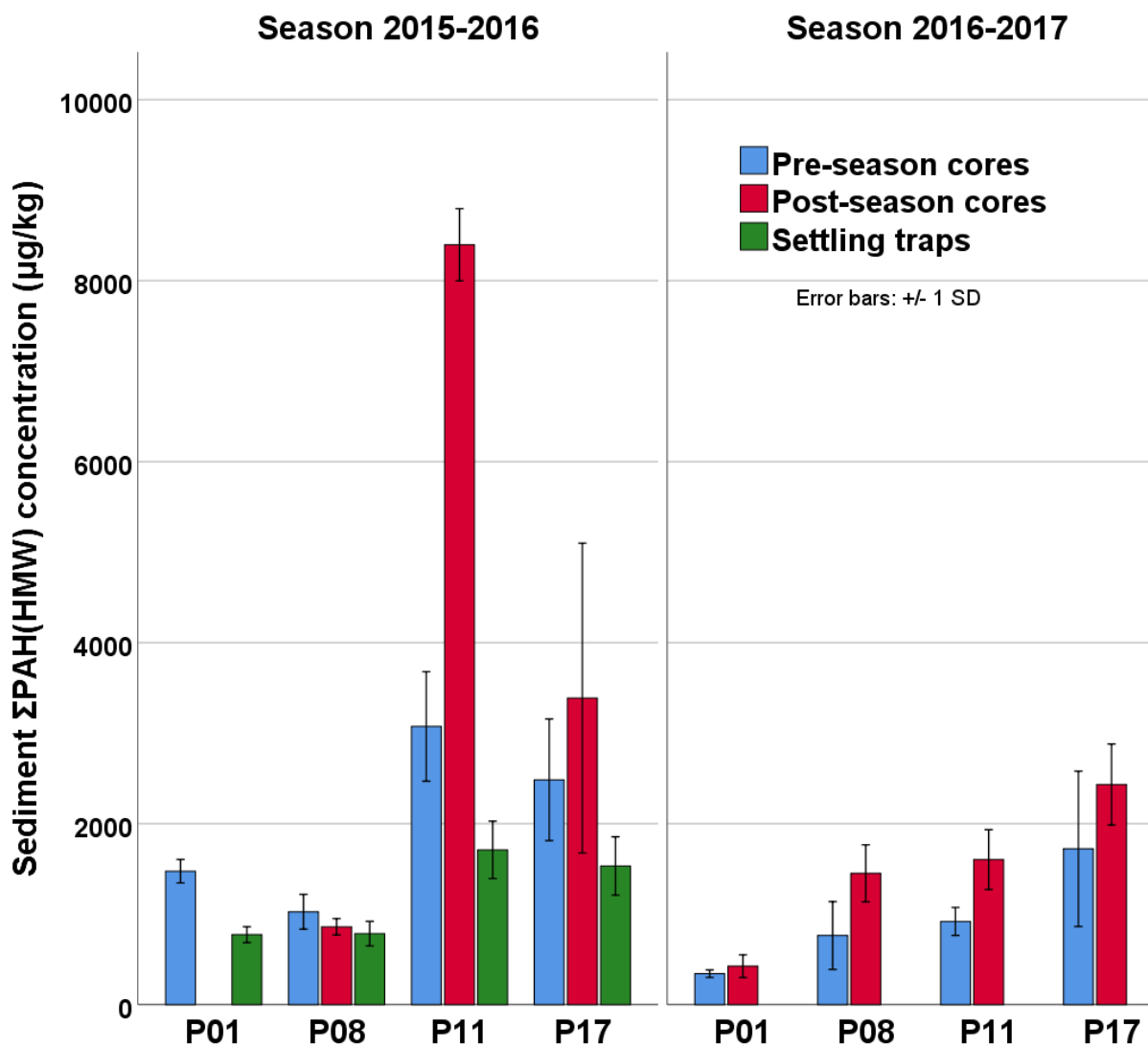


Figure 5-2: $\Sigma\text{PAH}_{\text{HMW}}$ concentrations of settling trap material and pre/post-storm sediment cores collected during seasons 2015-2016 and 2016-2017.

significant both in 2015-2016 (PStT⁸: $p=0.453$, WSRT⁹: $p=0.285$) and 2016-2017 (PStT: $p=0.146$, WSRT: $p=0.180$). Sediment in location P11 had statistically significant increases in 2015-2016 (PStT: $p=0.008$, WSRT: $p=0.109$) and 2016-2017 (PStT: $p=0.029$, WSRT: $p=0.109$). However, the increases observed during the 2015-2016 storm season in these locations, could not have originated from runoff as the $\Sigma\text{PAH}_{\text{HMMW}}$ concentrations of the particles collected in the settling traps was lower than pre and post storm sediment concentrations. This is a strong indication that runoff may not be leading to bulk sediment contamination in the receiving waters of Paleta creek.

The $\Sigma\text{PAH}_{\text{HMMW}}$ concentrations in location P11 traps and pre/post cores in 2015-2016 season, are higher than in location P17. This difference was significant in the pre (PStT: $p=0.062$, WSRT: $p=0.109$) and post (PStT: $p=0.052$, WSRT: $p=0.109$) storm cores but not statistically significant (PStT: $p=0.677$, WSRT: $p=0.593$) in the traps. During the 2016-2017 storm season, P17 sediment $\Sigma\text{PAH}_{\text{HMMW}}$ concentrations are higher than P11 both before the storm season¹⁰ (PStT: $p=0.400$, WSRT: $p=0.180$) and after (PStT: $p=0.032$, WSRT: $p=0.109$). These results are another indication that storm runoff is not necessarily leading to sediment contamination. There appear to be other processes (co)influencing bulk sediment concentrations and leading to seasonal fluctuations to the point of trend reversal.

⁸ PStT: Paired samples t-test (parametric)

⁹ WSRT: Wilcoxon signed rank test (non-parametric)

¹⁰ P17 pre-storm mean $\Sigma\text{PAH}_{\text{HMMW}}$ is calculated as the average of two values.

5.3.2 In-situ measurements

Both (Oct. 2015 – Jan. 2016 and Jan. 2016 – Feb. 2016) in-situ SPME deployments (Figure 5-3) showed that freely dissolved $\Sigma\text{PAH}_{\text{HMW}}$ concentrations in P17 were on the same level (approx. 20 ng L⁻¹) as locations P01 and P08 while location P11 had significantly higher concentrations by a factor of 5. This result was also observed in the July 2015 SPME deployment

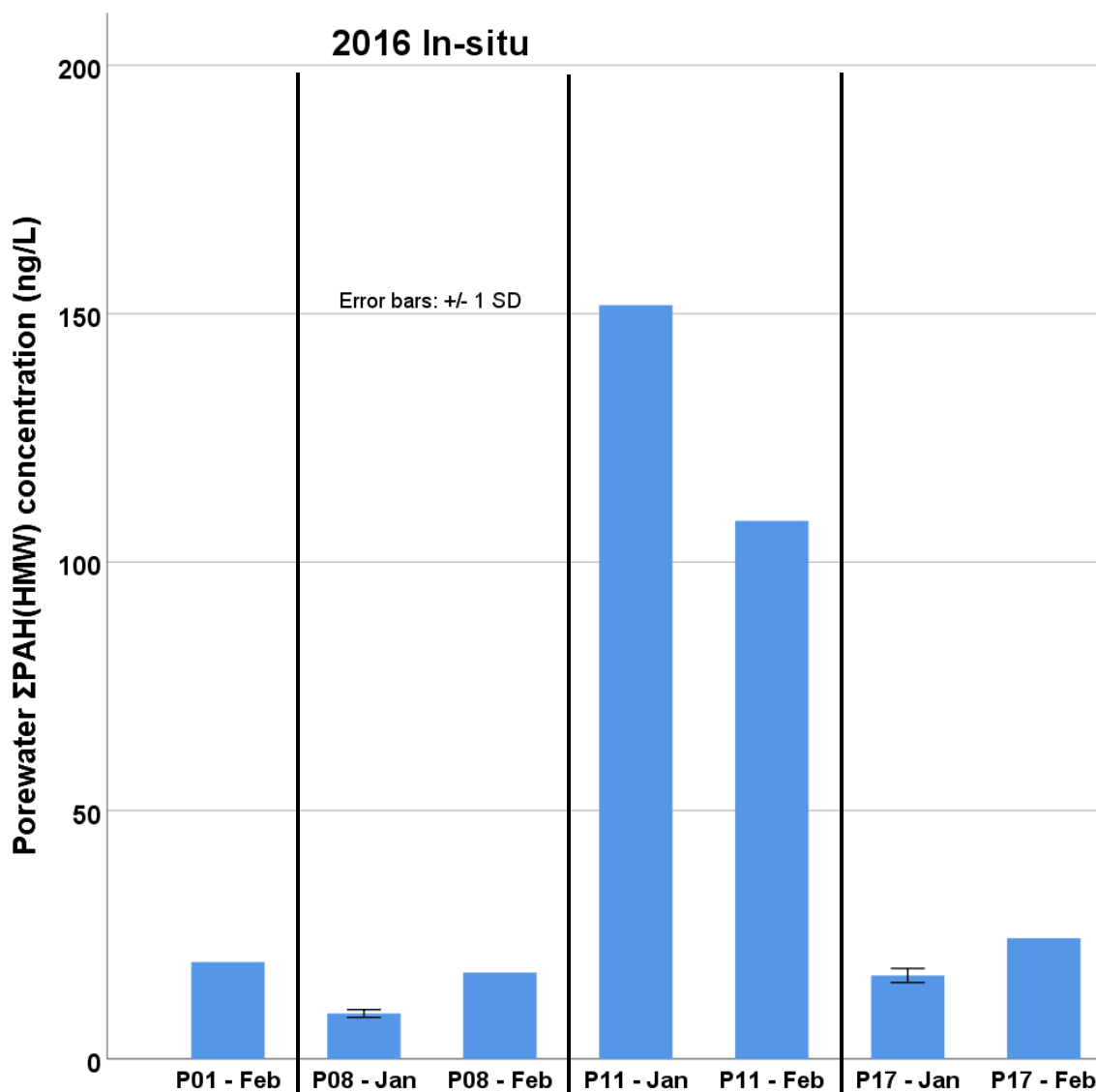


Figure 5-3: Season 2015/2016 In-situ porewater $\Sigma\text{PAH}_{\text{HMW}}$ concentrations per location for both SPME deployments.

(Figure A10) which measured $\Sigma\text{PAH}_{\text{HWM}}$ porewater concentrations around 25 ng L^{-1} with concentration in P11 being 3 times higher. These elevated freely dissolved $\Sigma\text{PAH}_{\text{HWM}}$ concentrations in P11 mirror the elevated bulk sediment $\Sigma\text{PAH}_{\text{HWM}}$ concentrations and cannot be attributed to stormwater discharges. Looking at P17 porewater concentrations, the consistency in low measurements and the similarity with freely dissolved concentrations in areas that are far from the influence of runoff discharges, also suggest that runoff does not appear to lead to near field contamination.

The in-situ bioaccumulation study on *Macoma Nasuta* with the SEA Rings (Figure 5-4) in 2016 (Jan. 2016 – Feb. 2016), revealed that sediment in location P17 led to the lowest lipid

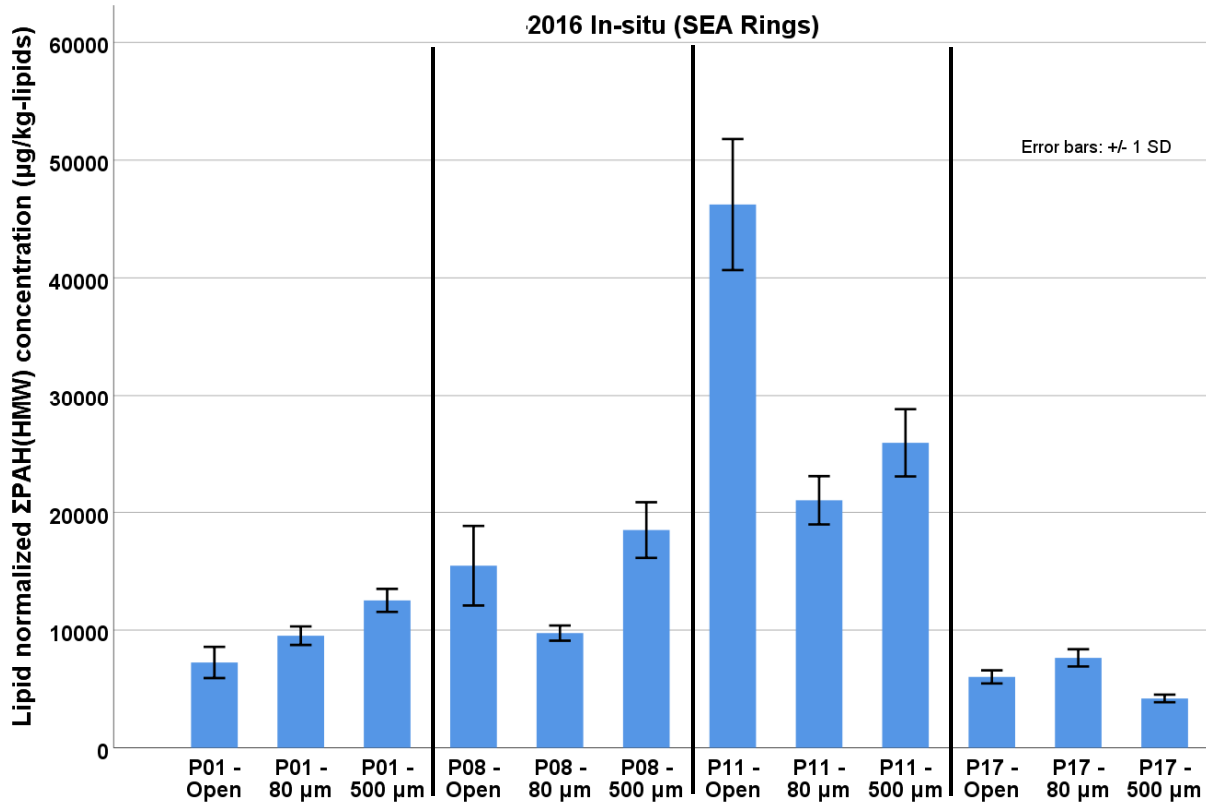


Figure 5-4: Season 2015/2016 In-situ lipid normalized $\Sigma\text{PAH}_{\text{HWM}}$ concentrations per location. Open, 80 μm and 500 μm refer to the existence or not of a pre-filter on the top of the bioassay chambers.

normalized $\Sigma\text{PAH}_{\text{HMW}}$ concentrations of any location. Taking into account that P17 is receiving the highest amounts of runoff solids and PAHs, leads to the conclusion that this contaminant load is largely unavailable to the clams. Native sediment in P11 led to the highest tissue concentrations by a factor of 5 (compared to P17) and this indicates that a source of PAHs is localized to the P11 area. This proportion and spatial distribution of tissue PAHs is very similar to the one we encountered in the porewater and is an indication that porewater seems to represent the PAH load the clams “see” in the sediment. This distribution is very different to the runoff effect distribution we were expecting in our 1-dimensional model in the previous chapter, which was exponentially diminishing from P17 outwards.

The pre-filters placed on top of the SEA Rings showed that the smaller filter (80 μm) led to lower bioaccumulation in almost all cases in locations P01, P08 and P11 while it led to an increase in P17. If we take into account that almost all sand (> 63 μm) particles in the runoff, settle at P17, this can be another indication that these particles are exceedingly desorption resistant even in the presence of lipids. In fact, if their presence leads to lower bioaccumulation, a case can be made that they act as a terminal sink of PAHs and thus the runoff is effectively removing contamination from the native near field sediment.

Summarizing the in-situ porewater and tissue results, we saw that the area represented by P17 which we would have expected to receive the highest runoff impact, was “cleaner” (or at worst equally contaminated) to the more distant parts of the receiving waters and this suggests that runoff is not having a measurable negative effect. There are multiple indications that there is a source of PAHs in location P11 that led to that area having the highest sediment, and in-situ freely dissolved and tissue concentrations. This source could potentially be vertical mixing of the sediment column, bringing to the surface legacy contaminated sediment.

5.3.3 *Ex-situ measurements*

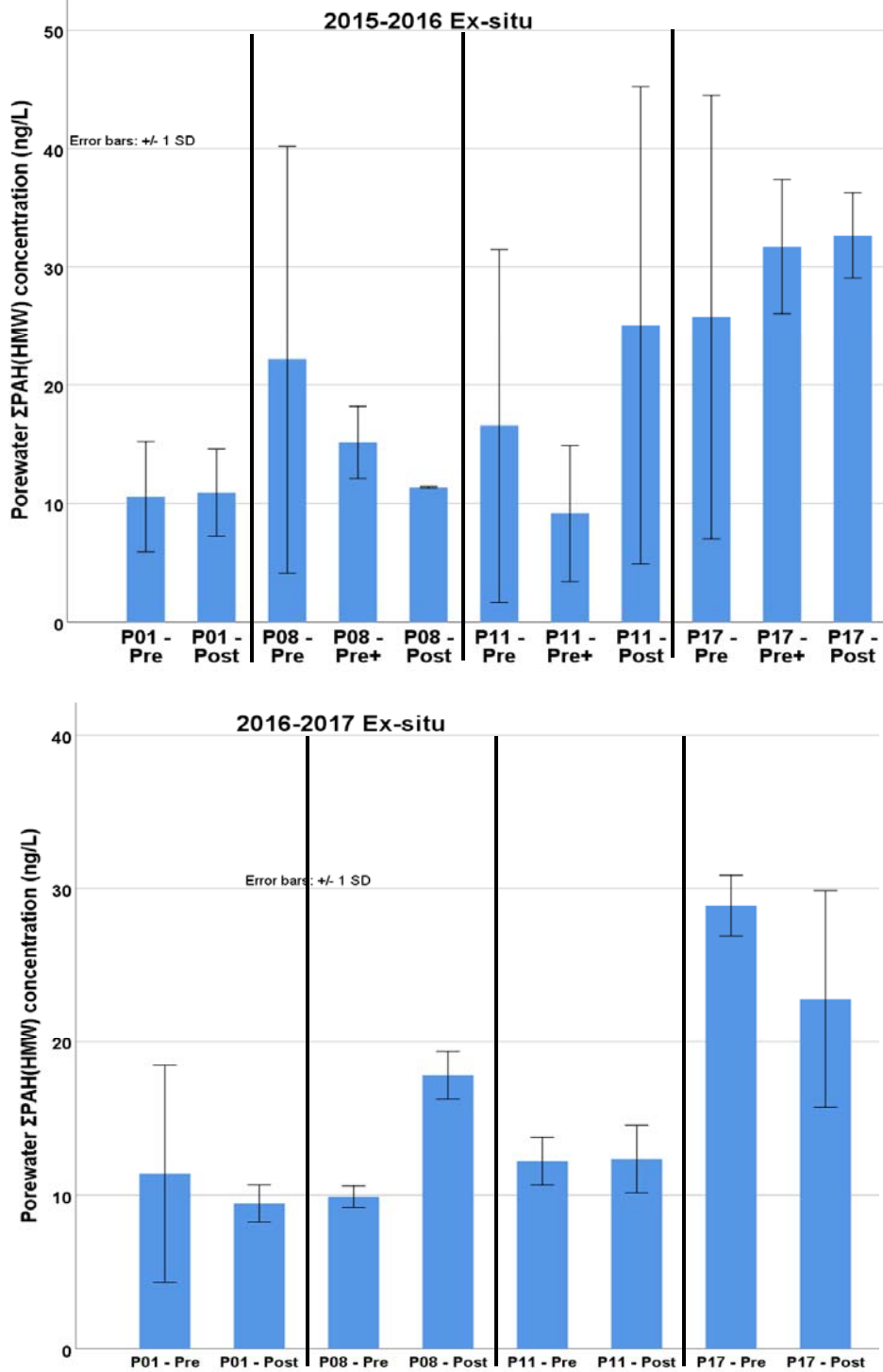


Figure 5-5: *Pre/post season 2015-2016 and 2016-2017 ex-situ porewater ΣPAH_{HMW} concentrations per location.*

Porewater measurements by SPMEs deployed ex-situ in bioassay cores during the 2015-2016 (Figure 5-5 - upper) and 2016-2017 seasons (Figure 5-5 - lower), show that freely dissolved $\Sigma\text{PAH}_{\text{HMW}}$ concentrations in location P17 remain consistently in the 20-30 ng L⁻¹ bracket. This range is the same as the one we saw in the in-situ measurements and can indicate that runoff contributions in the near field are generally stable over long time frames and this has allowed the local porewater to reach a state of equilibrium with the discharges. Location P11 has on average similar $\Sigma\text{PAH}_{\text{HMW}}$ concentrations to locations P01 and P08 and lower than P17 in both storm seasons. This result contrasts to the in-situ measurements and could strengthen the argument that the high in-situ porewater concentrations we saw earlier in P11 may not have originated from the runoff but possibly from a sedimentary process. That process must also have been very localized otherwise the post-storm ex-situ cores would have captured this increase and it would have been represented in the porewater. This argument can be also supported by the pre+ measurement (pre sediment with the addition of trap material on top) which shows that the depositing material actually led to the decrease of tissue concentrations compared to pre and post.

Tissue $\Sigma\text{PAH}_{\text{HMW}}$ concentrations as measured by the ex-situ bioaccumulation studies (Figure 5-6) show that sediment in location P17 led to lower (2015-2016) or approximately equal (2016-2017) tissue concentrations to the rest of the receiving sediments in the San Diego bay. Especially the 2015-2016 ex-situ results mirror the in-situ ones and in general suggest that stormwater runoff does not seem to have adverse effects on the uptake of HMW PAHs by benthic clams. The large increases of lipid normalized $\Sigma\text{PAH}_{\text{HMW}}$ concentrations in locations P01 (+823%) and P08 (+131%) during the 2015-2016 season, cannot be attributed to runoff influence due to the large distance from the main area of expected runoff effects (P17).

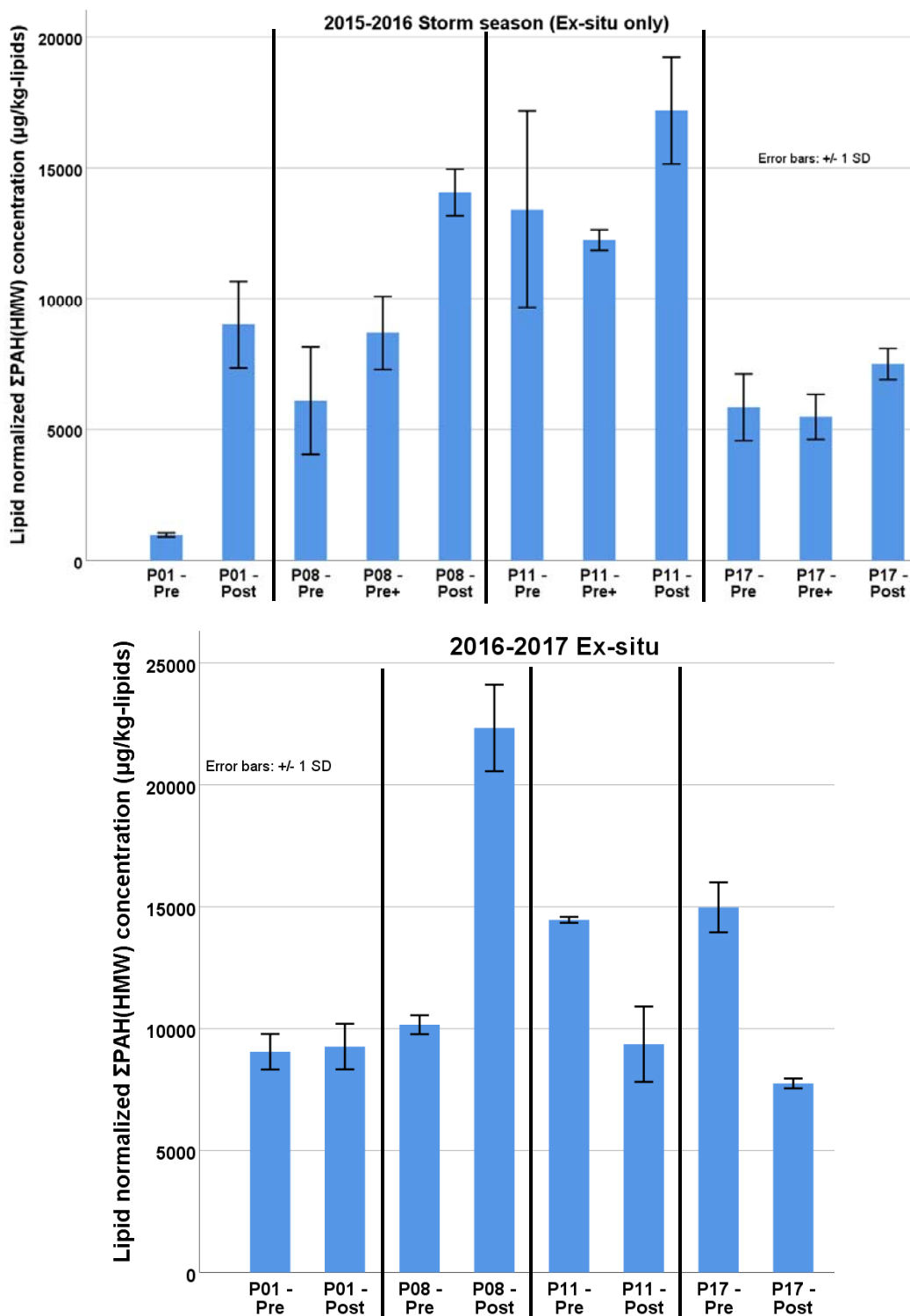


Figure 5-6: Pre/post season 2015-2016 and 2016-2017 ex-situ lipid normalized ΣPAH_{HMW} concentrations per location.

The addition of the trap material on the pre cores does not lead to significant tissue

$\Sigma\text{PAH}_{\text{HMMW}}$ concentration changes compared to tissues exposed only to pre storm cores. This result is similar to the one we encountered in ex-situ porewater measurements and supports the idea that runoff contributions are generally consistent and this has led the sediments to have reached as much of an equilibrium with the runoff as such a dynamic system can allow. In any case, we can say with more confidence that freshly depositing material in the San Diego bay does not lead to increased tissue burdens.

Tissue $\Sigma\text{PAH}_{\text{HMMW}}$ concentrations significantly decrease in locations P11 (PStT: $p=0.058$) and P17 (PStT: $p=0.011$) during the 2016-2017 storm season. This change is different to the increases observed in the sediment cores, unchanged $\Sigma\text{PAH}_{\text{HMMW}}$ porewater concentrations in P11 and smaller decrease of $\Sigma\text{PAH}_{\text{HMMW}}$ porewater concentrations in P17. These observations are revealing that increases in bulk sediment $\Sigma\text{PAH}_{\text{HMMW}}$ concentrations do not necessarily imply additional body burden to the benthos. This is a very important message given that the current regulatory framework relies on bulk sediment measurements to assess exposure and risk. Lastly, $\Sigma\text{PAH}_{\text{HMMW}}$ concentrations of sediment, porewater and tissue at P08 in the 2016-2017 season, increased significantly but this change cannot have originated from the storm runoff given our previous discussions.

Summarizing the results from ex-situ measurements, tissue $\Sigma\text{PAH}_{\text{HMMW}}$ concentrations in P17 are similar or lower to the other locations and that is a strong indication that runoff is not having a direct negative effect on the receiving benthos. The consistency of P17 $\Sigma\text{PAH}_{\text{HMMW}}$ porewater concentrations in the 20-30 ng L⁻¹ range combined with the general similarity of pre+ to pre/post porewater and tissue measurements can be an indication that the sediment may be in equilibrium with the runoff. If runoff particles have been having similar composition for years, this may have led to a state of balance between the newly depositing and previously deposited

material that has been subjected to erosion and mixing. There are many processes that affect sediments which are usually at work at the same time and it is difficult to imply causality from a single process, however in the case of runoff, we have multiple lines of evidence suggesting that it doesn't have significant impact on the receiving ecosystem.

5.3.4 Relating bioaccumulation to freely dissolved and bulk sediment concentrations

When individual lipid normalized PAH (FLA, PYR, CHR, BaA, BbF, BkF and BaP separately) concentrations are plotted against respective normalized porewater PAH

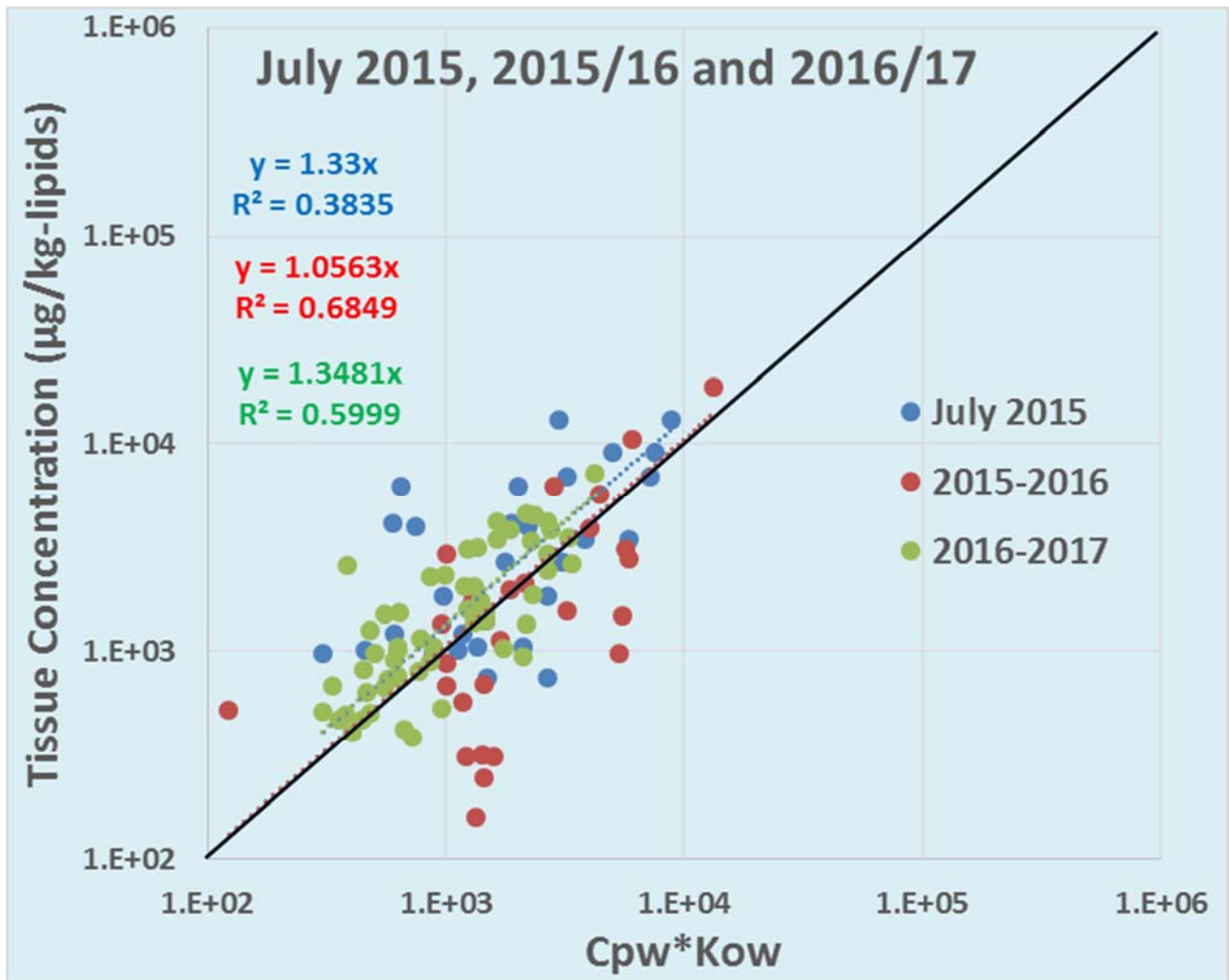


Figure 5-7: Log-log graph of measured normalized porewater concentrations versus lipid normalized ΣPAH_{HMW} concentrations for all sampling events.

concentrations ($C_{pw} * K_{ow}$) on log-log graph with the intercept set to 0, the BPAF (as defined in Eq. 4) is estimated to be around 1 (Figure 5-7). A slope of approximately 1 (as indicated by the black diagonal line) indicates that K_{ow} is a reasonable estimate of the bioconcentration factor (Eq. 7). Irrespective of sampling method (in- vs ex-situ), location, sampling period and compound, data behave agnostically and cluster around the 1:1 line. This is a very powerful result that hints at the robustness of the technique as a bioaccumulation predicting mechanism.

$$BPAF \sim 1 \rightarrow \frac{\frac{C_{tissue}}{f_{lipids}}}{C_{pw} * K_{ow}} \sim 1 \rightarrow K_{ow} \sim \frac{C_{tissue}}{C_{pw}} = BCF \quad (7)$$

A more vigorous statistical analysis of the above regression confirms the observations. There is a strong correlation (slope= 1.203, R=0.873) between the variables when looking at the dataset as a whole (N=111) and not separated in seasons. The $R^2=0.762$ value tells us that more than 75% of the variability in lipid normalized ΣPAH_{HMW} concentrations, can be accounted for by the porewater concentrations. The above correlation is statistically significant by Pearson correlation (Sig. (1-tailed) < 0.000) and ANOVA (F=351.5, Sig. < 0.000). The statistical significance of the correlation is also supported by the t-distribution (t=18.75, Sig. < 0.000). The 95% confidence interval for the slope is 1.076-1.331 and the residuals follow a fairly normal distribution (Figure A11). All the above confirm the observation from the graph that porewater concentrations as measured by SPMEs provide a good estimation of the PAH load residing in the clam lipids, a sediment ingesting organism nonetheless.

This observation has been reported in the literature (Lu et al., 2011; Mackay, 1982) for other organisms and suggests that lipids can be satisfactorily proxied by octanol. It is also strongly indicating that passive sampling can be an acceptable surrogate for measuring/predicting bioaccumulation. The importance of this conclusion in our study is that it

confirms the observation that different measurement conditions over a 2-year period, produce a consistent trend.

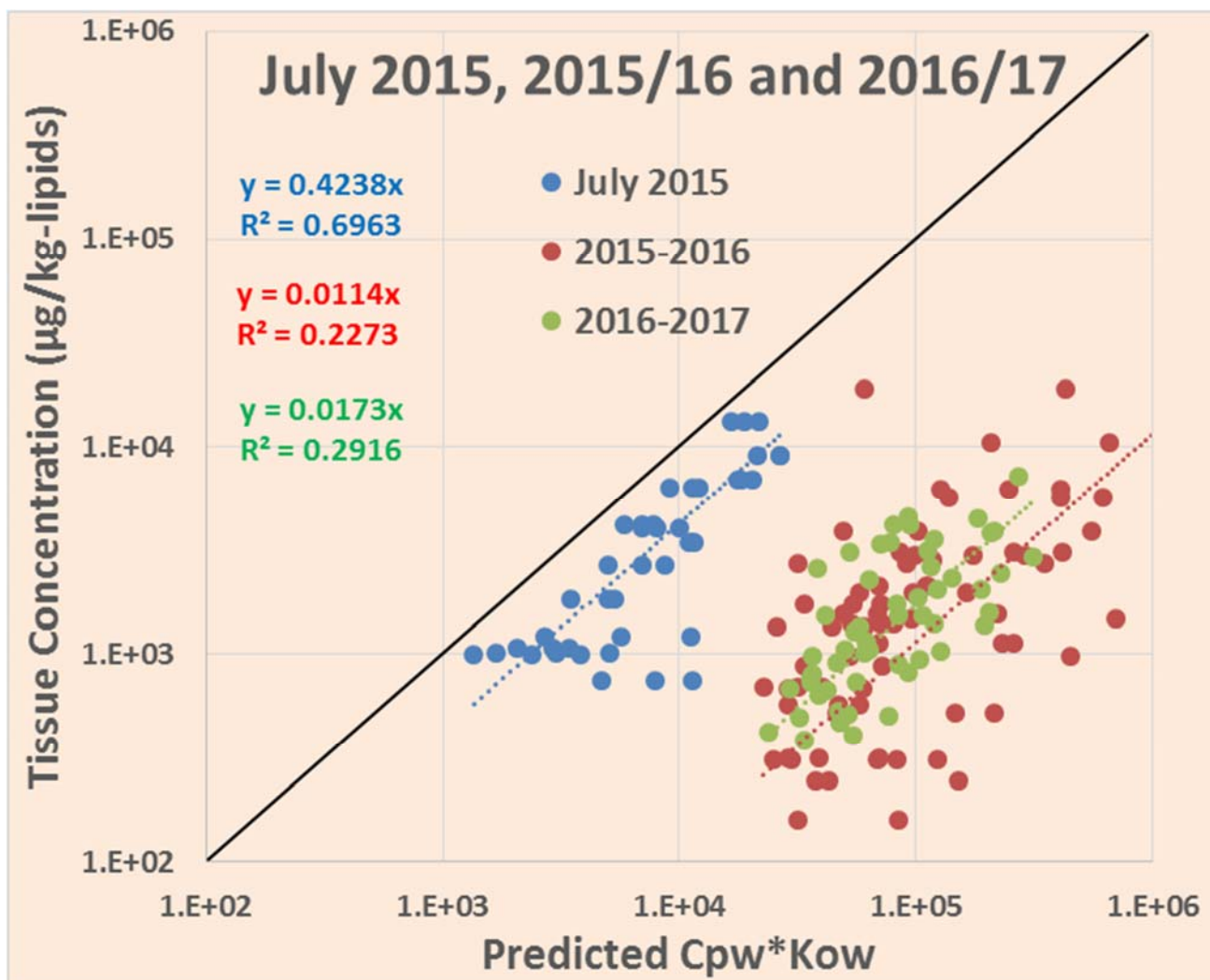


Figure 5-8: Log-log graph of predicted porewater concentrations versus lipid normalized ΣPAH_{HMW} concentrations for all sampling events.

Next, a similar log-log graph is presented using the predicted rather than the measured porewater PAH concentrations (Figure 5-8) and at first glance, the plot exhibits more variance and scattering. The data here originate from organic carbon normalized sediment concentrations for the same 7 HMW PAHs and are calculated according to Eq. 6. It appears that sediment is

$$\text{Predicted BPAF} = \frac{\frac{c_{tissue}}{f_{lipids}}}{118 \frac{c_{sed}}{f_{oc} * K_{ow}}} \quad (6)$$

over-predicting porewater (and tissue) concentrations by 1-2 orders of magnitude as indicated by the smaller slopes (all data are below the 1:1 line). This observation has been well documented (Cornelissen et al., 2005; Cornelissen and Gustafsson, 2004; Lohmann et al., 2005) and is especially true in urban sediments where the increased presence of soot disproportionately dominates PAH speciation (Accardi-Dey and Gschwend, 2002; Bucheli and Gustafsson, 2000; Chan et al., 2002).

Sediment collected in July 2015 (before the 2015/2016 storm season) exhibits greater bioavailability than the 2015/2016 and 2016/2017 storm seasons as indicated by its closer proximity to the 1:1 line. The reduced rainfall observed in the 2012-2015 period (Figure A12) and the subsequent storm seasons suggest that stormwater may lead to sediment recontamination but have less significant effect on bioaccumulation likely due to association of the PAHs in stormwater with less available forms such as BC (Gschwend and Wu, 1985; McGroddy and Farrington, 1995). One question that cannot be answered by this study is whether the stormwater recontamination will become more available over time and move toward the 2015 levels.

In summary we see the challenges associated with sediment measurements. Being a very complex matrix, analysis is affected by highly sorptive black carbon particles like the ones transported by stormwater (previous chapter), that exhibit reduced PAH bioavailability. On the other hand, porewater passive sampling is less affected by those issues and remains generally consistent in predicting bioaccumulation.

5.3.5 *Effects of storm runoff on receiving sediments*

Despite the many similarities between runoff and near field particles that we saw in the previous chapter, we did not see compelling evidence in this study that runoff is definitively leading to bulk sediment contamination while it was clearer that it does not lead to increased freely dissolved $\Sigma\text{PAH}_{\text{HMW}}$ concentrations and bioaccumulation.

In the previous chapter, multiple lines of evidence indicated that the most pronounced effects of stormwater runoff on sediment are manifesting in the near field. Our analysis showed that coarse silt and sand particles in the runoff, have high total organic carbon (TOC), black carbon (BC) and PAH content. The analysis of the material collected in the receiving waters by settling traps, shows very similar characteristics in location P17 which is at the mouth of the creek. The strong relation of runoff with the near field was confirmed by PAH ratios which also revealed that these particles are aged and of petrogenic origin. This petrogenic origin was affirmed by the observed abundance of lighter PAHs, as represented by phenanthrene (Phe) and pyrene (Pyr), compared to heavier PAHs, represented by benzo(a)pyrene (BaP) that have larger proportions in particles originating from pyrolytic sources.

Despite the above link between runoff and the near field, there was not conclusive evidence that storm runoff actually leads to increased sediment concentrations. In season 2015-2016, the settling trap material collected in P17 had lower ΣPAH , Pyr and BaP concentrations compared to sediment core material collected both before and after the storm season; if anything, this means that runoff material is not contaminating the sediment. This result also cannot explain the increase of sediment PAH concentrations from the beginning to the end of the storm season; based on the previous observation, the increases in sediment PAH concentrations should be attributed to another process and not runoff deposition. Furthermore, the higher PAH

concentrations in location P11 compared to P17, could not have been caused by the runoff which as we said before, has the highest influence in P17.

All of our bioaccumulation and most of our porewater measurements showed that sediment in location P17 led to similar or lower $\Sigma\text{PAH}_{\text{HMW}}$ concentrations compared to the other sampling locations. These results lead to the conclusion that stormwater runoff is not contributing to further contamination in the receiving waters and there is no ambiguity to this conclusion as there was in the sediment discussion above.

This increased certainty was provided by the demonstrated strong positive correlation of porewater to lipid normalized HMW PAH concentrations. This correlation confirmed the observations of other studies which concluded that freely dissolved PAH concentrations as measured by SPME passive samplers are a good surrogate for inferring tissue PAH concentrations. Sediment is the matrix that controls sorption of PAHs through its organic carbon fraction and is thus affected much more than porewater when varying amounts of desorption resistant BC are present. This leads not only to overprediction of bioaccumulation but also inconsistency between sampling measurements.

Another interesting observation was the constancy of $\Sigma\text{PAH}_{\text{HMW}}$ porewater concentrations in the 20-30 ng L⁻¹ range which combined with the similarity between pre+ and pre/post measurements, indicate that runoff could have a non-changing signature which over time has led to a relative state of equilibrium of sediment porewater. Other processes than deposition (resuspension, vertical mixing, and bioturbation), seem to add variability (not necessarily seasonal) to bulk sediment concentrations and sometimes lead to localized effects.

This was shown in our in-situ measurements which revealed elevated $\Sigma\text{PAH}_{\text{HMW}}$ porewater and tissue concentrations in location P11 during the 2015-2016 storm season, which

cannot be attributed to stormwater discharges. The ex-situ study did not confirm this result (P11 had lower concentrations than P17) and this can point to the assumption that there must have been a localized sediment process which was not represented in the trap and post season measurements that led to the observed in-situ increases. This discrepancy between some of the in-situ and ex-situ results is a reminder that ex-situ studies can be used only as an indicator of the sediment state but remain ignorant to ongoing and spatially limited sedimentary processes.

5.4 Conclusions

Our measurements provided the ability to directly compare porewater, sediment and tissue measurements from the same sampling locations and periods and demonstrated through different lines of evidence, that PAHs in urban stormwater runoff do not have a degrading effect on the receiving sediment ecosystem. Such a conclusion could not have been reached by bulk sediment concentrations alone and underlines the need to reassess the regulatory framework which considers bulk sediment as the basis for estimating biological and human health risk. The bottom line is that sediment recontamination measured by bulk sediment concentration is not the “whole story”.

From a risk assessment point of view, an important conclusion of this study was the improved assessment of bioavailability through the use of SPME porewater measurements. By demonstrating that porewater concentrations predicted bioaccumulation in bioassays with an effective bioaccumulation factor approximately equal to the octanol-water partition coefficient, we can suggest replacing bulk sediment measurements with porewater measurements to achieve improved risk assessment.

5.5 References

- Accardi-Dey, A.M., Gschwend, P.M., 2002. 23 Assessing the combined roles of natural organic matter and black carbon as sorbents in sediments. *Environ. Sci. Technol.* 36, 21–29. <https://doi.org/10.1021/es010953c>
- Bucheli, T.D., Gustafsson, O., 2000. 24 Qualification of the soot-water distribution coefficient of PAHs provides mechanistic basis for enhanced sorption observations. *Environ. Sci. Technol.* 34, 5144–5151. <https://doi.org/10.1021/es000092s>
- Chan, C., MacFarlane, J., Gustafsson, Ö., Haghseta, F., Gschwend, P.M., 2002. 22 Quantification of the Dilute Sedimentary Soot Phase: Implications for PAH Speciation and Bioavailability. *Environ. Sci. Technol.* 31, 203–209. <https://doi.org/10.1021/es960317s>
- Cornelissen, G., Gustafsson, Ö., 2004. 26 Sorption of Phenanthrene to Environmental Black Carbon in Sediment with and without Organic Matter and Native Sorbates. *Environ. Sci. Technol.* 38, 148–155. <https://doi.org/10.1021/es034776m>
- Cornelissen, G., Gustafsson, Ö., Bucheli, T.D., Jonker, M.T.O., Koelmans, A.A., Van Noort, P.C.M., 2005. 21 Extensive sorption of organic compounds to black carbon, coal, and kerogen in sediments and soils: Mechanisms and consequences for distribution, bioaccumulation, and biodegradation. *Environ. Sci. Technol.* 39, 6881–6895. <https://doi.org/10.1021/es050191b>
- Di Toro, D.M., Zarba, C.S., Hansen, D.J., Berry, W.J., Swartz, R.C., Cowan, C.E., Pavlou, S.P., Allen, H.E., Thomas, N.A., Paquin, P.R., 1991. 3 Technical basis for establishing sediment quality criteria for nonionic organic chemicals using equilibrium partitioning. *Environ. Toxicol. Chem.* 10, 1541–1583. <https://doi.org/10.1002/etc.5620101203>
- F.A.P.C. Gobas, Assessing Bioaccumulation Factors of Persistent Organic Pollutants in Aquatic Food-Chains. In: Harrad S. (eds) *Persistent Organic Pollutants (2001)* 145-165
- Greenberg, M.S., Chapman, P.M., Allan, I.J., Anderson, K.A., Apitz, S.E., Beegan, C., Bridges, T.S., Brown, S.S., Cargill, J.G., McCulloch, M.C., Menzie, C.A., Shine, J.P., Parkerton, T.F., 2014. 7 Passive sampling methods for contaminated sediments: risk assessment and management. *Integr. Environ. Assess. Manag.* 10, 224–236. <https://doi.org/10.1002/ieam.1511>
- Gschwend, P.M., Wu, S.C., 1985. 5 On the Constancy of Sediment-Water Partition Coefficients of Hydrophobic Organic Pollutants. *Environ. Sci. Technol.* 19, 90–96. <https://doi.org/10.1021/es00131a011>
- Hylleberg, J., Gallucci, V.F., 1975. 0 Selectivity in feeding by the deposit-feeding bivalve *Macoma nasuta*. *Mar. Biol.* 32, 167–178. <https://doi.org/10.1007/BF00388509>
- Kraaij, R., Mayer, P., Busser, F.J.M., Van Het Bolscher, M., Seinen, W., Tolls, J., Belfroid,

- A.C., 2003. 2 Measured pore-water concentrations make equilibrium partitioning work - A data analysis. *Environ. Sci. Technol.* 37, 268–274. <https://doi.org/10.1021/es020116q>
- Lohmann, R., Macfarlane, J.K., Gschwend, P.M., 2005. 25 Importance of black carbon to sorption of native PAHs, PCBs, and PCDDs in Boston and New York Harbor sediments. *Environ. Sci. Technol.* 39, 141–148. <https://doi.org/10.1021/es049424+>
- Lu, X., Skwarski, A., Drake, B., Reible, D.D., 2011. 1 Predicting bioavailability of PAHs and PCBs with porewater concentrations measured by solid-phase microextraction fibers. *Environ. Toxicol. Chem.* 30, 1109–1116. <https://doi.org/10.1002/etc.495>
- Mackay, D., 1982. 4 Correlation of Bioconcentration Factors. *Environ. Sci. Technol.* 16, 274–278. <https://doi.org/10.1021/es00099a008>
- Mcgroddy, S.E., Farrington, J.W., 1995. 6 Sediment Porewater Partitioning of Polycyclic Aromatic Hydrocarbons in Three Cores from Boston Harbor, Massachusetts. *Environ. Sci. Technol.* 29, 1542–1550. <https://doi.org/10.1021/es00006a016>
- Reible, D.D., 2014. *Processes, Assessment and Remediation of Contaminated Sediments*, SERDP/ESTCP Environmental Remediation Technology. Springer New York, New York, NY. <https://doi.org/10.1007/978-1-4614-6726-7>
- X.X. Lu, Y. Hong, D.D Reible. Assessing Bioavailability of Hydrophobic Organic Compounds and Metals in Sediments Using Freely Available Porewater Concentrations. In: Reible D. (eds) *Processes, Assessment and Remediation of Contaminated Sediments*. SERDP ESTCP Environmental Remediation Technology, (2014) vol 6
- You, J., Landrum, P.F., Lydy, M.J., 2006. 9 Comparison of chemical approaches for assessing bioavailability of sediment-associated contaminants. *Environ. Sci. Technol.* 40, 6348–6353. <https://doi.org/10.1021/es060830y>

Chapter 6

Conclusions and Future Works

This work can provide guidance in analytical laboratory methods as well as decision making around the impact of urban runoff on receiving sediment. The PLE method proposed in chapter 2 can be utilized in the extraction of urban weathered sediment as it takes into account its inherent challenges and can thus increase the productivity and sample turnaround in relatively small labs. The findings from the study on the physical, chemical and biological effects of urban runoff on receiving waters, can be useful in two ways. Firstly, they can provide an estimation of the recontamination potential of urban runoff and assist in decision making regarding sediment remediation considerations. Secondly, the characteristics of urban runoff as presented in this work can be useful in the development of better best management practices (BMPs) solutions.

The initial phase of this study focused on developing a well-rounded and robust method of extracting PAHs from sediment. Although there is an EPA Method (3545A) on PLE, the proposed high mass of extracting solids can lead to high levels of NOM in the extracts that will require multiple time consuming cleanup steps in order to generate low interference final extracts. That can reduce productivity and increase processing costs in relatively small labs with a large turnaround of samples. Our trials of several different PLE methods for the extraction of PAHs from weathered sediment, we concluded that a mixture of 80% DCM - 20% Hex, 2 static cycles of 5 mins, 100 °C and in-cell silica cleanup are conditions that consistently provide an extract that has low background during analysis. This method has been used for all subsequent sediment analysis in our lab for this and other projects.

The measurements we conducted on urban stormwater showed that its contamination potential is limited to the area close to the discharge point. This contamination consists of large particles ($> 20 \mu\text{m}$) that have higher than background concentrations of petrogenic PAHs. A possible origin of those particles is a nearby highway that crosses the watershed and contributes eroded pieces of tarmac coated with motor oil and fuel as well as tire and brake lining debris. There are indications of a second source of particles in our study area that deposits material disproportionately in the outer bay. Considering specific characteristics of the location, this source is potentially an aggregate of atmospheric deposition and propeller wash resuspension from ships operating within the San Diego bay.

An important novelty of this work was the chemical analysis of size fractionated runoff. Looking into PAH loads on different size particles in runoff and comparing them to the deposition profile of settling material in the receiving waters, proved to be a good combination in describing both their origin and fate. In contrast, sediment cores were not a useful tool in this study because they do not accurately reflect freshly depositing material but rather a vertical integration of multiple years of deposition.

The observed increases in sediment PAH concentrations in the near field were not mirrored in our bent-nosed clam bioaccumulation studies. As we suspected in our chemical measurements of runoff and settling material, the high BC content of the solids depositing in location P17 plays a role in the limited partitioning of PAHs in the freely dissolved phase and thus bioavailability. This result reaffirms relatively recent studies in their conclusions that bulk sediment concentrations are not necessarily an accurate measure of exposure risk.

Our study also suggested that PAHs in the porewater might be controlling steady state bioaccumulation despite sediment ingestion being the route of uptake. This was shown by the

good and consistent correlation between porewater and lipid normalized tissue concentrations. These results are also suggesting that passive sampling of porewater can be a relatively inexpensive surrogate for measuring bioaccumulation.

Below is a list of propositions for future work on PAH extraction from sediment as well as assessing the effects of runoff on sediments:

- 1) The composition of sediments is complex and varies for different locations. As such, further studies should be conducted on extracting multiple certified reference sediments with a wide array of TOC and BC contents in order to assess their potential correlations with PAH extraction recoveries.
- 2) Using the results of the above proposition, create a model that will predict PAH recoveries from previously unknown sediment based on simple TOC or BC measurements.
- 3) More urban drainage basins should be studied and fully characterized in order to obtain a more rounded impact assessment of urban runoff.
- 4) Future studies on runoff and its effects on sediment should consider deploying atmospheric deposition traps. That way they will also have information about the solids distribution of atmospheric particles in the area of study. PAH analysis should also be considered in order to derive PAH ratios and compare them to the ratios of the solids carried by the runoff and the settling traps in the receiving waters.
- 5) Although stormwater management entails reducing runoff contaminant loads by reducing runoff volume, it is not yet widely applied in urban watersheds and thus does not significantly address the loads themselves.
- 6) Results from this study should be utilized in designing more effective and efficient BMPs

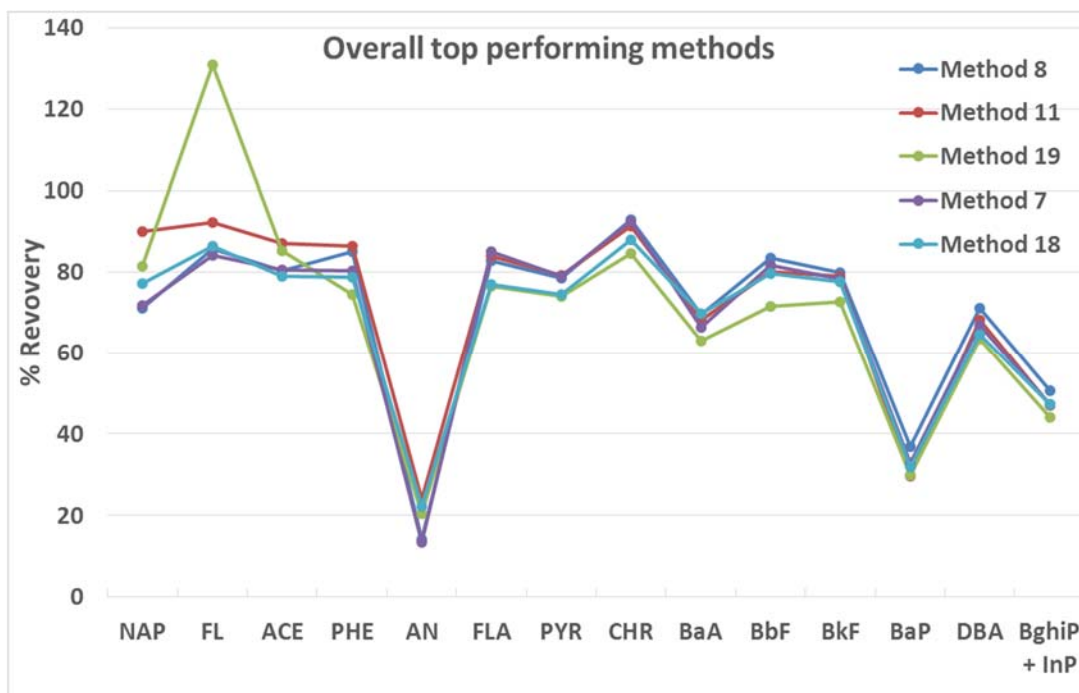


Figure A2: Comparison of CRM PAH recovery signatures of the 5 best extraction methods.

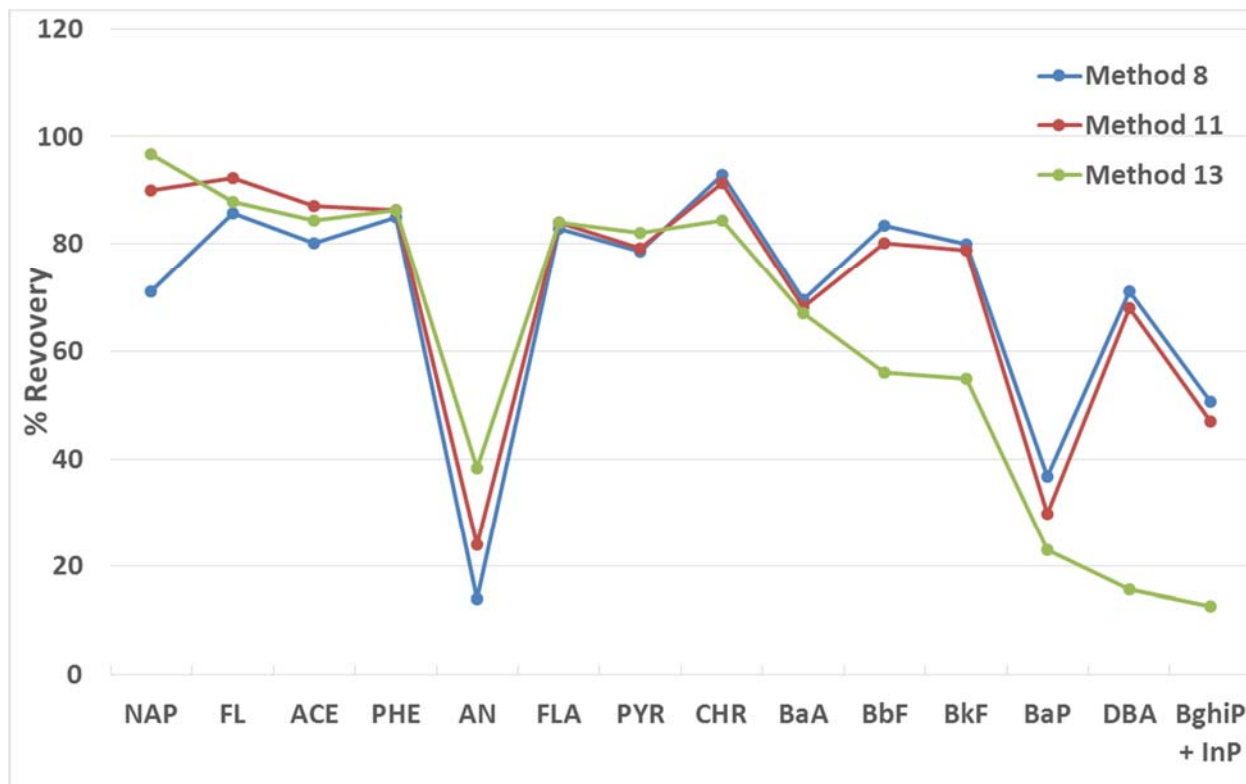


Figure A3: Comparison of CRM PAH recovery signatures of methods 8, 11 and 13.

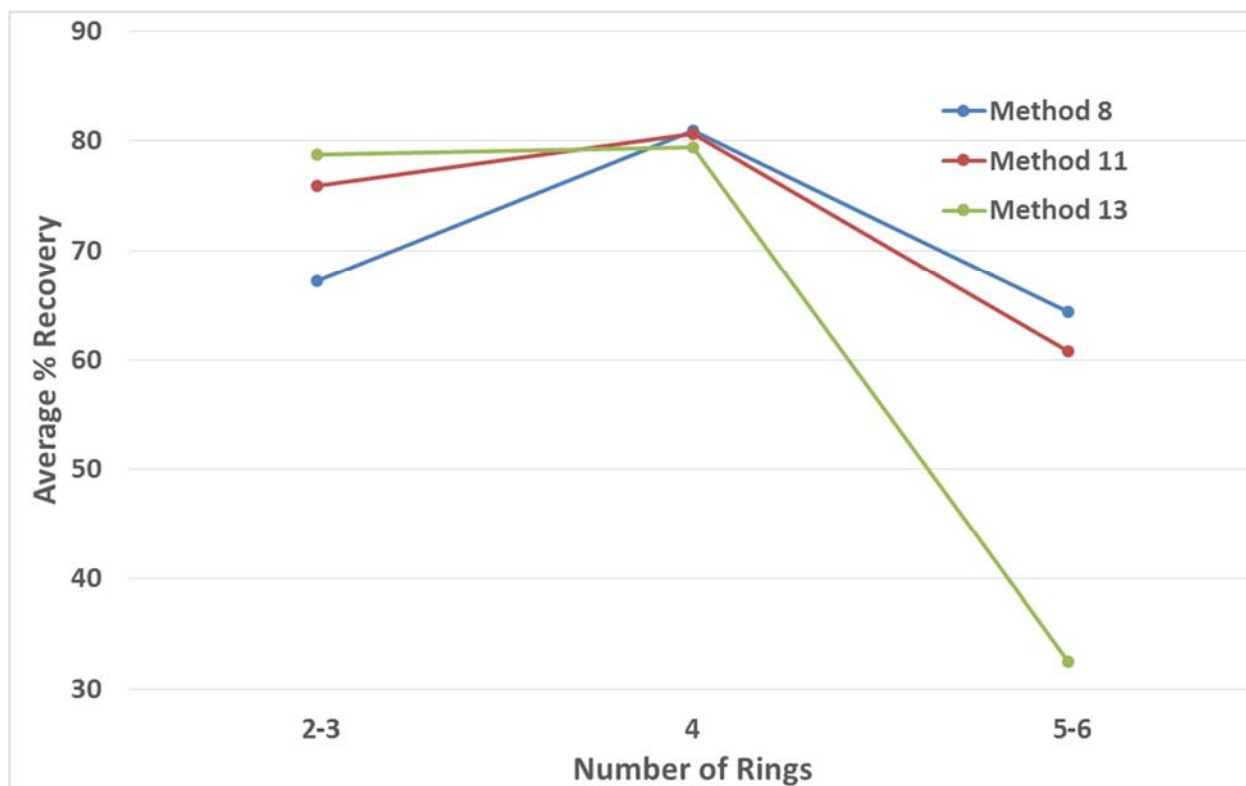


Figure A4: Comparison of the average recoveries of 3 groups (2-3, 4 and 5-6 ring) of PAHs from CRM for methods 8, 11 and 13.

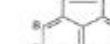
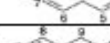
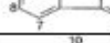
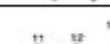
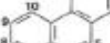
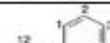
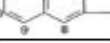
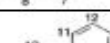
	Compound	Structure	MW (g/mol)	C_w^{sat} (mg/L)	p^{*o} (mm Hg)	$\log K_{ow}$	$\log K_{oo}^o$	TEF	PLHS Rank ^d
Low Molecular Weight PAHs	Naphthalene		128.1	31.0	1.8×10^{-2}	3.37		–	80
	Acenaphthylene		152.1	16.1	2.9×10^{-2}	4.0	3.40	–	343
	Acenaphthene		154.2	3.80	1.6×10^{-3}	3.92	3.65	–	168
	Fluorene		166.2	1.90	7.1×10^{-4}	4.18	3.86	–	300
	Phenanthrene		178.2	1.10	9.6×10^{-4}	4.57	4.15	–	248
	Anthracene		178.2	0.045	1.7×10^{-5}	4.54	4.15	–	306
High Molecular Weight PAHs	Fluoranthene		202.3	0.26	5.0×10^{-6}	5.22	4.58	–	138
	Pyrene		202.3	0.132	2.5×10^{-6}	5.18	4.58	–	255
	Benz[a]anthracene		228.3	0.011	2.2×10^{-8}	5.91	6.14	0.1	38
	Chrysene		228.3	0.002	6.3×10^{-9}	5.65	5.30	0.001	141
	Benzo[b]fluoranthene		252.3	0.0015	5.0×10^{-7}	5.80	5.74	0.1	10
	Benzo[k]fluoranthene		252.3	0.0008	5.1×10^{-7}	6.0	5.74	0.01	61
	Benzo[a]pyrene		252.3	0.0038	5.6×10^{-9}	6.04	6.74	1	8
	Benzo[g,h,i]perylene		276.3	0.0003	1×10^{-10}	6.50	6.52	–	321
	Dibenz[a,h]anthracene		278.4	0.0006	1.0×10^{-10}	6.75	6.20	1	15
	Indeno[1,2,3-c,d]pyrene		276.3	0.062	1.0×10^{-1}	7.66	6.20	0.1	174

Figure A5: Chemical structures and selected properties of the 16 USEPA priority pollutant PAHs. (source: [www.enviro.wiki/index.php?title=Polycyclic_Aromatic_Hydrocarbons_\(PAHs\)](http://www.enviro.wiki/index.php?title=Polycyclic_Aromatic_Hydrocarbons_(PAHs)))

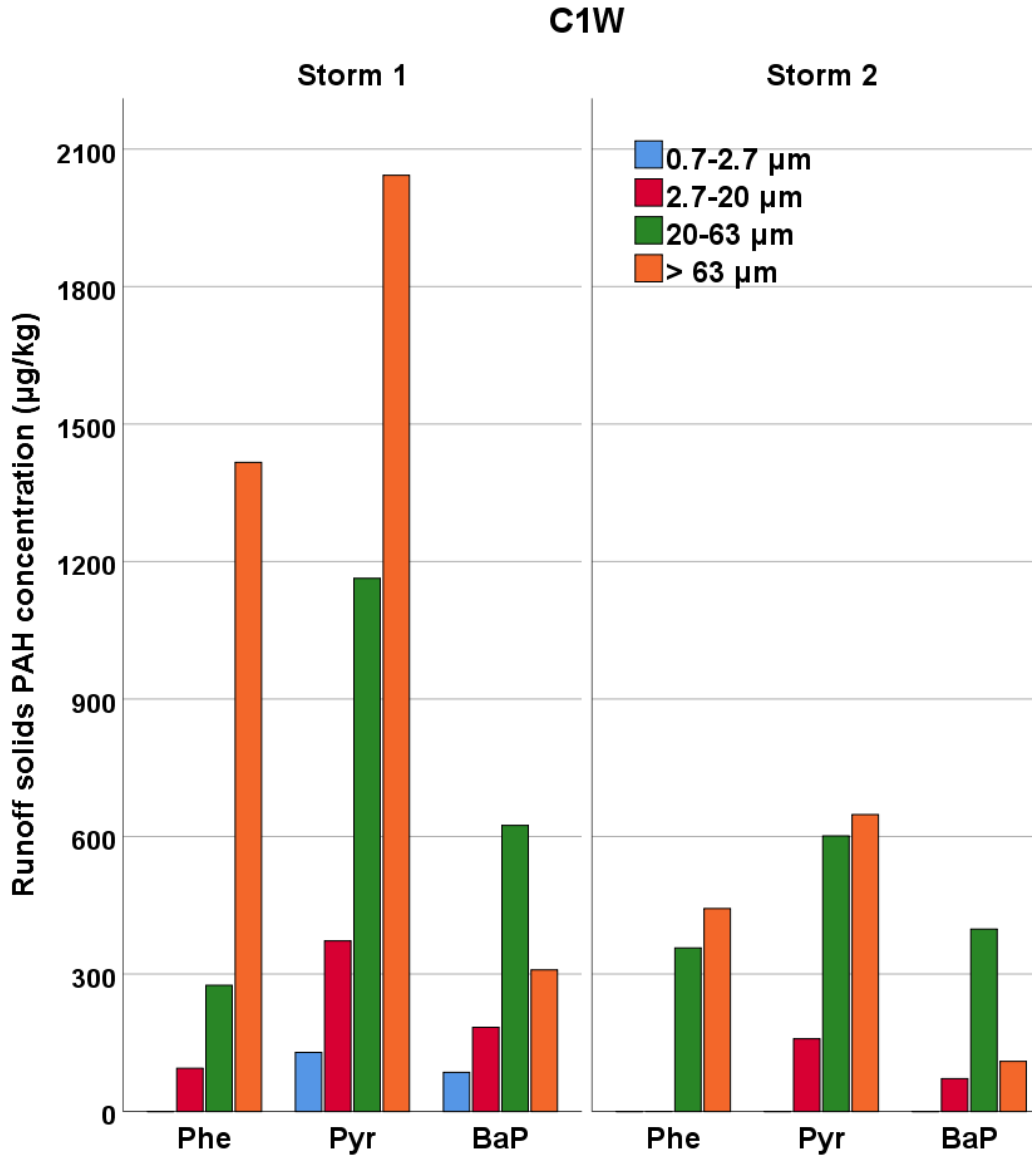


Figure A6: Concentrations of PHE, PYR and BaP in different fractions of composite runoff solids for both storms at Paleta creek. All values are from single measurements.

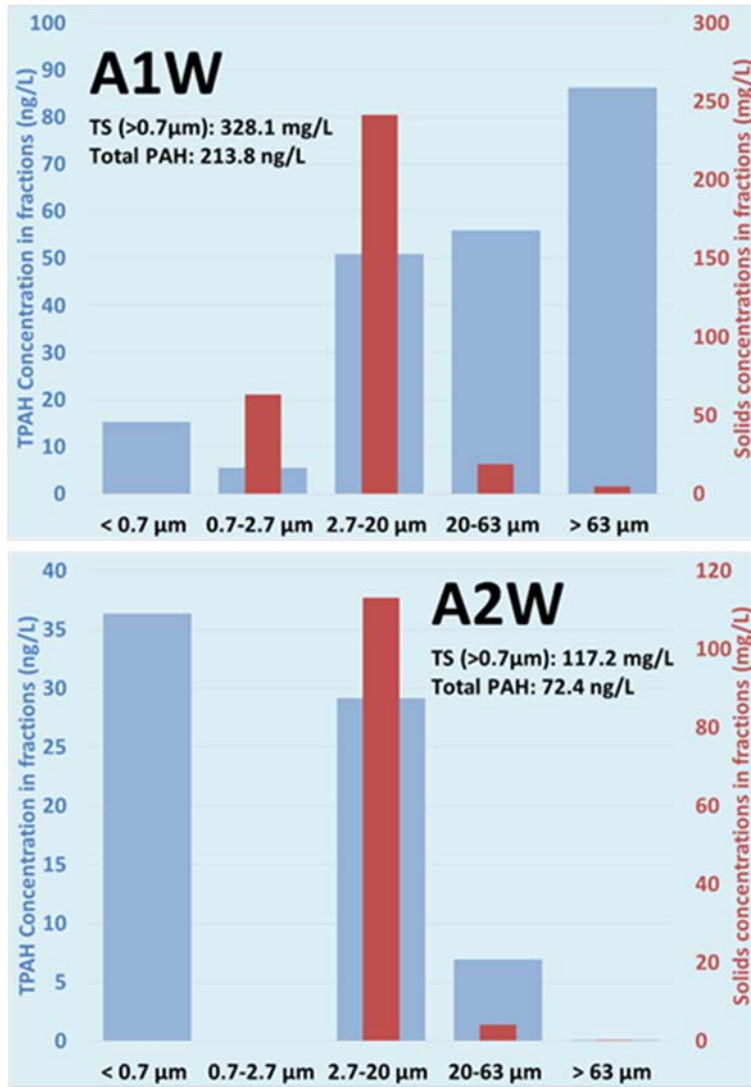


Figure A7: Storm 2 - Total solids and total PAH concentrations in different solid fractions of runoff grab samples at progressing time points at Paleta creek.

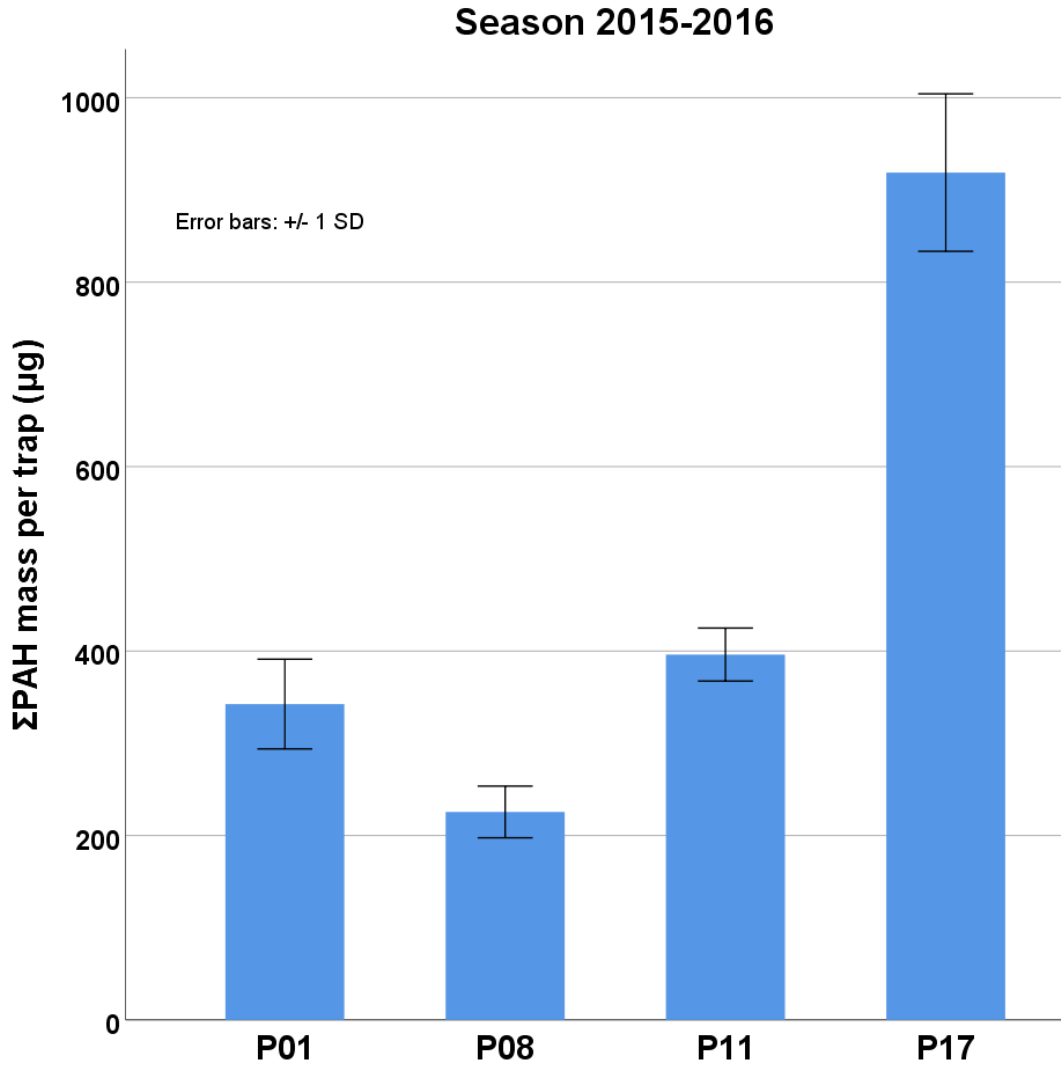


Figure A8: ΣPAH of settling particles collected by the deployed traps during season 2015-2016.

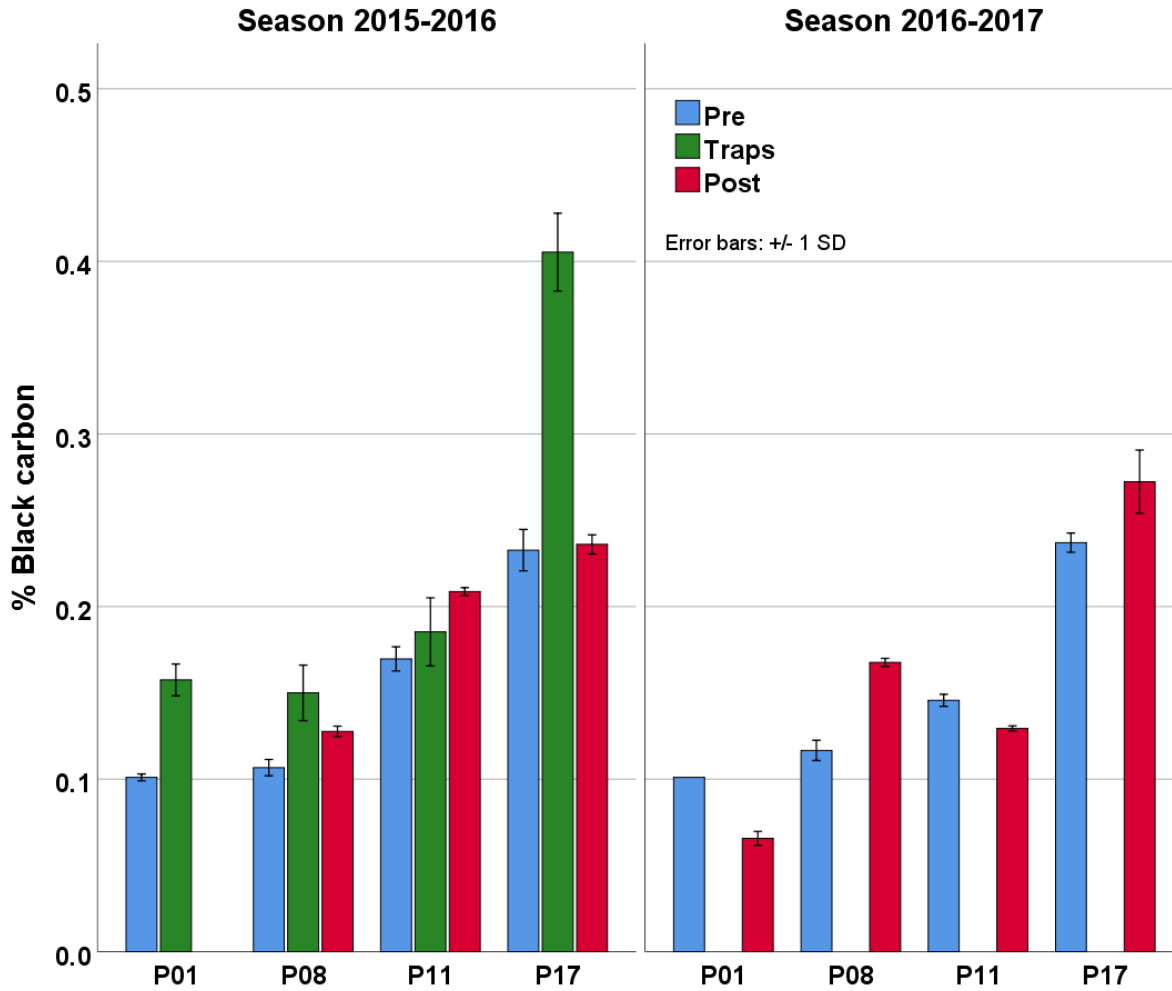


Figure A9: Receiving sediment (Pre and Post) and settling trap BC content in all sampling locations during storm seasons 2015-2016 and 2016-2017.

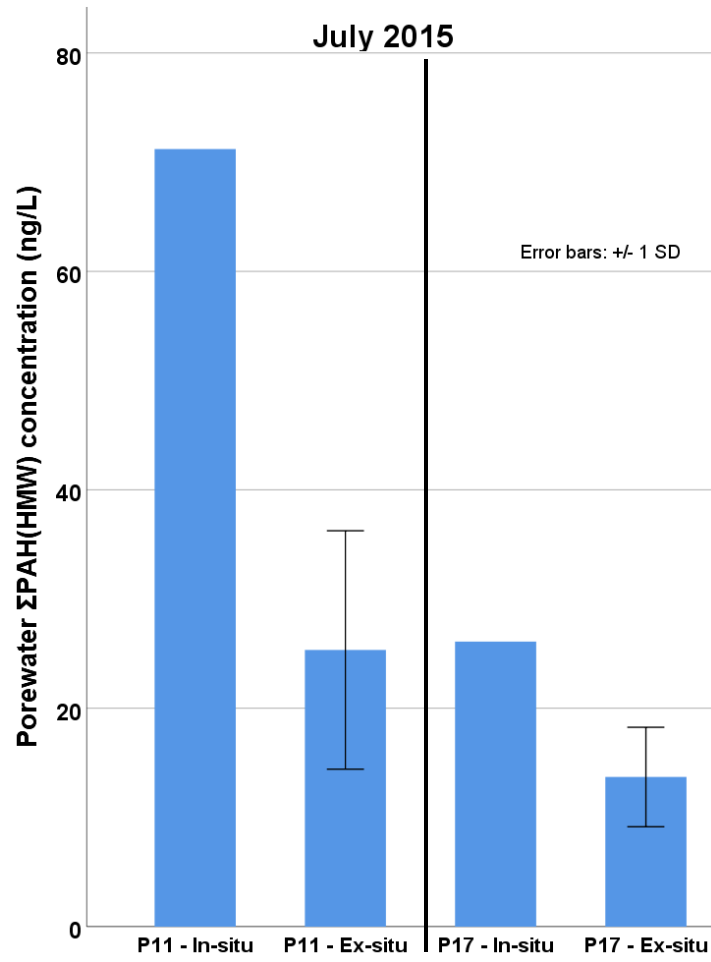


Figure A10: July 2015 in-situ and ex-situ porewater $\Sigma\text{PAH}_{\text{HMW}}$ concentrations per location.

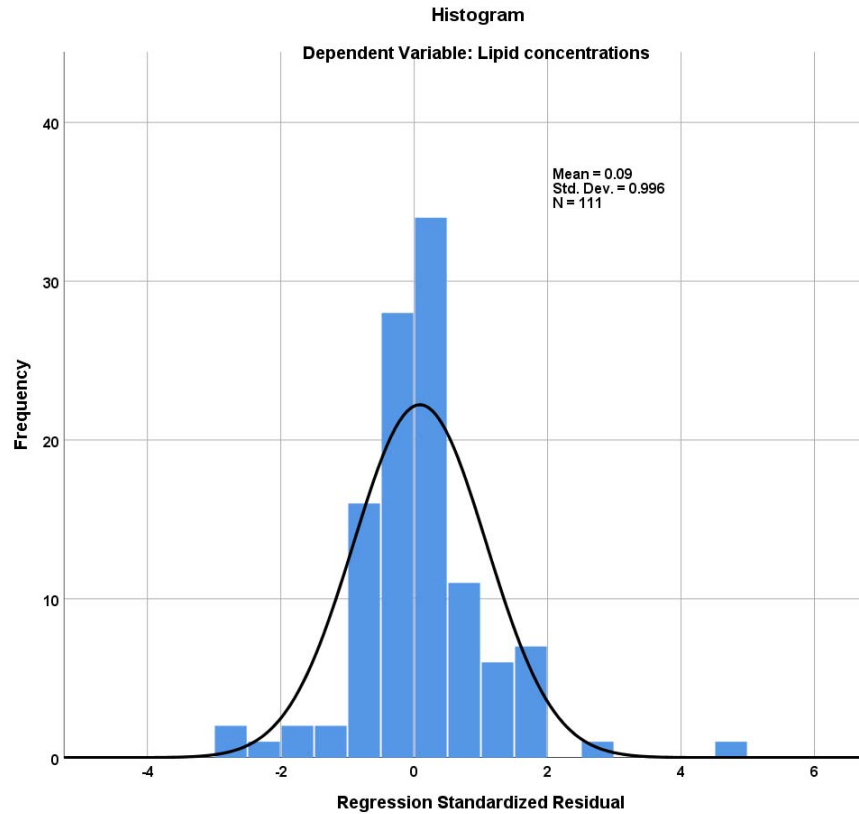


Figure A11: Histogram showing the distribution of the residuals following the regression of porewater and tissue measurements.

Water Year (Oct-Sep)	Actual Rainfall (inches)	Normal Rainfall (inches)	% of Normal
2011	12.70	10.34	123
2012	7.90	10.34	76
2013	6.55	10.34	63
2014	5.09	10.34	49
2015	11.91	10.34	115
2016	8.18	10.34	79
2017	12.73	10.34	123
2018	3.34	10.34	32

*Normal rainfall is the average of a previous period of multiple years

Figure A12: Annual precipitation in San Diego during the 2011-2018 period. (source: <https://www.sdcwa.org/annual-rainfall-lindbergh-field>)

Table A1: Extraction % recoveries of 15 PAHs from CRM for the 25 tested methods. In parenthesis the % relative standard deviation.

	1	2	3	4	5	6	7	8	9	10	11	12	13
NAP	68.4 (15.4)	73.8 (2)	76.2 (7.8)	72.2 (2)	71.7 (2.8)	66.7 (17.7)	71.7 (3.3)	71.1 (2.8)	51.5 (22.7)	75.6 (1.5)	90 (3.4)	87.2 (4.3)	96.8 (2.2)
FL	125 (13.5)	129.4 (2.5)	121.7 (8.5)	86 (1)	87.1 (2)	81.1 (11.8)	84.1 (2.3)	85.7 (1.9)	56.3 (23.5)	72 (2.4)	92.2 (0.2)	79.1 (6)	87.9 (3.1)
ACE	69.7 (12.7)	74.9 (4.5)	77.5 (7.6)	75.1 (1.9)	72.2 (4.5)	70 (16.2)	80.5 (3.2)	80.2 (0.8)	48.9 (21.2)	68.4 (1.7)	87 (1.5)	73.3 (5.1)	84.3 (2.9)
PHE	64.6 (9.4)	77.3 (5.5)	77.3 (9.9)	64.3 (1.9)	71.4 (1.5)	73.9 (6.3)	80.3 (1)	85 (4.2)	51.9 (21.5)	73.8 (0.7)	86.2 (0.9)	82.9 (5.5)	86.3 (2.2)
AN	16 (11.5)	14.5 (16)	15.5 (6.1)	15.5 (6.2)	15.4 (7.2)	16.7 (1.4)	13.5 (15.9)	14 (58.4)	18.2 (23.4)	24.8 (4.6)	24 (13.3)	26.6 (2.8)	38.3 (0)
FLA	65.8 (10.7)	74.8 (5.9)	71.4 (6.3)	70 (2.8)	68.3 (1.4)	67.8 (4.9)	85.1 (2.8)	82.8 (0.9)	53.8 (21)	75 (5)	83.9 (2)	74.7 (4.2)	84 (2.6)
PYR	62.6 (5.1)	70.1 (4)	65.3 (7.2)	64 (3)	62.6 (1.9)	65.1 (3)	79 (1.8)	78.5 (2.1)	55.7 (22)	72.9 (3.6)	79.2 (0.4)	71.7 (4.1)	82.1 (1.3)
CHR	74.1 (5)	81.4 (5.4)	73.7 (6.6)	74.4 (3.8)	71.6 (1.2)	70.1 (2.2)	92.4 (1.8)	92.9 (1.7)	61.2 (22.1)	82 (3.4)	91.2 (1)	87.6 (5)	84.4 (0.7)
BaA	55.6 (6.7)	56.9 (4.7)	54.4 (6)	55.1 (2.7)	54.2 (3.5)	52.7 (4.9)	66.3 (1.9)	69.4 (4.4)	44.9 (21.7)	60.5 (2.1)	68.1 (1.4)	65.5 (6.3)	67.1 (0.5)
BbF	64 (3.8)	63.9 (8.7)	58.6 (10.4)	63.6 (4.3)	60 (2.1)	54.5 (2.8)	81.6 (0.6)	83.4 (3)	51.1 (24)	72.3 (3.8)	80.1 (0.8)	74.5 (6.5)	56 (0.8)
BkF	63.3 (4.5)	67.1 (3.8)	59.7 (9.6)	65.8 (2.5)	59 (1.1)	54.2 (2.1)	78.2 (0.9)	79.9 (2.5)	48.5 (25.9)	69.3 (3.6)	78.9 (0.9)	73.3 (7.6)	54.8 (2.6)
BaP	22.2 (2.9)	21.9 (1.4)	20.6 (13.8)	25.2 (1.4)	24.2 (4.1)	21.1 (7.7)	32.7 (7.9)	36.8 (8.6)	18.9 (22.6)	24.5 (2.4)	29.7 (7.9)	31 (8.6)	23.1 (2.7)
DBA	61.1 (4.5)	56.6 (5.9)	47 (18.1)	60.7 (3.9)	46.6 (8)	37.8 (2.9)	66.7 (2.2)	71.1 (2.3)	36.1 (27.8)	58.7 (2.8)	68 (0.1)	59.1 (15.3)	15.8 (50.4)
BghiP + InP	40.5 (2.8)	36 (3.9)	28.6 (21.1)	40.6 (2.9)	32 (2.3)	25.7 (4.4)	47.2 (1.8)	50.7 (1.8)	27.4 (23.9)	40.8 (2)	47 (3.2)	37.4 (18)	12.6 (21.9)
Average	60.9 (7.8)	64.2 (5.3)	60.5 (9.9)	59.5 (2.9)	56.9 (3.1)	54.1 (6.3)	68.5 (3.4)	70.1 (6.8)	44.6 (23.1)	62.2 (2.8)	71.8 (2.6)	66 (7.1)	62.4 (6.7)
CRM % Recovery													
	14	15	16	17	18	19	20	21	22	23	24	25	
NAP	80.8 (7.5)	79.5 (8.4)	83.1 (5.3)	75.6 (5.6)	77.2 (10.9)	81.3 (7.1)	71.7 (1.6)	60.5 (5.1)	59.1 (9.7)	42.3 (9.3)	67.7 (8.1)	76.1 (0.2)	
FL	79.3 (6.6)	82.3 (1.8)	81.9 (2.4)	81.1 (4.3)	86.4 (8.2)	130.9 (12.1)	98.9 (2.6)	78.4 (4.3)	66.8 (1.9)	51.9 (13.9)	69.3 (4.9)	75.5 (2.6)	
ACE	76.2 (8.5)	74.3 (3.2)	77.4 (3.7)	77.8 (4.3)	78.9 (10.5)	85.3 (6.6)	80.3 (2.8)	72.2 (4.7)	60 (4.3)	48.5 (10.2)	65.4 (6.5)	69.9 (1.3)	
PHE	78.8 (3.1)	74.3 (0.1)	78.3 (2)	74.8 (4.5)	78.8 (7.7)	74.4 (5.2)	73 (2.7)	69.1 (2.7)	67.5 (1.9)	52.6 (13)	67.2 (8.1)	78 (0.7)	
AN	22.6 (7.3)	34.5 (1.4)	31 (21.4)	22.1 (7.4)	22.2 (9.2)	20.4 (4)	21.2 (1.1)	17 (4.3)	16.8 (11.3)	5.3 (41)	5 (6.1)	5.8 (10.2)	
FLA	76.2 (2.6)	79.1 (2)	76.5 (4)	75.7 (6.6)	76.8 (7.6)	76.5 (1.7)	75.6 (2.6)	72.4 (3.2)	69.9 (2.9)	59.9 (15.3)	71.5 (9.7)	72.8 (1)	
PYR	73.5 (2.3)	77.8 (2.3)	74.2 (2.6)	72 (5.5)	74.5 (7.8)	73.9 (3.5)	73.2 (1.5)	68.9 (2.1)	69.4 (0.5)	56.1 (15.4)	67.7 (8.3)	65.2 (3.3)	
CHR	86.5 (1.8)	82.9 (3.8)	75.1 (2)	86.7 (4.9)	87.8 (3.9)	84.5 (1.9)	83.3 (2.6)	87 (2)	81.7 (5.1)	68 (20.8)	83.5 (9.2)	79.8 (1.1)	
BaA	64.8 (1.5)	64.9 (4)	56 (2.1)	66.5 (4.6)	69.7 (7.4)	63 (1.3)	63.5 (3.5)	62.6 (1.2)	61.9 (1.7)	49.4 (27.5)	53.3 (11.4)	51.1 (0.9)	
BbF	76.3 (1.5)	62.9 (8.4)	56.4 (4.4)	77.5 (5.1)	79.6 (7.2)	71.5 (0)	73 (2.9)	77.3 (1.9)	78.7 (1.6)	59.3 (13.3)	73 (9.6)	68.6 (1)	
BkF	75.1 (1.3)	64.2 (8.2)	55.6 (4.6)	75.8 (4.8)	77.5 (8.3)	72.6 (1.8)	72.5 (3.2)	75.9 (1.8)	74.4 (2)	52.9 (23.6)	69.6 (9.3)	65.5 (3.8)	
BaP	30.9 (1.8)	26.3 (8)	21.1 (17.2)	28.1 (4.3)	31.9 (10.6)	29.8 (3.1)	31.8 (2.2)	25.5 (4)	28.5 (3.6)	14 (18.6)	14.8 (8)	14.8 (20)	
DBA	65.3 (1.7)	38.3 (13.3)	27 (33.3)	62.9 (6.5)	64.4 (8.7)	63.4 (3.1)	65.3 (3.5)	69.1 (1.3)	68 (3.1)	28 (23.9)	57.1 (9.7)	57.5 (3)	
BghiP + InP	47.2 (1.2)	24.5 (11.4)	21.5 (28)	43.8 (5.6)	47.1 (8)	43.9 (0.9)	45.3 (2.6)	47.6 (0.9)	51.3 (3.8)	28 (23.2)	41.5 (9.2)	37.9 (6.4)	
Average	66.7 (3.5)	61.8 (5.5)	58.2 (9.5)	65.7 (5.3)	68.1 (8.3)	69.4 (3.7)	66.3 (2.5)	63.1 (2.8)	61 (3.8)	44 (19.2)	57.6 (8.4)	58.5 (4)	

$$\text{Average \% Recovery} = \text{Average}(\text{Average}(\text{triplicates}))$$

$$\text{Average RSDs} = \text{Average}(100 * \frac{\text{St. Dev. (triplicates)}}{\text{Average (triplicates)}})$$

Table A2: *Extraction % recoveries of 15 PAHs from SRM for the 5 tested methods. In parenthesis the % relative standard deviation.*

	SRM % Recovery				
	1	2	3	4	5
NAP	78.7 (5.1)	46.2 (12.5)	109.7 (4.6)	62.9 (17.4)	53.4 (1.4)
FL	45.6 (6.4)	42.7 (51.4)	52.6 (20)	60.8 (57.4)	55.6 (31.5)
ACE	23.6 (1.6)	70.8 (31.8)	37.1 (12.2)	82.3 (54.3)	58.5 (55.2)
PHE	93.1 (8.8)	78 (0.3)	115.4 (3.3)	88.4 (2.9)	80.5 (0.9)
AN	77 (21.8)	72.4 (13)	85.8 (1.8)	84.8 (23.7)	77.6 (21.3)
FLA	70.3 (13.1)	66.5 (3)	91.7 (20.4)	88.6 (5)	79.4 (6.1)
PYR	71.3 (2.8)	72.5 (3.7)	99 (22.9)	71.6 (0.6)	75.3 (18.8)
CHR	65.8 (7.3)	68.6 (4.4)	73.7 (3.7)	68.1 (17.9)	41.7 (50.7)
BaA	66.5 (8.7)	65.9 (4.3)	74.3 (3.4)	44.6 (44.6)	58.3 (2.7)
BbF	94.5 (5.9)	94.3 (4)	102.3 (2.7)	93.9 (0.9)	84.4 (0.7)
BkF	75.6 (7.9)	75.2 (3.1)	81.5 (4.6)	75.5 (2.9)	68.5 (1.3)
BaP	60.4 (3.2)	66.7 (6.6)	67.7 (0.5)	69.5 (3.6)	56.1 (5.6)
DBA	78.5 (15.3)	54.8 (16.1)	76.7 (11.9)	42.1 (27.6)	54.4 (27.3)
BghiP + InP	38.3 (5)	37.2 (5.6)	40.5 (4.8)	37.1 (1.2)	32.5 (3.6)
Average	67.1 (8.1)	65.1 (11.4)	79.1 (8.3)	69.3 (18.6)	62.6 (16.2)

Table A3: Storm 1 - Calculated aqueous runoff PAH concentrations in the corresponding size intervals.

Location ID	Size Interval	Measured Concentration (ng/L)																												Total PAH-15
		Naphthalene		Fluorene		Acenaphthene		Phenanthrene		Anthracene		Fluoranthene		Pyrene		Chrysenes		Benzo[a]anthracene		Benzo[b]fluoranthene		Benzo[k]fluoranthene		Benzo[a]pyrene		Dibenzo[a,h]anthracene		Benzo[ghi]perylene+Indeno[1,2,3-cd]pyrene		
		Value	Flag	Value	Flag	Value	Flag	Value	Flag	Value	Flag	Value	Flag	Value	Flag	Value	Flag	Value	Flag	Value	Flag	Value	Flag	Value	Flag	Value	Flag	Value	Flag	
C2W	< 0.7 µm	12.6		39.1		1.1		19.0		2.1		9.1		8.6		1.2		1.1		1.2		0.3		0.8		0.5		2.3		99.1
	> 0.7 µm	19.7		0.0	<0	0.0	<0	21.2		0.0	<0	590.1		240.8		30.4		49.5		239.4		9.8		17.4		3.7		3.9		1225.7
	0.7-2.7 µm	0.0	<0	0.0	<0	0.0	<0	0.0	<0	0.0	<0	18.1		5.8		1.9		1.0		3.4		0.9		1.7		0.4		5.2		38.4
	2.7-20 µm	14.4		5.2		4.4		38.3		0.0	<0	56.1		75.1		19.5		14.0		26.8		10.0		17.2		7.7		48.0		336.7
	20-63 µm	0.0	<0	0.0	<0	0.0	<0	3.9		9.6		52.8		30.9		17.9		18.1		45.0		15.5		26.7		6.2		72.1		298.6
> 63 µm	21.8		0.0	<0	0.0	<0	0.0	<0	0.0	<0	463.1		129.0		0.0	<0	16.4		164.1		0.0	<0	0.0	<0	0.0	<0	0.0	<0	794.5	
O4W	< 0.7 µm	9.6		1.9		0.8		5.6		1.5		13.8		6.8		0.7		0.5		0.2	J	0.6		0.8		0.8		43.9		
	> 0.7 µm	15.7		9.4		1.1		31.7		8.6		69.8		73.3		17.4		8.1		27.1		8.0		16.2		5.1		42.4		
	0.7-2.7 µm	1.4		1.2		0.3		2.7		0.4		0.0	<0	1.2		0.5		0.0	<0	1.1		0.1		0.0	<0	1.5		10.5		
	2.7-20 µm	0.0	<0	0.0	<0	0.0	<0	0.0	<0	0.0	<0	17.7		10.9		3.3		2.1		7.4		2.0		3.7		1.1		11.0		
	20-63 µm	0.9		0.0	<0	3.3		4.0		0.0	<0	48.6		2.2		10.9		6.4		4.8		0.7		1.5		1.7		5.8		
> 63 µm	19.0		9.8		0.0	<0	25.2		9.9		11.4		59.1		2.7		0.0	<0	13.8		5.2		10.9		2.8		24.1			
O3W	< 0.7 µm	8.5		3.3		2.6		9.9		1.2		5.1		6.0		0.4		0.5		0.3	J	0.2		0.2		0.4		38.6		
	> 0.7 µm	27.5		0.0	<0	0.9		34.0		33.7		279.9		79.5		20.3		22.9		59.2		17.5		35.2		30.1		654.3		
	0.7-2.7 µm	0.2		0.0	<0	0.3		0.0	<0	0.2		6.5		6.1		2.2		1.2		4.6		1.8		3.6		0.6		5.7		
	2.7-20 µm	0.0	<0	0.0	<0	0.0	<0	0.0	<0	0.0	<0	22.0		13.1		5.2		3.9		11.7		4.9		10.5		2.1		11.6		
	20-63 µm	0.0	<0	0.1		0.7		0.3		1.4		4.0		0.0	<0	0.7		0.4		2.4		0.6		1.5		0.2		1.9		
> 63 µm	30.1		0.2		1.1		34.5		32.9		247.4		60.8		12.3		17.3		40.6		10.1		19.6		10.8		528.5			
C1W	< 0.7 µm	17.0		6.7		3.1		13.8		0.9		16.1		9.1		1.1		0.5		0.6		0.3		0.4		0.9		71.1		
	> 0.7 µm	6.3		0.0	<0	23.2		98.5		17.4		211.1		218.2		104.6		54.8		130.1		41.1		74.8		19.7		144.4		
	0.7-2.7 µm	0.0	<0	0.0	<0	1.9		0.0	<0	0.4		0.0	<0	1.6		1.9		0.9		2.4		0.7		1.1		0.6		2.9		
	2.7-20 µm	2.5		1.4		1.6		14.9		3.1		102.0		58.9		27.2		19.8		54.4		18.9		29.1		10.1		57.4		
	20-63 µm	0.2		0.0	<0	0.0	<0	12.8		7.9		169.7		54.2		16.0		21.6		62.7		20.0		29.1		1.6		36.9		
> 63 µm	9.2		1.5		23.0		71.8		6.0		0.0	<0	103.6		59.6		12.5		10.7		1.5		15.7		7.5		47.2			
O1W	< 0.7 µm	18.2		10.2		2.4		16.7		2.3		5.7		6.1		3.1		1.8		3.1		1.3		2.1		1.5		2.6		
	> 0.7 µm	11.6		13.7		43.1		93.2		1.6		114.1		43.8		45.8		64.5		124.3		24.2		78.2		2.6		97.2		
	0.7-2.7 µm	0.0	<0	0.0	<0	0.0		0.0	<0	0.0	<0	1.7		0.0	<0	0.0	<0	0.0	<0	0.0	<0	0.0	<0	0.0	<0	0.0	<0	1.7		
	2.7-20 µm	1.4		0.0	<0	0.0	<0	10.6		1.0		24.0		12.8		7.8		7.9		14.6		4.5		9.8		3.5		23.1		
	20-63 µm	0.0	<0	1.2		3.3		17.3		2.8		33.9		9.6		10.0		10.2		29.7		5.3		15.3		0.0	<0	22.5		
> 63 µm	16.8		15.1		40.0		67.7		0.0	<0	54.5		21.9		28.4		46.8		80.1		14.7		53.8		1.1		52.4			
O2W	< 0.7 µm	0.5		4.6		5.3		14.6		5.0		74.4		68.6		17.8		10.4		33.2		13.1		12.4		3.3		9.1		
	> 0.7 µm	2.2		0.0	<0	57.1		88.2		20.4		896.3	E	619.5	E	195.3		148.5		306.4		132.9		142.2		55.4		94.1		
	0.7-2.7 µm	0.0	<0	0.0	<0	0.0		0.0	<0	0.0	<0	0.0	<0	0.0	<0	0.0	<0	1.4		0.0	<0	0.0	<0	0.0	<0	0.1		0.1		
	2.7-20 µm	2.1		0.9		1.6		14.5		5.0		99.9		116.5		45.9		33.7		78.0		32.6		33.1		6.8		19.9		
	20-63 µm	0.0	<0	0.0	<0	0.0	<0	0.1		8.7		0.0	<0	0.0	<0	0.0	<0	0.0	<0	0.0	<0	0.0	<0	0.0	<0	0.0	<0	0.0		
> 63 µm	0.9		0.0	<0	56.9		79.7		7.8		831.9	E	536.1	E	158.7		119.9		244.7		107.7		115.9		49.4		2388.5			
A1W	< 0.7 µm	4.7		0.0	U	0.0	U	3.5		0.0	U	5.0		4.0		1.5		0.9		0.5		0.2		0.2		0.4		0.6		
	> 0.7 µm	12.3		5.4		23.9		269.8		41.6		775.4		609.7		281.6		195.2		420.8		157.8		274.6		72.3		425.5		
	0.7-2.7 µm	0.0	<0	0.0	U	0.5		0.0	<0	0.5		2.5		3.0		0.0	<0	0.0	<0	2.3		0.7		1.0		0.3		1.8		
	2.7-20 µm	1.9		0.0	U	1.4		47.0		5.5		137.6		108.2		53.2		56.8		128.1		47.8		76.8		22.5		125.3		
	20-63 µm	7.0		0.0	U	0.0	<0	84.4		8.1		230.9	E	31.2	E	15.3		0.0	<0	0.0	<0	60.4		104.0		5.4		132.0		
> 63 µm	3.5		5.4		22.0		138.8		27.5		404.4		467.2		213.3		153.1		298.7		49.0		92.9		44.1		166.4			
A2W	< 0.7 µm	13.3		55.5		3.1		10.0		0.8		11.4		5.0		0.9		0.5		0.5		0.2		0.4		0.2		0.9		
	> 0.7 µm	11.4		0.0	<0	9.3		25.6		9.0		214.1		123.5		15.6		10.3		38.2		13.8		21.7		10.5		23.1		
	0.7-2.7 µm	0.0	<0	0.0	<0	2.5		0.0	<0	0.0	<0	3.6		4.4		1.8		1.4		6.1		1.9		2.7		0.7		5.0		
	2.7-20 µm	0.0	<0	0.0	<0	0.0	<0	3.4		0.9		34.3		29.1		13.1		8.8		29.4		10.2		13.8		4.3		21.5		
	20-63 µm	0.0	<0	0.0	<0	1.7		0.0	<0	0.0	<0	28.0		2.6		2.0		0.2		0.1		0.0	<0	0.0	<0	0.6	<0	0.0		
> 63 µm	15.7		5.8		6.0		25.0		8.8		148.2		87.4		0.0	<0	0.0	<0	2.6		3.2		8.8		4.9		0.0			
A3W	< 0.7 µm	38.5		11.1		17.4		19.9		1.8		10.2		7.2		1.0		0.8		1.3		0.5		0.8		0.5		1.3		
	> 0.7 µm	0.0	<0	0.0	<0	0.0	<0	1.8		0.1		10.2		5.7		2.3		2.5		5.7		2.0		4.1		0.4		6.1		
	0.7-2.7 µm	0.0	<0	0.5		3.2		0.0	<0	0.0	<0	7.2		3.1		1.5		1.1		3.5		1.3		2.1		0.7		3.3		
	2.7-20 µm	0.0	<0	0.0	<0	0.0	<0	0.0	<0	1.0		4.1		1.7		0.2		0.7		2.1		0.7		1.1		0.5		1.3		
	20-63 µm	0.0	<0	0.0	<0	0.0	<0	0.0	<0	1.1		5.2		1.3		0.6		0.1		0.6		0.2		0.1		0.3	<0	9.7		
> 63 µm	6.6		2.1		1.5		7.5		0.0	<0	0.0	<0	0.0	<																

Table A4: Storm 2 - Calculated aqueous runoff PAH concentrations in the corresponding size intervals.

Location ID	Size Interval	Measured Concentration (ng/L)																										Total PAH-15		
		Naphthalene		Fluorene		Acenaphthene		Phenanthrene		Anthracene		Fluoranthene		Pyrene		Chrysene		Benzo[a]anthracene		Benzo[b]fluoranthene		Benzo[k]fluoranthene		Benzo[a]pyrene		Dibenzo[a,h]anthracene			Benzo[ghi]perylene+Indeno[1,2,3-cd]pyrene	
		Value	Flag	Value	Flag	Value	Flag	Value	Flag	Value	Flag	Value	Flag	Value	Flag	Value	Flag	Value	Flag	Value	Flag	Value	Flag	Value	Flag	Value	Flag		Value	Flag
C2W	< 0.7 µm	7.6		1.7		10.6		0.0	U	0.0	U	2.5		3.4		0.5		0.3		0.6		0.1	J	0.2		0.5		0.9		28.9
	> 0.7 µm	7.9		28.4		35.6		287.2		0.0	U	216.7		167.5		57.2		41.3		117.5		27.5		50.7		0.0	<0	150.8		1188.2
	0.7-2.7 µm	0.0	<0	0.0	<0	1.9		0.0	U	0.0	U	0.0	<0	0.3		0.0	<0	0.0		0.0	<0	0.0		0.2		0.0	<0	0.0	<0	2.5
	2.7-20 µm	3.8		56.4		0.0	<0	0.0	U	0.0	U	22.0		30.2		11.5		5.8		17.6		4.8		10.3		2.7		38.3		203.3
	20-63 µm	52.3		300.5		1.8		0.0	U	0.0	U	135.0		50.9		20.0		7.8		34.7		10.3		22.8		25.4		90.9		752.3
> 63 µm	0.0	<0	0.0	<0	43.8		287.2		0.0	U	59.8		86.1		25.7		27.6		65.2		12.5		17.4		0.0	<0	21.6		646.9	
O4W	< 0.7 µm	14.2		1.9		1.5		6.6		0.0	U	0.0	U	2.6		0.0	U	0.0	U	0.0	U	0.0	U	0.0	U	0.0	U	0.0	U	26.8
	> 0.7 µm	3.7		0.0	<0	0.8		0.0	<0	1.3		4.3		1.8		1.9		0.9		1.8		0.2		0.5		1.7		1.8		20.8
	0.7-2.7 µm	0.3		0.0	<0	0.0	<0	0.0	<0	0.0	U	0.0	U	0.0	<0	0.0	U	0.0	U	0.0	U	0.0	U	0.0	U	0.0	U	0.0	U	0.3
	2.7-20 µm	1.4		0.4		1.7		1.6		0.0	U	3.3		0.7		0.0	U	0.0	U	0.0	U	0.1		0.0	U	0.0	U	0.3		9.6
	20-63 µm	0.0	<0	0.0	<0	0.0	<0	0.0	<0	0.0	U	0.0	<0	1.0		1.1		0.5		0.9		0.1		0.5		0.0	U	0.9		5.0
> 63 µm	6.4		0.0	<0	0.7		1.1		1.3		1.5		0.3		0.8		0.4		0.9		0.1		0.0	<0	1.7		0.6		15.9	
C1W	< 0.7 µm	6.6		1.2		1.9		7.9		0.0	U	3.7		3.5		0.6		0.5		0.3		0.1		0.1		0.3		0.4		27.1
	> 0.7 µm	0.4		4.0		10.1		20.9		0.0	U	21.4		43.7		27.2		18.1		26.4		10.0		18.5		4.1		47.6		252.4
	0.7-2.7 µm	0.3		0.0	<0	0.0	<0	0.0	<0	0.0	U	0.6		0.4		0.1		0.0	<0	0.2		0.0		0.2		0.0		0.3		2.1
	2.7-20 µm	0.0	<0	0.0	<0	0.0	<0	0.0	<0	0.3		8.5		10.1		3.8		2.5		7.9		2.6		4.6		1.2		12.3		53.9
	20-63 µm	2.4		0.0		0.0	<0	9.9		0.4		19.6		16.6		6.4		4.6		17.2		5.9		11.0		2.0		30.3		126.3
> 63 µm	0.4		4.3		11.5		11.3		0.0	<0	0.0	<0	16.6		16.9		11.0		1.0		1.4		2.8		0.8		4.7		82.8	
O2W	< 0.7 µm	3.1		5.2		5.4		7.6		1.7		9.2		6.5		0.7		0.4		1.2		0.4		0.3		0.5		0.4		42.5
	> 0.7 µm	2.7		0.0	<0	0.0		7.2		0.0	<0	14.6		28.7		20.5		8.0		20.9		9.2		11.7		3.6		16.9		143.9
	0.7-2.7 µm	3.3		0.0	<0	0.0	<0	0.0	<0	0.0	<0	0.0	<0	0.0	<0	0.2		0.1		0.0		0.1		0.0		0.0		0.2		4.0
	2.7-20 µm	1.0		2.8		5.4		0.0	<0	0.0	<0	3.3		2.8		1.6		0.9		5.3		1.9		1.8		0.7		3.0		30.5
	20-63 µm	0.0	<0	0.0	<0	3.1		0.0	U	0.0	U	4.3		2.9		1.2		1.0		5.7		1.5		2.1		0.2		3.9		26.0
> 63 µm	1.1		0.0	<0	0.0	<0	14.8		0.8		7.4		23.4		17.4		5.9		9.9		5.8		7.6		2.7		9.7		106.5	
A1W	< 0.7 µm	4.0		1.1		1.9		3.8		0.0	U	1.7		2.5		0.0	U	0.0	U	0.0	U	0.0	U	0.0	U	0.0	U	0.2		15.2
	> 0.7 µm	0.7		1.4		3.0		25.1		1.0		39.3		31.3		13.0		7.6		17.5		5.6		10.3		2.8		29.3		187.8
	0.7-2.7 µm	0.0	<0	0.0	<0	0.1		1.0		2.6		0.6		0.0	<0	0.3		0.2		0.2		0.1		0.2		0.3		0.0	<0	5.5
	2.7-20 µm	1.2		5.1		3.2		10.7		0.0	<0	7.7		5.9		2.9		1.8		4.5		1.3		2.0		0.6		4.0		50.9
	20-63 µm	0.0	<0	0.0	<0	0.0	<0	0.0	<0	0.0	<0	12.6		9.2		3.4		2.1		5.8		2.0		3.7		3.1		14.0		55.9
> 63 µm	1.0		0.0		1.3		13.9		0.4		18.4		16.9		6.4		3.5		7.0		2.2		4.4		0.0	<0	11.4		86.7	
A2W	< 0.7 µm	1.8		12.0		12.7		0.2		0.0	U	5.7		3.3		0.0	U	0.0	U	0.2		0.0	J	0.1		0.3		0.1		36.4
	> 0.7 µm	5.0		0.0	<0	0.0	<0	7.9		0.3		1.5		4.8		2.6		1.9		8.6		2.2		4.6		2.5		6.4		48.3
	0.7-2.7 µm	0.0	<0	0.0	<0	0.0	<0	4.8		0.6		0.5		0.4		0.5		0.3		0.1		0.1		0.1		0.1		0.2		7.5
	2.7-20 µm	0.9		0.0	<0	1.2		2.3		2.0		5.2		3.8		1.7		1.5		3.5		1.0		1.6		0.6		3.9		29.2
	20-63 µm	1.8		0.0	<0	0.0	<0	0.0	<0	0.0	<0	0.0	<0	0.7		0.2		0.4		1.5		0.4		0.6		0.0	<0	1.2		6.9
> 63 µm	2.5		0.9		0.1		2.1		0.3		0.0	<0	0.0	<0	0.2		0.0	<0	3.5		0.7		2.3		2.3		1.1		16.0	

Flags	Description
J	Indicates an estimated value. Data indicate the presence of an analyte, but the result is below the calibration range, but greater than zero.
U	Indicates compound was analyzed for, but not detected.
E	Identifies analytes whose concentrations exceed the calibration range of the HPLC instrument for that specific analysis.
N	Not calculated. Due to salinity, there is low confidence on the calculated value.
LS	Low solids mass that corresponds to <10mg/L solids concentration
<0	Indicates a negative outcome in concentration or TFS calculations
NA	Not analyzed (Insufficient sample) / Not applicable

Table A5: Storm 1 – TFS and calculated runoff solids concentrations of PAHs in the corresponding size intervals.

Location ID	Size Interval	TFS (mg/L)		Measured Concentration																												Total PAH-15	Units
				Naphthalene		Fluorene		Acenaphthene		Phenanthrene		Anthracene		Fluoranthene		Pyrene		Chrysene		Benzo[a]ant hracene		Benzo[b]fluor anthene		Benzo[k]fluor anthene		Benzo[a]pyr ene		Dibenzo[a,h] anthracene		Benzo[ghi]perylene + Indeno[1,2,3-cd]pyrene			
		Value	Flag	Value	Flag	Value	Flag	Value	Flag	Value	Flag	Value	Flag	Value	Flag	Value	Flag	Value	Flag	Value	Flag	Value	Flag	Value	Flag	Value	Flag	Value	Flag	Value	Flag		
C2W	Bulk (ng/L)	NA		32.3		0.0	U	0.0	U	40.2		0.0	U	599.2		249.4		31.6		50.6		240.6		10.1		18.1		4.2		6.2		1282.4	ng/L
	> 0.7µm (µg/kg)	259.1		75.9		0.0	U	0.0	U	81.7		0.0	U	2277.3		929.2		117.2		190.9		923.8		37.9		67.1		14.3		15.0		4730.4	µg/kg
	0.7-2.7 µm (µg/kg)	11.4		0.0	<0	0.0	<0	0.0	<0	0.0	<0	0.0	<0	1587.0		504.6		165.0		90.1		300.0		83.3		148.2		34.0		459.9		3372.2	µg/kg
	2.7-20 µm (µg/kg)	146.9		97.9		35.6		29.8		260.7		0.0	U	382.0		511.4		132.8		95.2		182.6		68.1		117.2		52.7		326.5		2292.5	µg/kg
	20-63 µm (µg/kg)	45.1		0.0	<0	0.0	<0	0.0	<0	86.5		212.1		1169.9		685.3		397.5		400.6		997.1		344.1		591.8		137.7		1597.8		6620.5	µg/kg
	> 63 µm (µg/kg)	55.7		391.5		0.0	U	0.0	U	0.0	<0	0.0	U	8307.8		2314.2		0.0	<0	294.2		2944.6		0.0	<0	0.0	<0	0.0	<0	0.0	<0	14252.4	µg/kg
O4W	Bulk (ng/L)	NA		25.2		11.3		1.9		37.3		10.2		83.6		80.1		18.1		8.7		27.4		8.2		16.8		5.9		43.2		377.9	ng/L
	> 0.7µm (µg/kg)	186.6		84.0		50.1		6.1		169.9		46.3		374.3		392.8		93.2		43.6		145.4		42.8		86.8		27.1		227.3		1789.6	µg/kg
	0.7-2.7 µm (µg/kg)	58.4		24.7		20.3		6.0		45.8		6.6		0.0	<0	20.4		8.7		0.0	<0	18.9		2.4		0.2		0.0	<0	26.0		180.1	µg/kg
	2.7-20 µm (µg/kg)	95.1		0.0	<0	0.0	<0	0.0	<0	0.0	<0	0.0	<0	186.0		114.1		34.4		22.4		78.2		20.9		39.3		11.7		116.0		623.1	µg/kg
	20-63 µm (µg/kg)	33.1		27.3		0.0	<0	98.6		120.6		0.0	<0	1467.6		65.0		328.8		193.0		144.8		20.7		45.0		52.6		174.5		2738.4	µg/kg
	> 63 µm (ng/L)	0.0		19.0		9.8		0.0	<0	25.2		9.9		11.4		59.1		2.7		0.0	<0	13.8		5.2		10.9		2.8		24.1		193.9	ng/L
O3W	Bulk (ng/L)	NA		35.9		2.3		3.5		43.9		34.8		285.0		85.4		20.8		23.4		59.5		17.6		35.4		14.0		30.5		692.0	ng/L
	> 0.7µm (µg/kg)	N	S	N	S	N	S	N	S	N	S	N	S	N	S	N	S	N	S	N	S	N	S	N	S	N	S	N	S	N	S	µg/kg	
	0.7-2.7 µm (µg/kg)	N	TFS<0, S	N	S	N	S	N	S	N	S	N	S	N	S	N	S	N	S	N	S	N	S	N	S	N	S	N	S	N	S	µg/kg	
	2.7-20 µm (µg/kg)	N	S	N	S	N	S	N	S	N	S	N	S	N	S	N	S	N	S	N	S	N	S	N	S	N	S	N	S	N	S	µg/kg	
	20-63 µm (µg/kg)	2.8	LS	NA	LS	NA	LS	NA	LS	NA	LS	NA	LS	NA	LS	NA	LS	NA	LS	NA	LS	NA	LS	NA	LS	NA	LS	NA	LS	NA	LS	µg/kg	
	> 63 µm (µg/kg)	1.8	LS	NA	LS	NA	LS	NA	LS	NA	LS	NA	LS	NA	LS	NA	LS	NA	LS	NA	LS	NA	LS	NA	LS	NA	LS	NA	LS	NA	LS	µg/kg	
C1W	Bulk (ng/L)	NA		23.3		4.3		26.3		112.3		18.3		227.2		227.3		105.8		55.3		130.7		41.4		75.2		20.3		145.2		1213.0	ng/L
	> 0.7µm (µg/kg)	267.8		23.5		0.0	<0	86.5		367.6		65.0		788.2		814.7		390.7		204.6		485.8		153.5		279.4		73.4		539.0		4272.0	µg/kg
	0.7-2.7 µm (µg/kg)	12.5		0.0	<0	0.0	<0	148.5		0.0	<0	30.0		0.0	<0	129.0		152.2		68.7		191.5		58.3		85.5		44.6		233.2		1141.5	µg/kg
	2.7-20 µm (µg/kg)	158.1		15.6		8.8		9.9		94.4		19.8		645.0		372.4		171.7		125.5		343.8		119.2		183.8		63.6		363.1		2536.8	µg/kg
	20-63 µm (µg/kg)	46.6		4.4		0.0	<0	0.0	<0	275.3		169.8		3645.6		1163.5		343.3		464.6		1347.1		430.3		624.1		34.3		791.9		9294.1	µg/kg
	> 63 µm (µg/kg)	50.7		182.4		29.6		453.1		1416.5		118.3		0.0	<0	2042.8		1175.8		246.0		210.2		29.5		308.8		147.2		930.6		7290.7	µg/kg
O1W	Bulk (ng/L)	NA		29.9		23.9		45.6		109.9		3.9		119.8		49.9		48.9		66.3		127.4		25.5		80.3		4.2		99.8		835.2	ng/L
	> 0.7µm (µg/kg)	120.1		97.0		114.1		359.4		776.3		13.2		950.6		364.7		381.6		537.1		1035.5		201.6		651.4		21.9		809.2		6313.6	µg/kg
	0.7-2.7 µm (µg/kg)	0.0	TFS<0	0.0	<0	0.0	<0	0.0	<0	0.0	<0	0.0	<0	0.0	<0	0.0	<0	0.0	<0	0.0	<0	0.0	<0	0.0	<0	0.0	<0	0.0	<0	0.0	<0	0.0	µg/kg
	2.7-20 µm (µg/kg)	29.6		47.2		0.0	<0	0.0	<0	359.9		32.3		810.0		433.1		264.9		266.2		492.5		150.8		330.2		119.7		779.1		4085.9	µg/kg
	20-63 µm (µg/kg)	58.6		0.0	<0	20.4		56.6		296.0		48.2		579.0		163.1		170.1		174.8		507.5		90.0		260.8		0.0	<0	383.1		2749.7	µg/kg
	> 63 µm (µg/kg)	31.9		528.5		474.3		1255.3		2125.6		0.0	<0	1710.2		686.8		892.5		1468.2		2514.0		461.7		1687.5		33.2		1644.4		15482.4	µg/kg
O2W	Bulk (ng/L)	NA		2.6		1.1		62.4		102.8		25.4		970.7		688.1		213.2		158.9		339.6		146.0		154.7		58.8		103.3		3027.5	ng/L
	> 0.7µm (µg/kg)	1110.7		1.9		0.0	<0	51.4		79.4		18.3		807.0		557.8		175.9		133.7		275.9		119.6		128.1		49.9		84.8		2483.6	µg/kg
	0.7-2.7 µm (µg/kg)	28.8		0.0	<0	0.0	<0	0.0	<0	0.0	<0	0.0	<0	0.0	<0	0.0	<0	0.0	<0	0.0	<0	0.0	<0	0.0	<0	0.0	<0	2.8		3.8		56.7	µg/kg
	2.7-20 µm (µg/kg)	1053.4		2.0		0.9		1.5		13.8		4.8		94.8		110.6		43.6		32.0		74.0		31.0		31.4		6.4		18.9		465.7	µg/kg
	20-63 µm (µg/kg)	20.6		0.0	<0	0.0	<0	0.0	<0	6.5		419.5		0.0	<0	0.0	<0	0.0	<0	0.0	<0	0.0	<0	0.0	<0	0.0	<0	0.0	<0	0.0	<0	426.1	µg/kg
	> 63 µm (µg/kg)	7.9	LS	NA	LS	NA	LS	NA	LS	NA	LS	NA	LS	NA	LS	NA	LS	NA	LS	NA	LS	NA	LS	NA	LS	NA	LS	NA	LS	NA	LS	µg/kg	
A1W	Bulk (ng/L)	NA		17.0		5.4		23.9		273.3		41.6		780.4		613.7		283.2		196.1		421.3		158.0		274.9		72.7		426.1		3587.5	ng/L
	> 0.7µm (µg/kg)	241.8		51.1		22.3		98.7		1116.1		172.1		3207.2		2521.8		1164.9		807.5		1740.6		652.9		1135.9		299.2		1759.9		14750.4	µg/kg
	0.7-2.7 µm (µg/kg)	0.0	TFS<0	0.0	<0	0.0	U	0.0	<0	0.0	<0	0.0	<0	0.0	<0	0.0	<0	0.0	<0	0.0	<0	0.0	<0	0.0	<0	0.0	<0	0.0	<0	0.0	<0	0.0	µg/kg
	2.7-20 µm (µg/kg)	115.9		16.6		0.0	U	12.4		405.7		47.8		1187.5		933.8		458.8		490.2		1105.2		412.1		662.3		193.8		1081.3		7007.3	µg/kg
	20-63 µm (µg/kg)	101.7		68.4		0.0	U	0.0	<0	829.5		79.2		2269.8		307.0	E	150.2		0.0	<0	0.0	<0	593.5		1022.1		53.5		1296.9		6670.1	µg/kg
	> 63 µm (µg/kg)	24.1		144.6		223.7		911.9		5757.7		1141.4		16768.0		19374.1		8843.3		6350.0		12385.3		2032.2		3851.1		1828.9		6900.6		86512.8	µg/kg
A2W	Bulk (ng/L)</																																

Table A6: Storm 2 – TFS and calculated runoff solids concentrations of PAHs in the corresponding size intervals.

Location ID	Size Interval	TFS (mg/L)		Measured Concentration																								Total PAH-15	Units							
				Naphthalene		Fluorene		Acenaphthene		Phenanthrene		Anthracene		Fluoranthene		Pyrene		Chrysene		Benzo[a]anthracene		Benzo[b]fluoranthene		Benzo[k]fluoranthene		Benzo[a]pyrene				Dibenzo[a,h]anthracene		Benzo[ghi]perylene + Indeno[1,2,3-cd]pyrene				
		Value	Flag	Value	Flag	Value	Flag	Value	Flag	Value	Flag	Value	Flag	Value	Flag	Value	Flag	Value	Flag	Value	Flag	Value	Flag	Value	Flag	Value	Flag			Value	Flag	Value	Flag	Value	Flag	
C2W	Bulk (ng/L)	NA		15.5		30.1		46.2		287.2		0.0	U	219.2		170.9		57.7		41.5		118.1		27.6		50.9		0.0	U	151.7		1216.5	ng/L			
	> 0.7µm (µg/kg)	784.4		10.1		36.2		45.4		366.1		0.0	U	276.2		213.5		73.0		52.6		149.7		35.1		64.7		0.0	U	192.2		1514.7	µg/kg			
	0.7-2.7 µm (µg/kg)	0.0	TFS<0	0.0	<0	0.0	<0	0.0	<0	0.0	<0	0.0	<0	0.0	<0	0.0	<0	0.0	<0	0.0	<0	0.0	<0	0.0	<0	0.0	<0	0.0	<0	0.0	<0	0.0	<0	0.0	µg/kg	
	2.7-20 µm (µg/kg)	62.9		60.7		896.1		0.0	<0	0.0	U	0.0	U	349.3		479.3		182.6		92.8		279.5		75.6		163.6		42.1		608.5		3230.2	µg/kg			
	20-63 µm (µg/kg)	190.7		274.0		1575.5		9.4		0.0	U	0.0	U	707.7		266.7		105.0		40.9		182.0		53.8		119.7		133.1		476.4		3944.3	µg/kg			
	> 63 µm (µg/kg)	530.7		0.0	<0	0.0	<0	82.5		541.1		0.0	U	112.6		162.3		48.5		51.9		122.9		23.6		32.7		0.0	U	40.8		1218.9	µg/kg			
O4W	Bulk (ng/L)	NA		17.9		1.6		2.3		5.7		1.3		4.3		4.4		1.9		0.9		1.8		0.2		0.5		1.7		1.8		46.4	ng/L			
	> 0.7µm (µg/kg)	N	S	N	S	N	S	N	S	N	S	N	S	N	S	N	S	N	S	N	S	N	S	N	S	N	S	N	S	N	S	N	S	µg/kg		
	0.7-2.7 µm (µg/kg)	N	TFS<0, S	N	S	N	S	N	S	N	S	N	S	N	S	N	S	N	S	N	S	N	S	N	S	N	S	N	S	N	S	N	S	N	S	µg/kg
	2.7-20 µm (µg/kg)	N	S	N	S	N	S	N	S	N	S	N	S	N	S	N	S	N	S	N	S	N	S	N	S	N	S	N	S	N	S	N	S	N	S	µg/kg
	20-63 µm (µg/kg)	1.9	LS	NA	LS	NA	LS	NA	LS	NA	LS	NA	LS	NA	LS	NA	LS	NA	LS	NA	LS	NA	LS	NA	LS	NA	LS	NA	LS	NA	LS	NA	LS	NA	LS	µg/kg
	> 63 µm (µg/kg)	1.1	LS	NA	LS	NA	LS	NA	LS	NA	LS	NA	LS	NA	LS	NA	LS	NA	LS	NA	LS	NA	LS	NA	LS	NA	LS	NA	LS	NA	LS	NA	LS	NA	LS	µg/kg
C1W	Bulk (ng/L)	NA		6.9		5.1		12.0		28.9		0.0	U	25.1		47.2		27.7		18.6		26.7		10.1		18.6		4.5		47.9		279.5	ng/L			
	> 0.7µm (µg/kg)	116.8		3.2		33.9		86.7		179.2		0.0	U	183.2		374.2		232.7		155.3		225.8		85.4		158.4		35.2		407.2		2160.4	µg/kg			
	0.7-2.7 µm (µg/kg)	0.0	TFS<0	0.0	<0	0.0	<0	0.0	<0	0.0	<0	0.0	<0	0.0	<0	0.0	<0	0.0	<0	0.0	<0	0.0	<0	0.0	<0	0.0	<0	0.0	<0	0.0	<0	0.0	<0	0.0	µg/kg	
	2.7-20 µm (µg/kg)	63.6		0.0	<0	0.0	<0	0.0	<0	0.1		4.8		134.3		158.7		60.1		39.1		124.9		41.5		71.6		19.3		193.3		847.8	µg/kg			
	20-63 µm (µg/kg)	27.6		86.3		0.4		0.0	<0	357.0		13.6		708.9		601.3		233.4		167.4		624.1		214.1		397.9		74.1		1098.2		4576.7	µg/kg			
	> 63 µm (µg/kg)	25.6		14.5		168.7		449.5		442.7		0.0	U	0.0	<0	647.7		657.8		431.1		38.9		54.3		109.5		31.2		183.4		3229.4	µg/kg			
O2W	Bulk (ng/L)	NA		5.8		4.2		5.4		14.8		0.8		23.7		35.2		21.2		8.4		22.1		9.6		11.9		4.1		17.3		184.4	ng/L			
	> 0.7µm (µg/kg)	N	S	N	S	N	S	N	S	N	S	N	S	N	S	N	S	N	S	N	S	N	S	N	S	N	S	N	S	N	S	N	S	µg/kg		
	0.7-2.7 µm (µg/kg)	N	TFS<0, S	N	S	N	S	N	S	N	S	N	S	N	S	N	S	N	S	N	S	N	S	N	S	N	S	N	S	N	S	N	S	N	S	µg/kg
	2.7-20 µm (µg/kg)	N	S	N	S	N	S	N	S	N	S	N	S	N	S	N	S	N	S	N	S	N	S	N	S	N	S	N	S	N	S	N	S	N	S	µg/kg
	20-63 µm (µg/kg)	9.8	LS	NA	LS	NA	LS	NA	LS	NA	LS	NA	LS	NA	LS	NA	LS	NA	LS	NA	LS	NA	LS	NA	LS	NA	LS	NA	LS	NA	LS	NA	LS	NA	LS	µg/kg
	> 63 µm (µg/kg)	5.9	LS	NA	LS	NA	LS	NA	LS	NA	LS	NA	LS	NA	LS	NA	LS	NA	LS	NA	LS	NA	LS	NA	LS	NA	LS	NA	LS	NA	LS	NA	LS	NA	LS	µg/kg
A1W	Bulk (ng/L)	NA		4.7		2.5		4.9		28.9		1.0		41.0		33.8		13.0		7.6		17.5		5.6		10.3		2.8		29.5		203.0	ng/L			
	> 0.7µm (µg/kg)	N	S	N	S	N	S	N	S	N	S	N	S	N	S	N	S	N	S	N	S	N	S	N	S	N	S	N	S	N	S	N	S	N	S	µg/kg
	0.7-2.7 µm (µg/kg)	N	S	N	S	N	S	N	S	N	S	N	S	N	S	N	S	N	S	N	S	N	S	N	S	N	S	N	S	N	S	N	S	N	S	µg/kg
	2.7-20 µm (µg/kg)	N	S	N	S	N	S	N	S	N	S	N	S	N	S	N	S	N	S	N	S	N	S	N	S	N	S	N	S	N	S	N	S	N	S	µg/kg
	20-63 µm (µg/kg)	18.6		0.0	<0	0.0	<0	0.0	<0	0.0	<0	0.0	<0	677.7		493.9		183.0		112.6		312.2		106.2		197.6		166.3		749.7		2999.2	µg/kg			
	> 63 µm (µg/kg)	4.5	LS	NA	LS	NA	LS	NA	LS	NA	LS	NA	LS	NA	LS	NA	LS	NA	LS	NA	LS	NA	LS	NA	LS	NA	LS	NA	LS	NA	LS	NA	LS	NA	LS	µg/kg
A2W	Bulk (ng/L)	NA		6.8		2.8		4.2		8.2		0.3		7.1		8.1		2.6		1.9		8.8		2.2		4.7		2.8		6.5		66.9	ng/L			
	> 0.7µm (µg/kg)	N	S	N	S	N	S	N	S	N	S	N	S	N	S	N	S	N	S	N	S	N	S	N	S	N	S	N	S	N	S	N	S	N	S	µg/kg
	0.7-2.7 µm (µg/kg)	N	TFS<0, S	N	S	N	S	N	S	N	S	N	S	N	S	N	S	N	S	N	S	N	S	N	S	N	S	N	S	N	S	N	S	N	S	µg/kg
	2.7-20 µm (µg/kg)	N	S	N	S	N	S	N	S	N	S	N	S	N	S	N	S	N	S	N	S	N	S	N	S	N	S	N	S	N	S	N	S	N	S	µg/kg
	20-63 µm (µg/kg)	3.9	LS	NA	LS	NA	LS	NA	LS	NA	LS	NA	LS	NA	LS	NA	LS	NA	LS	NA	LS	NA	LS	NA	LS	NA	LS	NA	LS	NA	LS	NA	LS	NA	LS	µg/kg
	> 63 µm (ng/L)	0.0		2.5		0.9		0.1		2.1		0.3		0.0	<0	0.0	<0	0.2		0.0	<0	3.5		0.7		2.3		2.3		1.1		16.0	ng/L			

Table A7: Average measured sediment core and settling trap ΣPAH concentrations at the receiving waters of Paleta creek.

	Average Sediment Concentration (µg/Kg-dw)																						
	July 2015				2015-2016								2016-2017										
	Cores		Traps		Pre-storm cores				Post-storm cores				Traps				Pre-storm cores				Post-storm cores		
	P11	P17	P11	P17	P01	P08	P11	P17	P08	P11	P17	P01	P08	P11	P17	P01	P08	P11	P17	P01	P08	P11	P17
%TOC	1.38	4.46	3.51	6.28	0.79	1.17	1.75	3.63	1.51	2.06	3.86	2.39	2.38	3.14	4.45	0.98	1.25	1.93	3.94	0.72	1.96	1.87	5.16
%BC	0.12	0.28	0.13	0.20	0.10	0.11	0.17	0.23	0.13	0.21	0.24	0.16	0.15	0.19	0.41	0.10	0.12	0.15	0.24	0.07	0.17	0.13	0.27
Naphthalene	64.0	84.3	156	136	73.8	85.2	84.0	90.5	80.0	160	70.2	19.0	13.1	27.3	23.6	11.1	12.8	15.9	17.1	58.2	82.4	126	164
Fluorene	6.8	8.2	ND	ND	ND	ND	ND	ND	ND	ND	ND	ND	ND	ND	22.3	ND	ND	ND	ND	7.2	14.9	14.8	20.5
Acenaphthene	ND	ND	ND	ND	ND	ND	ND	ND	ND	ND	ND	ND	ND	2.4	13.5	ND	ND	ND	8.0	ND	ND	ND	ND
Phenanthrene	39.6	65.6	265.2	516	66.8	79.7	80.7	144	73.8	157	306	41.2	41.2	91.2	233	18.9	29.3	34.0	98.7	30.5	67.1	108	209
Anthracene	13.2	10.9	117	52.5	45.3	25.0	52.3	59.1	24.0	0.0	0.0	34.1	23.9	50.1	56.7	6.7	22.8	11.3	42.7	7.4	22.8	24.7	36.3
Fluoranthene	126	120	410	681	58.8	87.9	221	240	83.0	1409	384	86.2	76.3	194	390	44.1	86.6	100	346	41.3	156	216	498
Pyrene	299	210	561	694	72.0	105	950	515	104	2713	538	103	103	241	393	45.9	97.1	129	405	54.9	233	294	606
Chrysene	139	75.6	236	310	63.4	64.5	81.9	147	68.0	437	559	72.7	65.2	206	159	31.5	64.8	72.1	135	33.0	118	137	207
Benz[a]anthracene	108	60.3	199	233	53.2	45.7	155	138	46.9	700	263	57.8	52.8	96.5	125	23.0	58.2	54.8	140	22.6	106	93.7	192
Benzo[b]fluoranthene	295	225	906	530	569	340	814	597	263	1600	702	199	215	465	221	83.7	190	249	312	117	376	411	436
Benzo[k]fluoranthene	152	91.8	393	209	261	141	333	219	107	625	350	92.1	102	198	96.8	41.8	97.5	118	144	54.5	166	174	179
Benzo[a]pyrene	245	156	616	323	397	242	519	385	188	914	591	164	170	310	148	72.6	170	198	241	102	295	277	314
Dibenz[a,h]anthracene	42.6	25.0	118	65.4	59.8	35.4	61.7	41.8	22.8	88.3	275	32.0	36.1	71.3	20.8	14.6	35.1	35.5	33.6	20.6	54.7	53.8	55.7
Benzo[ghi]perylene + Indeno[1,2,3-cd]pyrene	188	158	599	491	241	208	417	354	158	706	601	157	160	299	225	70.9	144	175	261	86.3	246	259	324

Table A8: TOC content of solids deposited on filters/sieves of composite runoff collected during both storms.

		0.7µm			2.7µm			20µm			63µm		
		%TOC	StDev	RSD	%TOC	StDev	RSD	%TOC	StDev	RSD	%TOC	StDev	RSD
Storm 1	C2W	10.37	0.72	6.98	11.88	0.77	6.45	15.82	2.44	15.41	19.83	1.84	9.29
	O4W	3.50	0.06	1.67	5.22	0.20	3.83	9.26			47.24		
	O3W	4.75	0.08	1.67	2.02	0.37	18.29	NA			NA		
	C1W	8.32	0.66	7.88	8.35	0.43	5.19	14.08	0.33	2.38	21.29		
	O1W	19.15	4.80	25.04	14.91	4.00	26.79	21.23	1.66	7.83	23.68		
	O2W	3.37	0.05	1.34	2.77	0.13	4.81	6.04			10.06		
	A1W	13.90	0.80	5.74	13.05	0.77	5.91	17.08			20.34		
	A2W	3.47	0.09	2.68	3.03	0.25	8.11	8.06			NA		
	A3W	3.76	0.14	3.80	0.99	0.59	59.87	32.08			NA		
		0.7µm			2.7µm			20µm			63µm		
		%TOC	StDev	RSD	%TOC	StDev	RSD	%TOC	StDev	RSD	%TOC	StDev	RSD
Storm 2	A A1W	10.97	0.95	8.67	1.17	0.11	9.77	12.89			19.13		
	B A1W	1.27	0.11	8.75	2.70	0.09	3.34	13.56			NA		
	A A2W	3.09	0.06	2.09	1.18	0.05	4.49	NA			NA		
	B A2W	2.78	0.28	10.18	1.11	0.14	12.56	10.49			NA		
	A O2W	4.45	0.42	9.45	3.26	0.58	17.81	19.03			NA		
	B O2W	5.55	0.20	3.64	3.90	0.41	10.44	16.10			21.63		
	O4W	1.95	0.10	4.89	0.68	0.05	7.80	NA			NA		
	A C1W	9.09	0.40	4.44	10.91	0.99	9.08	10.46			15.31		
	B C1W	9.53	0.40	4.19	8.35	0.37	4.45	7.81			17.12		
	C2W	11.02	0.77	6.95	10.00	0.21	2.10	6.43	1.48	23.07	2.24	0.87	38.89
		=	No solids mass										
		=	Single run										
		=	Duplicates										
		=	Triplicates										

Table A9: July 2015 - Average measured tissue, sediment and porewater concentrations for 7 PAHs at the receiving waters of Paleta creek.

	Average Tissue Concentration ($\mu\text{g}/\text{kg-lipids}$)		Average Sediment Concentration ($\mu\text{g}/\text{Kg-dw}$)				Average Porewater Concentration (ng/L)			
			Cores		Traps		Insitu SPMEs		Exsitu SPMEs	
	P11	P17	P11	P17	P11	P17	P11	P17	P11	P17
%TOC			1.38	4.46	3.51	6.28				
%BC			0.12	0.28	0.13	0.20				
Fluoranthene	6275	1218	126	120	410	681	10.4	6.0	3.3	3.1
Pyrene	13163	739	299	210	561	694	49.5	15.1	16.8	8.4
Chrysene	4009	1009	139	75.6	236	310	2.8	1.4	0.9	0.6
Benz[a]anthracene	4147	982	108	60.3	199	233	2.7	1.3	0.9	0.4
Benzo[b]fluoranthene	9067	2652	295	225	906	530	2.0	0.8	1.3	0.5
Benzo[k]fluoranthene	3418	1056	152	91.8	393	209	1.9	0.7	1.2	0.4
Benzo[a]pyrene	6902	1841	245	156	616	323	2.1	0.8	0.9	0.3

Table A10: *In-situ 2015-2016 - Average measured tissue, sediment and porewater concentrations for 7 PAHs at the receiving waters of Paleta creek.*

	Average Tissue Concentration (µg/kg-lipids)											
	P01-Open	P01-80µm	P01-500µm	P08-Open	P08-80µm	P08-500µm	P11-Open	P11-80µm	P11-500µm	P17-Open	P17-80µm	P17-500µm
%TOC												
%BC												
Fluoranthene	675	724	608	1354	621	1030	3902	667	2118	1405	1521	852
Pyrene	881	585	844	1730	789	1475	18833	1469	8233	2112	2807	1451
Chrysene	159	253	198	566	207	351	1561	1949	1887	243	307	171
Benz[a]anthracene	308	436	468	694	326	618	2725	2816	1388	311	402	209
Benzo[b]fluoranthene	2786	3945	5282	6231	4166	8163	10456	7633	6773	1132	1527	878
Benzo[k]fluoranthene	971	1389	2019	1951	1463	2746	3082	1784	1921	309	419	239
Benzo[a]pyrene	1471	2192	3106	2944	2173	4113	5671	4706	3587	514	659	393

	Average Sediment Concentration (µg/Kg-dw)				Average Porewater Concentration (ng/L)							
	Traps				Jan Insitu SPMEs			Feb Insitu SPMEs				
	P01	P08	P11	P17	P08	P11	P17	P01	P08	P11	P17	
%TOC	2.39	2.38	3.14	4.45								
%BC	0.16	0.15	0.19	0.41								
Fluoranthene	86.2	76.3	194	390	2.3	24.7	3.9	5.1	4.9	20.5	7.6	
Pyrene	103	103	241	393	3.8	113	10.6	5.7	7.3	74.5	12.1	
Chrysene	72.7	65.2	206	159	0.7	4.9	0.9	1.7	1.5	4.1	1.8	
Benz[a]anthracene	57.8	52.8	96.5	125	0.8	4.0	0.8	2.2	2.0	4.6	2.0	
Benzo[b]fluoranthene	199	215	465	221	0.6	1.7	0.3	1.5	0.7	1.6	0.4	
Benzo[k]fluoranthene	92.1	102	198	96.8	0.6	1.8	0.4	1.7	0.6	1.8	0.4	
Benzo[a]pyrene	164	170	310	148	0.4	1.4	0.0	1.6	0.3	1.3	ND	

Table A11: Ex-situ 2015-2016 - Average measured tissue, sediment and porewater concentrations for 7 PAHs at the receiving waters of Paleta creek.

	Average Tissue Concentration ($\mu\text{g}/\text{kg-lipids}$)											Average Sediment Concentration ($\mu\text{g}/\text{Kg-dw}$)						
												Pre-storm cores				Post-storm cores		
	P01 - Pre	P01 - Post	P08 - Pre	P08 - Post	P08 - Pre+	P11 - Pre	P11 - Post	P11 - Pre+	P17 - Pre	P17 - Post	P17 - Pre+	P01	P08	P11	P17	P08	P11	P17
%TOC												0.79	1.17	1.75	3.63	1.51	2.06	3.86
%BC												0.10	0.11	0.17	0.23	0.13	0.21	0.24
Fluoranthene	73.4	772	487	919	663	753	1457	933	625	279	372	58.8	87.9	221	240	83.0	1409	384
Pyrene	50.5	1109	964	1745	1113	4476	7926	4295	2102	2933	2220	72.0	105	950	515	104	2713	538
Chrysene	63.5	762	610	1946	720	657	364	599	332	371	239	63.4	64.5	81.9	147	68.0	437	559
Benz[a]anthracene	152	583	171	679	394	846	417	658	287	331	236	53.2	45.7	155	138	46.9	700	263
Benzo[b]fluoranthene	230	2248	2001	4316	3533	4163	3070	3758	1105	1493	1210	569	340	814	597	263	1600	702
Benzo[k]fluoranthene	244	1549	841	1864	961	1217	2704	1008	489	497	453	261	141	333	219	107	625	350
Benzo[a]pyrene	161	1977	1014	2600	1302	1299	1254	996	896	1582	739	397	242	519	385	188	914	591
	Average Porewater Concentration (ng/L)																	
	SPMEs - Prestorm				SPMEs -			SPMEs - Poststorm										
	P01	P08	P11	P17	P08+	P11+	P17+	P01	P08	P11	P17							
%TOC																		
%BC																		
Fluoranthene	2.4	7.9	9.3	43.2	4.4	20.0	12.0	8.1	20.6	41.1	24.0							
Pyrene	4.1	93.0	57.2	103	7.5	48.3	33.8	35.1	118	150	69.9							
Chrysene	0.6	2.7	2.6	5.0	0.8	2.7	1.9	1.9	4.4	6.0	3.6							
Benz[a]anthracene	0.6	2.8	2.2	5.6	0.7	2.9	1.4	1.8	3.9	7.3	3.6							
Benzo[b]fluoranthene	1.1	2.2	1.6	2.3	0.7	1.6	0.9	1.6	3.1	3.4	1.5							
Benzo[k]fluoranthene	1.0	2.2	1.6	2.1	0.7	1.4	0.8	1.6	3.2	3.4	1.4							
Benzo[a]pyrene	0.8	1.7	1.2	1.8	0.5	1.2	0.7	1.2	2.5	2.6	1.2							

Table A12: Ex-situ 2016-2017 - Average measured tissue, sediment and porewater concentrations for 7 PAHs at the receiving waters of Paleta creek.

	Average Tissue Concentration ($\mu\text{g}/\text{kg-lipids}$)								Average Sediment Concentration ($\mu\text{g}/\text{Kg-dw}$)							
	Pre-storm				Post-storm				Pre-storm cores				Post-storm cores			
	P01	P08	P11	P17	P01	P08	P11	P17	P01	P08	P11	P17	P01	P08	P11	P17
%TOC									0.98	1.25	1.93	3.94	0.72	1.96	1.87	5.16
%BC									0.10	0.12	0.15	0.24	0.07	0.17	0.13	0.27
Fluoranthene	736	735	1512	3365	903	2275	812	3445	44.1	86.6	100	346	41.3	156	216	498
Pyrene	798	1143	3090	4161	1016	4177	2023	4588	45.9	97.1	129	405	54.9	233	294	606
Chrysene	382	406	630	763	464	1044	499	671	31.5	64.8	72.1	135	33.0	118	137	207
Benz[a]anthracene	416	464	677	967	493	1266	512	2577	23.0	58.2	54.8	140	22.6	106	93.7	192
Benzo[b]fluoranthene	3524	3861	4518	3150	2425	7144	2900	1391	83.7	190	249	312	117	376	411	436
Benzo[k]fluoranthene	1347	1526	1728	1047	939	2622	1035	528	41.8	97.5	118	144	54.5	166	174	179
Benzo[a]pyrene	1850	2029	2307	1524	1364	3805	1580	883	72.6	170	198	241	102	295	277	314

	Average Porewater Concentration (ng/L)							
	SPMEs - Prestorm				SPMEs - Poststorm			
	P01	P08	P11	P17	P01	P08	P11	P17
%TOC								
%BC								
Fluoranthene	3.0	2.9	2.9	11.7	3.1	4.4	2.3	8.5
Pyrene	4.3	4.4	6.9	14.9	3.5	9.2	7.4	12.2
Chrysene	0.9	0.5	0.6	0.8	0.6	0.8	0.6	0.7
Benz[a]anthracene	1.0	0.5	0.5	0.7	0.5	0.7	0.4	0.5
Benzo[b]fluoranthene	0.9	0.7	0.6	0.4	0.7	1.1	0.7	0.4
Benzo[k]fluoranthene	0.7	0.5	0.4	0.3	0.7	1.1	0.6	0.3
Benzo[a]pyrene	0.7	0.3	0.3	0.2	0.4	0.5	0.4	0.2